U.S.N.A.—Trident Scholar project report; no. 280 (2001)

Assessment of Radio Frequency Propagation in a Naval Shipboard Environment

by

Midshipman Daniel R.J. Estes, Class of 2001
United States Naval Academy
Annapolis, Maryland

_____
(signature)

Certification of Advisors Approval

Professor Antal A. Sarkady
Electrical Engineering Department

_____
(signature)

_____
(date)

Commander Thaddeus B. Welch
Electrical Engineering Department

_____
(signature)

_____
(date)

Acceptance for the Trident Scholar Committee

_____
(signature)

_____
(date)

USNA-1531-2

Form SF298 Citation Data

Report Date *("DD MON YYYY")* 07052001	**Report Type** N/A	**Dates Covered (from... to)** *("DD MON YYYY")*

Title and Subtitle Assessment of radio frequency propagation in a naval shipboard environment	**Contract or Grant Number**
	Program Element Number
Authors Estes, Daniel R.J.	**Project Number**
	Task Number
	Work Unit Number
Performing Organization Name(s) and Address(es) US Naval Academy Annapolis, MD 21402	**Performing Organization Number(s)**
Sponsoring/Monitoring Agency Name(s) and Address(es)	**Monitoring Agency Acronym**
	Monitoring Agency Report Number(s)
Distribution/Availability Statement Approved for public release, distribution unlimited	
Supplementary Notes	
Abstract	
Subject Terms	
Document Classification unclassified	**Classification of SF298** unclassified
Classification of Abstract unclassified	**Limitation of Abstract** unlimited
Number of Pages 130	

REPORT DOCUMENTATION PAGE

Form Approved
OMB No. 074-0188

1. AGENCY USE ONLY (Leave blank)	2. REPORT DATE	3. REPORT TYPE AND DATE COVERED
	7 May 2001	

4. TITLE AND SUBTITLE
Assessment of radio frequency propagation in a naval shipboard environment

5. FUNDING NUMBERS

6. AUTHOR(S)
Estes, Daniel R.J.

7. PERFORMING ORGANIZATION NAME(S) AND ADDRESS(ES)

8. PERFORMING ORGANIZATION REPORT NUMBER

9. SPONSORING/MONITORING AGENCY NAME(S) AND ADDRESS(ES)
US Naval Academy
Annapolis, MD 21402

10. SPONSORING/MONITORING AGENCY REPORT NUMBER
Trident Scholar project report no. 280 (2001)

11. SUPPLEMENTARY NOTES

12a. DISTRIBUTION/AVAILABILITY STATEMENT
This document has been approved for public release; its distribution is UNLIMITED.

12b. DISTRIBUTION CODE

13. ABSTRACT:
The Navy, in an effort to reduce costs and operate within future budgetary constraints, is planning to reduce the manning on combat ships. To support this reduction in manning, several wireless technologies are being considered, including wireless LANs and a wireless sensor system augmented by a computer-controlled log keeping system. The internal volume of a combat ship is a generally un-studied wireless environment. While a preliminary study demonstrated that radio energy can be radiated and received from compartment to compartment (room to room) within a ship, a detailed analysis of this environment has not been done. In this project, data was collected aboard decommissioned and active ships to characterize the wireless channel on combat ships and to attempt to determine the effect of bulkheads (walls) and hatches (doors) on the information path. Both narrowband and ultra-wideband techniques have been used to demonstrated and measure transmissions through the shipboard environment. Each bulkhead attenuated the test signal roughly 20dB. Computer modeling of the bulkhead supported the hypothesis that the radio energy is propagating through the non-conductive structures within the bulkhead - hatch seals, for example - rather than through the steel.

14. SUBJECT TERMS
wireless technology; combat ships; wireless signals; bulkheads; hatches; non-conductive structures

15. NUMBER OF PAGES
127

16. PRICE CODE

17. SECURITY CLASSIFICATION OF REPORT	18. SECURITY CLASSIFICATION OF THIS PAGE	19. SECURITY CLASSIFICATION OF ABSTRACT	20. LIMITATION OF ABSTRACT

Abstract

The Navy, in an effort to reduce costs and operate within the budgetary constraints of the near future, is planning to reduce the manning on combat ships. To accomplish this without reducing the readiness or capability of these ships, the remaining personnel must work more efficiently. To support this required increase in efficiency, several wireless technologies are being considered, including wireless LANs and a wireless sensor system augmented by a computer-controlled log keeping system.

The internal volume of a combat ship is a generally un-studied wireless environment. While a preliminary study demonstrated that radio energy can be radiated and received from compartment to compartment (room to room) within a ship, a detailed analysis of this environment has not been done.

In this project, data was collected aboard decommissioned and active ships to characterize the wireless channel on combat ships and to attempt to determine the effect of bulkheads (walls) and hatches (doors) in the information path. Both narrowband and ultra-wideband techniques have been used to demonstrate and measure transmissions through the shipboard environment. Each bulkhead attenuated the test signal roughly 20dB.

Computer modeling of the bulkhead supported the hypothesis that the radio energy is propagating through the non-conductive structures within the bulkhead—hatch seals, for example—rather than through the steel.

Acknowledgements

I would like to thank the US Naval Academy Electrical Engineering Department for providing me with the equipment and facilities to undertake this project. In particular, I would like to thank Professor Antal A. Sarkady, CDR Thaddeus B. Welch, Professor Murray S. Korman (Physics Department), and Associate Professor Deborah M. Mechtel for their instruction, expertise, support, and time.

This project was suggested and sponsored by Henry Whitesel and Jack Overby of the Machinery Research and Development Directorate at the Naval Surface Warfare Center Carderock Division (NSWCCD) in Philadelphia. Their support has been instrumental in every phase of this project.

Funding support for NSWCCD came from James Gagorik and LCDR Frank Novak of the Office of Naval Research, and from Dr. Patricia Tatem of the Naval Research Laboratory. Two projects at NSWCCD contributed funds to this investigation. They were the Reduced Ships-Crew by Virtual Presence program and Emerging Requirements for Damage Control Sensors.

I would also like to thank Don Garner for his personal attention to the installation and support of the computer simulation software used in this project.

I could not have completed this project without the support of my chain of command. They have allowed me, sometimes with short notice, to travel to wherever I needed to go. Their understanding and patience has been greatly appreciated.

Time Domain Corporation graciously lent one of their prototype ultra-wideband communication systems to USNA. The capabilities of their equipment allowed a more in-depth study of the shipboard wireless channel. In particular, I would like to thank James Mann for sharing his expertise in use of the equipment and in channel sounding, and for the assistance he gave me in testing aboard several ships.

This project could not have happened without the support of the ships that allowed me to perform this testing. My thanks go to the officers and crews of the *USS Ross, USS Leyte Gulf, USS Carr,* and *USS Oscar Austin*.

I would like to thank Nadeem Bunni and Bogdan Ionescu of the technical support division of Ansoft Corporation for their assistance with the use of Maxwell3D to simulate electromagnetic wave propagation.

Finally, I would like to thank my friends and family for their support. Without them I would not have found the strength to finish this project. I would especially like to thank my fiancée, Bridget Kramer, for the loving support she gave throughout this project.

Table of Contents

List of Figures

List of Tables

1. Introduction

The Navy is always trying to find cost-effective ways to improve the level of protection it provides to the country and our allies. One way identified to accomplish this is to reduce crew complements and employ sailors more efficiently aboard ship. As a consequence of maintaining a highly technical all-volunteer force, each sailor represents a significant operating cost in terms of training and salary. Therefore, reducing the number of personnel aboard ship and employing the crew in the most effective manner will allow funds to be applied to other uses to support the Navy's service to the country.

One means to achieve this is to build automation into the ship wherever possible. For example, a system of sensors which transmit their information directly back to a central monitoring station would free a watchstander from roaming about the ship recording data in a log. In the event of a casualty, such a system would also enhance the safety of the crew by providing information about the damage (fire, flooding, smoke, etc) without risking a crewmember to obtain it. If implemented, the extent of such a system throughout the internal structure of each ship, as well as the need for future reconfigurability, would require a wireless information path, as will be explained below. Other systems as well, such as a network for mobile computers, have been proposed and would also require a wireless link.

Why Wireless?

Wireless systems have several advantages in a shipboard environment. Electric or fiber-optic cables add significant weight to ships. They add some complexity to the design process. They are also expensive to procure, maintain, and replace. Passing the cables from compartment to compartment (room to room) requires that holes be cut in the bulkhead (wall), which weakens the bulkhead. To compensate, bulkheads must be made thicker, which increases the weight and cost of the ship.

Additionally, the cables are susceptible to damage. A casualty, whether the result of an accident or attack, could cause the information path to be damaged or destroyed. The information path for the distributed sensor system, for example, could fail precisely when information about the affected compartments is most important to allow the crew to minimize risk to personnel and focus damage control efforts most effectively.

Radio waves, however, travel through space. Space does not cost anything, weigh anything, or need to be routed through the structure of a ship. Space does not need to be maintained or replaced, and space cannot be damaged or destroyed. Wireless systems are easily (inexpensively) reconfigured as well. Overall, wireless systems can be more cost effective and survivable.

Obstacles to Wireless Communication

Several factors tend to limit the performance of wireless systems aboard ships. The most obvious factor is that bulkheads will tend to block signals. The bulkheads are made of metal, most often steel, which is conductive. When an electric field enters a perfect conductor, it collapses. Though steel is not a perfect conductor, it does attenuate (weaken) the signal severely (Fig. 81). However, there are many non-conductive structures within bulkheads that allow electromagnetic waves to pass—for example, hatch seals and insulation around power cables.

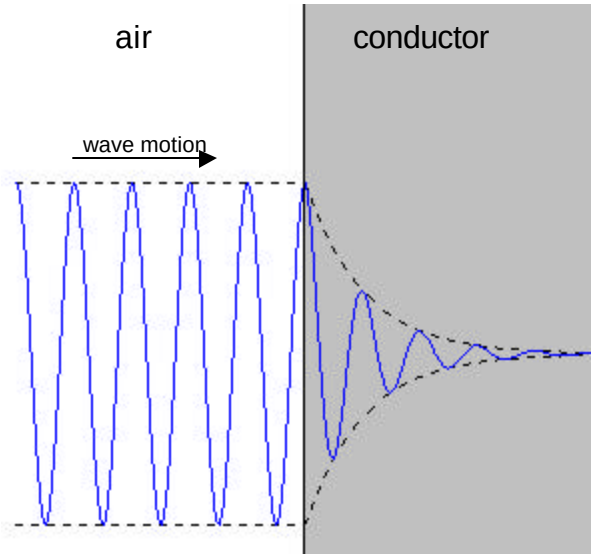

Figure 1 Electric Field of Radio Wave Entering Conductor.

Another factor that limits radio communication within ships is the multipath environment. Any signal transmitted within a ship is reflected, scattered, or diffracted by many different objects, resulting in multiple copies of the transmission arriving at the receiver. As light travels at a finite speed (c = 299e6 m / s = 983e6 ft / s), these multiple copies arrive at different times, and since the signal is a coherent waveform, mutual interference between them could result in signal degradation or cancellation at the receiver. This effect is highly dependent on wavelength and the various path lengths. Therefore, the multipath effect varies with frequency and location [1 p 147].

Channel Sounding

Since radio first began being used as a communications medium, the propagation of electromagnetic waves has been studied. Outdoor studies, such as references [2] and [3], attempt to describe the wireless channel over large areas according to the topography—such as urban or suburban environments.

Once wireless systems began being used within buildings, indoor wireless channels also began being studied. Some studies focused on specific wireless devices [4], others on frequency ranges [5-6]. Types of buildings in which wireless systems were likely to be implemented were also studied, including academic buildings [7], open-plan office buildings [8], and factory buildings [8-9].

There have been some wireless channel studies performed aboard ships, as well, but not nearly as many as there have been in buildings. Furthermore, the shipboard channel is not as well characterized. Several studies have been done to determine the performance of commercial, off-the-shelf (COTS) wireless LAN components in the hangar bay of a *Nimitz*-class carrier, aboard a *Los Angeles*-class submarine, and aboard an *Ohio*-class submarine [10-12]. However, these studies report the performance of specific components and do not address the channel characteristics. Another study, performed aboard the *ex-USS Shadwell*, attempted to identify the propagation modes [13]. Although the *Shadwell* study did not reach any major conclusions regarding how the electromagnetic waves were propagating from compartment to compartment, it did show that wireless communication is possible through closed hatches and between decks.

Project Goals

This paper will describe the wireless channel from 800 MHz to 2.5 GHz as measured aboard several Navy ships. The attenuation associated with transmitting through bulkheads will be reported, as will the effect of opening and closing hatches. The paper will report the results of ultra-wideband (approximately 1 GHz to 3 GHz) tests made using a prototype communication system. It will also, through the use of computer modeling, attempt to explain how the transmitted energy propagates from compartment to compartment through the non-conductive structures within bulkheads.

2. Narrowband Testing

To describe the wireless channel aboard ship, tests were performed on one inactive and four active Navy ships. Most tests were performed using narrowband equipment. One set of tests, using ultra-wideband equipment, will be discussed in chapter 3. Wireless measurements were made by placing a transmitter in one compartment of a ship and measuring the signal in another location.

Test Equipment

The narrowband test equipment consisted of a transmitter system, an antenna positioner, and a data logging system.

The transmitter system (Figs. 2 – 5) consisted of a radio frequency (RF) signal generator, a frequency doubler, a direct current (DC) power supply, an amplifier, an antenna, and connecting cables. The signal generator (HP8662A) was capable of creating sinusoidal waveforms from 10 kilohertz (kHz) to 1.28 gigahertz (GHz). If a frequency higher than 1.28 GHz was desired, the signal was passed through a frequency doubler (HP11721A). The signal was then passed through an amplifier, which was powered by the DC power supply (HP6205C). The DC power supply and the signal generator are powered by 120 Volt Alternating Current (120 V AC) power. Finally, the signal was transmitted by a whip antenna.

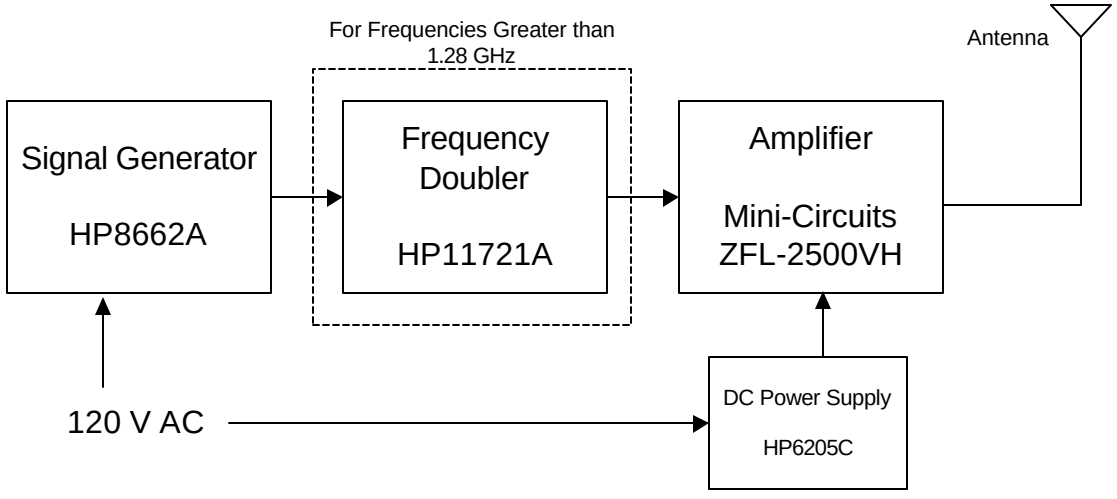

Figure 2 Transmitter Block Diagram.

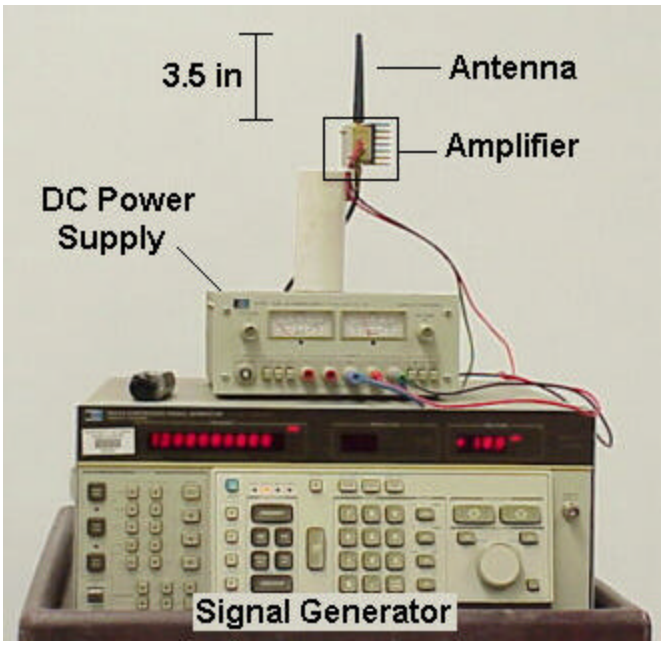

Figure 3 Transmitter System (Front).

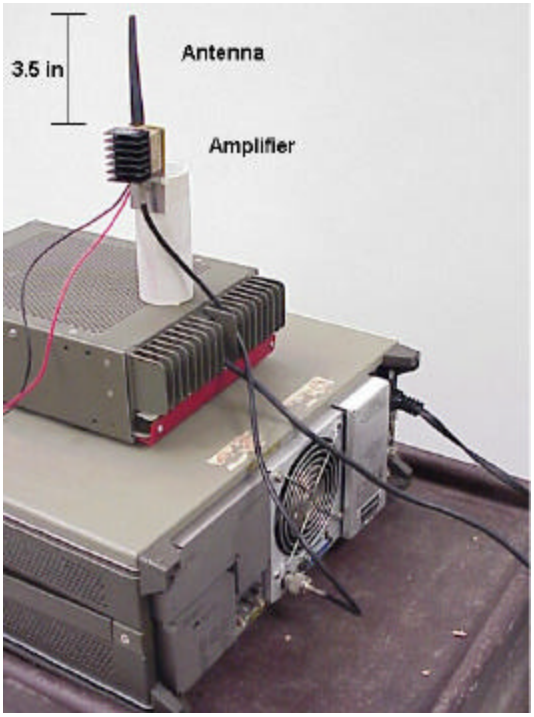

Figure 4 Transmitter Without Doubler.

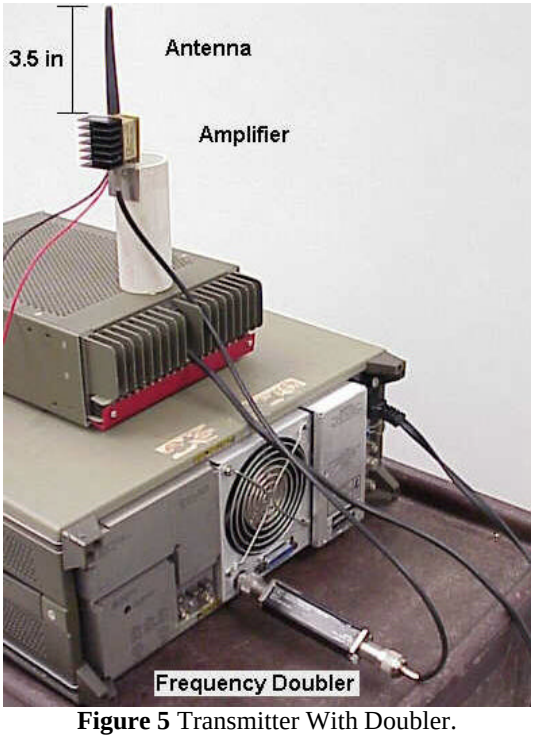

Figure 5 Transmitter With Doubler.

The receiver was composed of two systems: an antenna positioner and a data logging system. The antenna positioner (Figs. 6 – 7) was used to move the antenna smoothly through several wavelengths of travel while taking measurements. This provided a more complete sample of the multipath effect. The antenna was mounted on a

wooden cart, which was moved smoothly across a wooden track by a stepper motor. This process provided very accurate position and velocity control. The motor was controlled by a drive indexer (Parker Hann PDX 13), which was programmed using a laptop computer. Except for the motor, the positioning system was made entirely without metal in order to prevent interference with the antenna's near fields. The laptop and drive indexer are powered by 120 V AC power. The stepper motor draws power from the drive indexer.

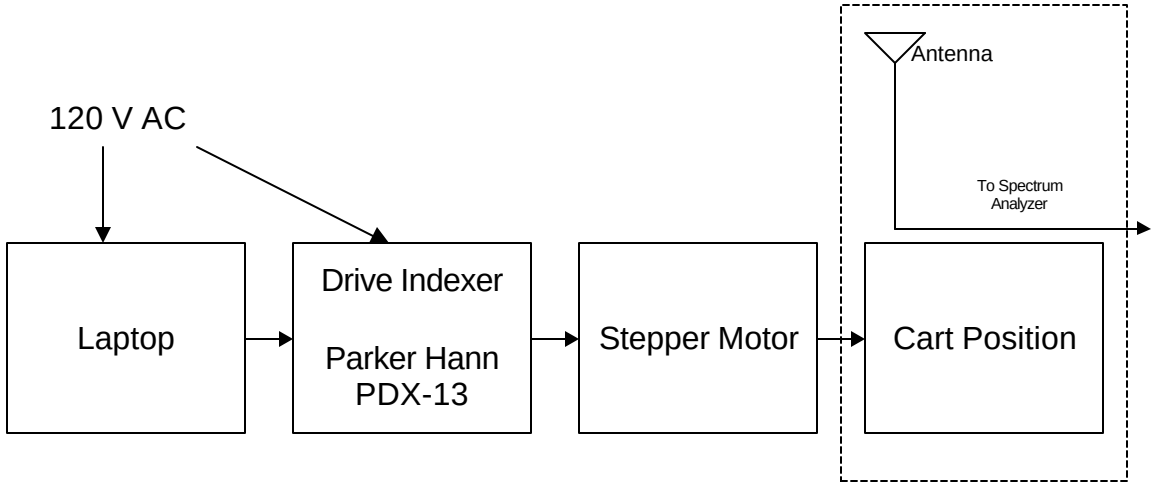

Figure 6 Antenna Positioning System Block Diagram.

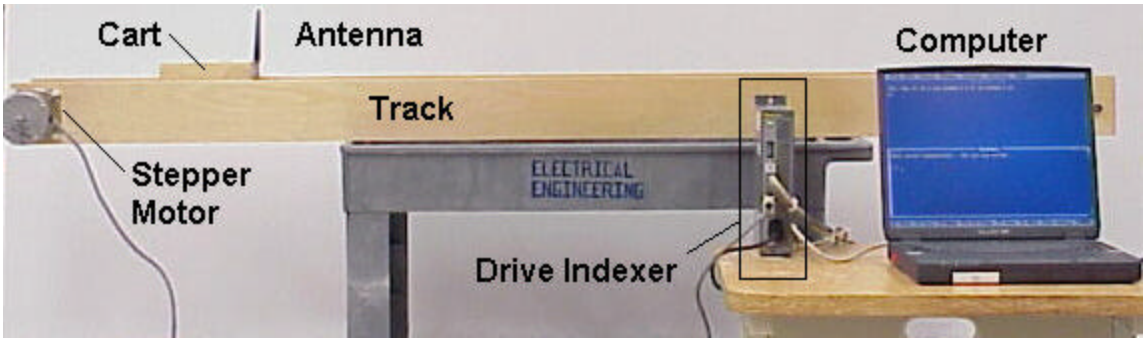

Figure 7 Antenna Positioning System.

The data logging system (Figs. 8 – 9) consisted of a spectrum analyzer (Agilent 8595E) and a laptop computer, both of which drew 120 V AC power. The computer was running the program HP Vee, which fed commands to the spectrum analyzer and recorded the data it returned. The program was set up to measure and record the power at a user-defined frequency. The system recorded approximately 4.6 samples per second. For each frequency tested, the data recording system measured and recorded the received signal power level while the positioner was moving the antenna smoothly through approximately four feet of space. The data for each measurement—each set of recorded

power levels measured at a particular location and frequency—was saved in a text file, for later analysis with MATLAB [14].

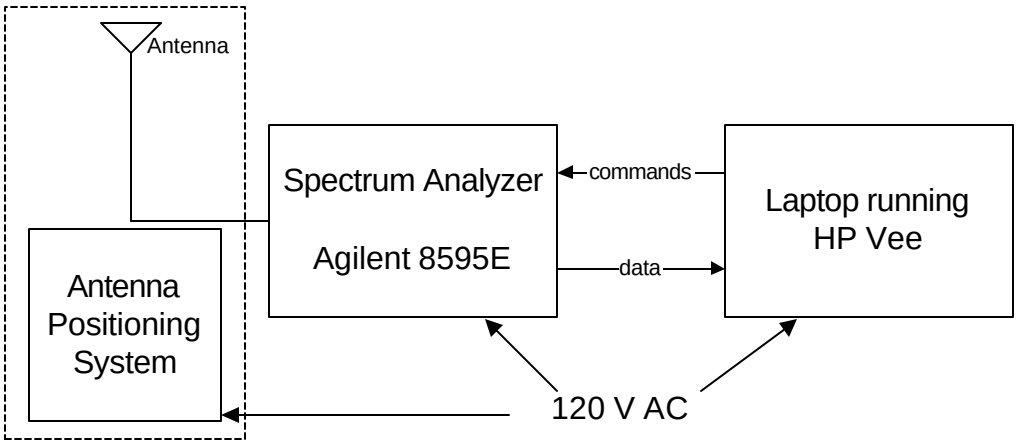

Figure 8 Data Logging System Block Diagram.

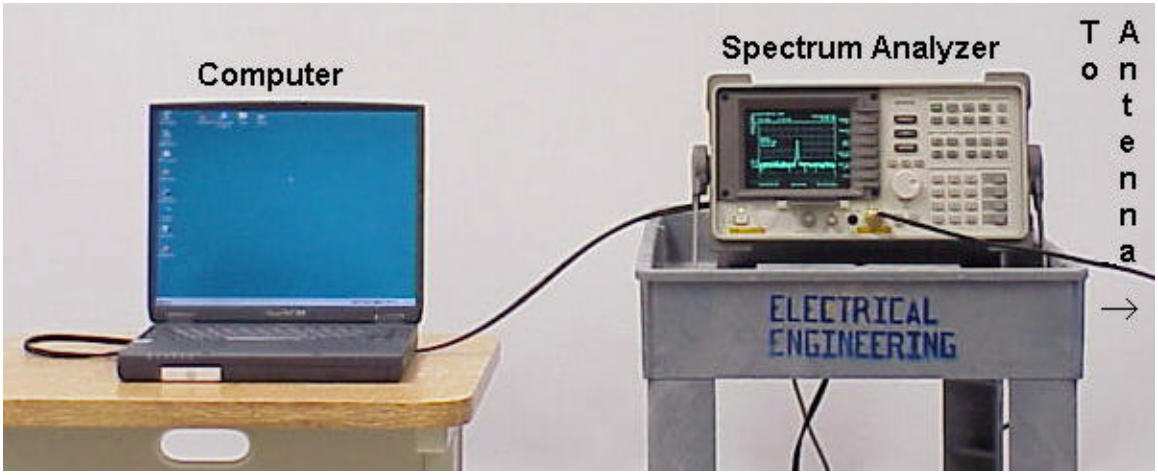

Figure 9 Data Logging System.

Statistical Analysis

The measured data were analyzed with MATLAB in the following manner.

Maximum (max), minimum (min), and average power: Due to the multipath effect, the received power showed extreme variation according to frequency and location, as shown by the raw data included in the discussion of tests aboard each ship. The maximum and minimum received power level for each measurement was determined.

The data had been stored as power level received, with units of dBm. These values were converted from dBm to milliwatt values and averaged. This must be done because the decibel is a unit of proportion (see Appendix A), which would cause lower-

power points to be over emphasized in the averaging operation. This average was then converted back to dBm for display and further analysis.

Power standard deviation: The standard deviation was calculated as the square root of the variance, which was calculated from the data in dBm rather than milliwatts. This is because the variance of a signal is better described in proportion to the average signal. Therefore, the variance is calculated from the data in proportional units.

Number of Points, N: The number of data points taken in the measurement, N, was recorded.

Error Value: The error value is an estimate of the error a calculated average value will have as compared to the true average value. It is the standard deviation of the sampled data divided by the square root of N [15].

K factor: The Ricean *K* factor describes distribution of received power levels. In a channel with a dominant propagation path, it describes the ratio of power received from that path, $P_{Dominant\ Path}$, to the power received from other paths, $P_{All\ Other\ Paths}$:

$$K = \frac{P_{DominantPath}}{P_{All\ Other\ Paths}}$$

K is a function of the geometry of the paths that the electromagnetic waves travel from the transmitter to the receiver. Therefore, the *K* factor varies with position, and must be measured at each location. The received power level of a channel containing no reflective paths (dominant path only, $K = \infty$) and subject only to additive white gaussian noise (AWGN) will, by definition, exhibit a gaussian probability density function (pdf). A channel containing no dominant path (reflective paths only, $K = 0$) will, by definition, exhibit a Rayleigh distribution. Any channel with both dominant and reflective paths will demonstrate a Ricean distribution [1 p.175]. The equation for the pdf, $p(r)$, of a Ricean channel is:

$$p(r) = \frac{r}{s^2} e^{-\frac{r^2+K^2}{2s^2}} I_0\left(\frac{Kr}{s^2}\right)$$

where r is the received signal level, s^2 is the noise power in the channel, and I_0 is a Bessel function of the first kind [1 p. 176].

The *K* factor is found within an accuracy of 0.1 by integrating the pdf to find the Ricean cumulative distribution function (CDF) that matches the CDF of the data most closely (Figs. 10 – 11). The *K* factor of this best-fit Ricean CDF is then adopted as the *K* factor of the measurement.

K MSE: The mean square error (MSE) of the *K* factor is a measurement of the quality of the measured data. The difference between the best-fit Ricean CDF and the data CDF is squared, and the average taken. Data sets that more closely follow a Ricean distribution have a smaller MSE than those that don't. It is generally accepted that a MSE of less than 0.0005 indicates a good fit Ricean distribution [16].

In practice it was found that the number of data points in each measurement was small, usually between 110 and 120. There is still confidence in the estimated *K* values, however, because the received signal was sampled along the length of the track at over 10 samples per wavelength, providing good resolution of the received power over distance along the track. Some MSE values were somewhat higher than 0.0005, which could be due to shadowing or diffraction patterns at the measurement location.

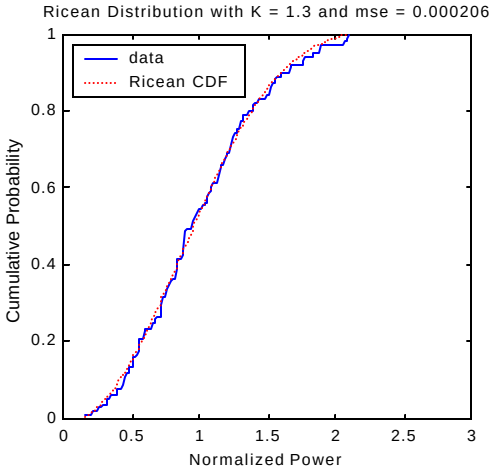

Figure 10 Good Fit Ricean Curve MSE = .000205.

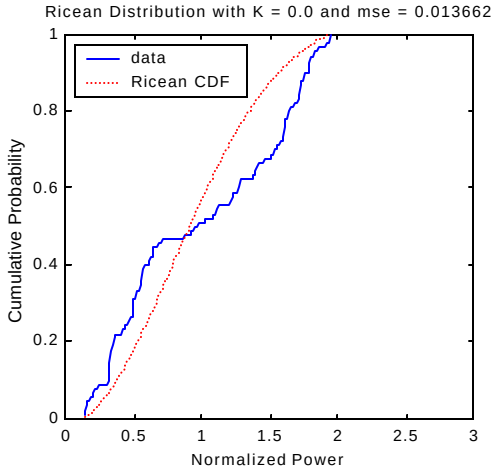

Figure 11 Poor Fit Ricean Curve MSE = .01366.

Attenuation: Attenuation is the loss in power associated with transmission through a volume or object. It is the proportion of signal power lost between two points. In the instance where power is measured in decibels (dB), as it is in this report, attenuation is simply the difference between the power levels. This is because the decibel is a logarithmic quantity, and a ratio operation in absolute units (watts) becomes a subtraction operation in logarithmic units (decibels).

The transmitter and receiver were not calibrated. The transmitter and receiver used many narrowband components, whose behavior would need to be calibrated at each test frequency. Wideband components, such as antennas, were cost prohibitive. Rather than calibrate the equipment at each frequency each time the test was to be performed, the channel was studied by comparing measurements to each other. This required that at least two measurements be taken for any meaningful information about attenuation, but eliminated the need to have the instruments calibrated before each test.

Therefore, to find signal attenuation, the results from measurements in different locations were compared. Attenuation was calculated as the loss of signal power

associated with transmission through a bulkhead or hatch. The attenuation associated with a bulkhead is the difference between the power received on the side nearest the transmitter and that received on the far side. The attenuation of a hatch is the difference between the power received on the far side with the hatch open and that when it was closed. That is (in dB):

$$A_{Bulkhead} = P_{Near} - P_{Far}$$
$$A_{Hatch} = P_{Open} - P_{Shut}$$

Attenuation Error: When two measured power levels are subtracted, the uncertainty in the value of each is combined into the uncertainty of the difference. Therefore, the error values associated with the measured power levels are added to find the worst-case error value of the attenuation.

Test Results

Ex-USS America

The *America* is a decommissioned aircraft carrier located in the Philadelphia shipyard. Initial testing was performed on the *America* to demonstrate that wireless transmissions could be received through closed hatches. For this set of tests, the positioning system and data logging system were not used. Rather, the antenna was hand-positioned to find the strongest signal within a local area, and the data were recorded by saving the spectrum analyzer trace to disk and printing out a hardcopy. Consequently, the number of data points recorded in each measurement was between one and six, and meaningful error bars could not be calculated for these measurements. The data recorded in these tests are presented at the end of this section.

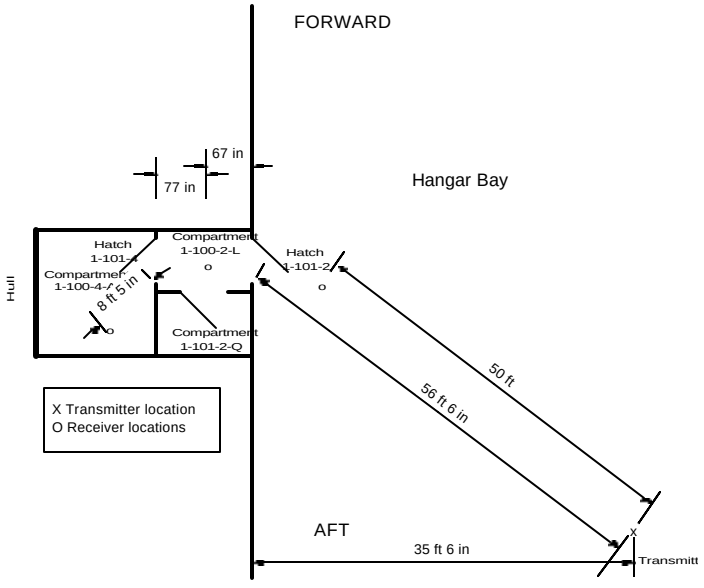

Figure 12 Test Layout Aboard *ex-USS America* For Tests Across 1-101-2 and 1-101-4.

The effect of hatches 1-101-2 and 1-101-4 was determined by comparing the signal on the near side of the hatch to that on the far side (Fig. 12). It should be noted that this particular test technique was different than that used for all other hatches—the effects of all other hatches are determined by comparing the received power level through the open hatch with the received power level through the shut hatch.

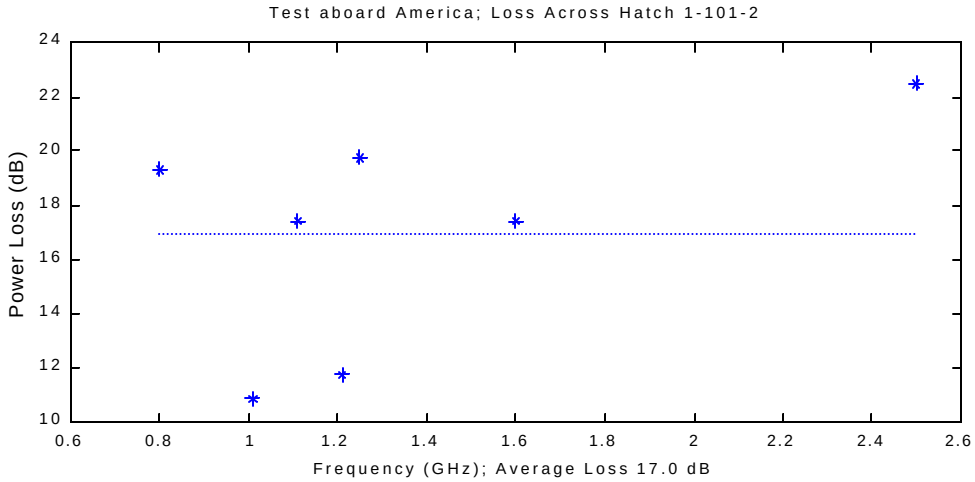

Figure 13 Loss Across Hatch 1-101-2 Aboard *ex-USS America.*

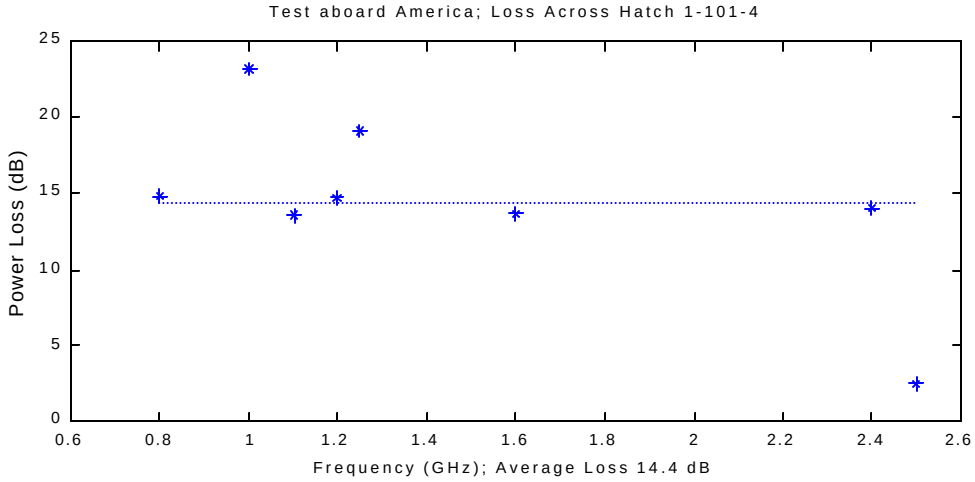

Figure 14 Loss Across Hatch 1-101-4 Aboard *ex-USS America.*

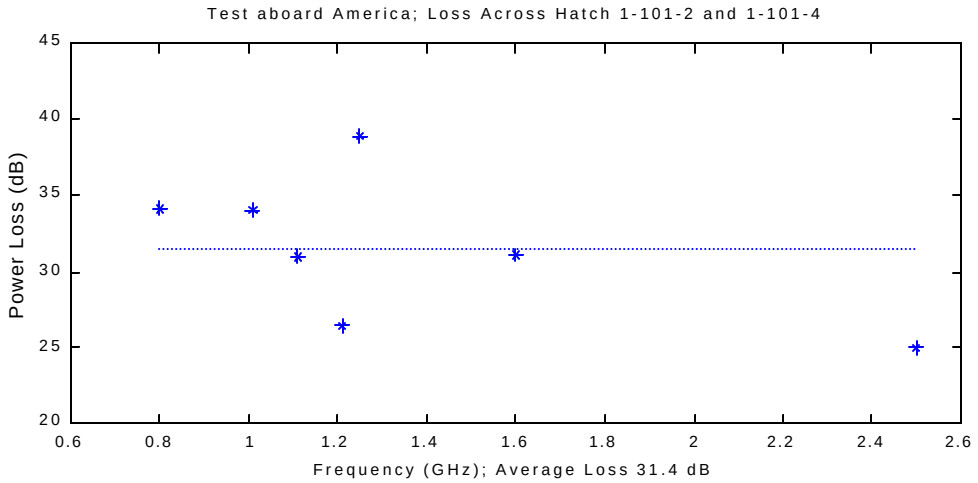

Figure 15 Loss Across Hatches 1-101-2 and 1-101-4.

Figures 13 – 15 are plots of the attenuation versus frequency associated with hatches 1-101-2 and 1-101-4. The difference in power received on each side of the hatch is attributed to the effect of that hatch. The average attenuation measured across hatch 1-101-2 was 17.0 dB. Similarly, hatch 1-101-4 attenuated the signal an average of 14.4 dB. The lower attenuation measured across hatch 1-101-4 could be attributed to the geometry of the tests: hatch 1-101-2 blocked an almost direct path from the transmitter, whereas hatch 1-101-4 did not.

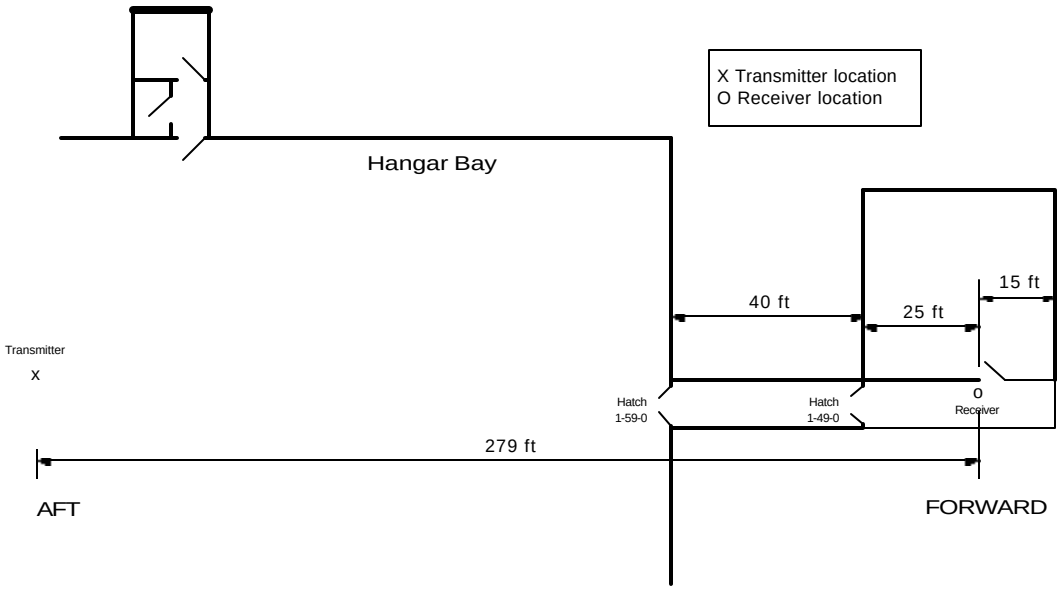

Figure 16 Test Layout Aboard *ex-USS America* For Tests Across 1-59-0.

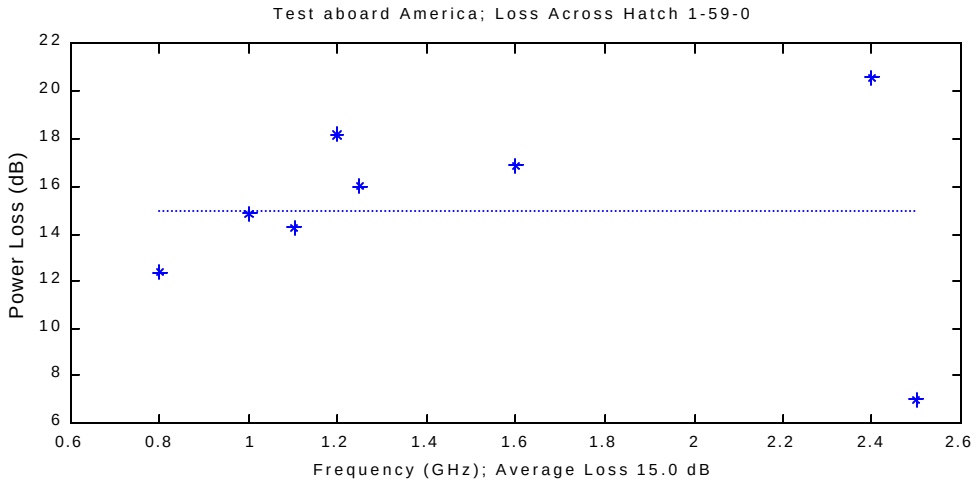

Figure 17 Loss Across Hatch 1-59-0 Aboard *ex-USS America*.

The attenuation associated with hatch 1-59-0 (Fig. 16) was calculated by comparing the signal strength with the hatch open to that with the hatch shut (Fig. 17). This technique was used to test all further hatches in order to determine the effect of the hatch *only*, without the effect of the bulkhead as well. Bulkheads were tested by measuring the signal on both sides and comparing the measurements. The average attenuation of hatch 1-59-0 was 15.0 dB.

Table 1 Results of Narrowband Measurements Aboard *ex-USS America*.

Trace	Receiver	Bulkheads	Hatches	Distance	Frequency	Receive	Standard	Samples
				(ft)	(GHz)	(dBm)	Dev (dB)	
tr00	hangar	0	0	7.42	1.11	-22.7		1
tr01	hangar	0	0	10.1				
tr02	hangar	0	0	50	1.10	-37.0		1
tr03	1-100-2-L	1	0	62.1	1.11	-46.1	0.4031	2
tr04	1-100-2-L	1	1	62.1	1.11	-52.3	1.8592	3
tr05	1-100-2-L	1	1	62.1	1.11			
tr06	1-100-2-L	1	1	62.1	1.11			
tr07	1-100-4-A	2	0	76.9	1.11	-50.6		1
tr08	1-100-4-A	2	1	76.9	1.11	-58.4		1
tr09	1-100-4-A	2	2	76.9	1.11	-60.4	0.1768	2
tr10	corridor	2	0	279	1.11	-46.5		1
tr11	corridor	2	1	279	1.11	-57.5		1
tr12	corridor	2	2	279	1.10	-74.7		1
tr13	corridor	2	1.5	279	1.10	-66.6	0.2899	2
tr14	1-39-2-Q	3	1	284	1.10	-74.0		1
tr15	hangar	0	0	10	1.01	-28.8	0.0141	2
tr16	hangar	0	0	10	1.11	-21.3		1
tr17	hangar	0	0	10	1.21	-22.6		1
tr18	hangar	0	0	10	2.21	-41.4		1
tr19	hangar	0	0	10	1.61	-36.3		1

Trace	Receiver	Bulkheads	Hatches	Distance	Frequency	Receive	Standard	Samples
				(ft)	(GHz)	(dBm)	Dev (dB)	
tr20	hangar	0	0	10	0.802	-39.1		1
tr21	hangar	0	0	10	1.26	-28.5		1
tr22	hangar	0	0	10	2.52	-43.0		1
tr23	hangar	0	0	50	1.01	-43.3		1
tr24	hangar	0	0	50	1.11	-32.5		1
tr25	hangar	0	0	50	1.21	-36.4		1
tr26	hangar	0	0	50	2.22	-43.6		1
tr27	hangar	0	0	50	1.61	-46.0		1
tr28	hangar	0	0	50	0.800	-44.4		1
tr29	hangar	0	0	50	1.26	-36.5		1
tr30	hangar	0	0	50	2.52	-52.3		1
tr31	1-100-2-L	1	1	62.1	1.01	-54.2	0.2773	3
tr32	1-100-2-L	1	1	62.1	1.11	-52.0	0.4063	3
tr33	1-100-2-L	1	1	62.1	1.21	-48.2	0.4325	3
tr34	1-100-2-L	1	1	62.1	2.40	-62.5	0.8858	3
tr35	1-100-2-L	1	1	62.1	1.60	-63.5	0.9205	3
tr36	1-100-2-L	1	1	62.1	0.800	-63.7	0.6293	2
tr37	1-100-2-L	1	1	62.1	1.25	-56.2	1.9001	3
tr38	1-100-2-L	1	1	62.1	2.50	-74.7	0.3842	3
tr39	1-100-4-A	2	2	76.9	1.00	-77.3	0.5244	3
tr40	1-100-4-A	2	2	76.9	1.10	-69.2	2.3058	3
tr41	1-100-4-A	2	2	76.9	1.20	-62.9	0.3387	3
tr42	1-100-4-A	2	2	76.9	2.40	-76.5	0.0693	3
tr43	1-100-4-A	2	2	76.9	1.60	-77.2	0.5565	3
tr44	1-100-4-A	2	2	76.9	0.800	-78.5	0.0404	3
tr45	1-100-4-A	2	2	76.9	1.25	-75.3	1.2309	3
tr46	1-100-4-A	2	2	76.9	2.50	-77.3	0.0924	3
tr47	corridor	1	0	279	1.01	-49.1	0.3672	3
tr48	corridor	1	0	279	1.11	-57.1	0.4285	3
tr49	corridor	1	0	279	1.21	-50.7	0.4258	3
tr50	corridor	1	0	279	2.41	-53.7	0.5248	3
tr51	corridor	1	0	279	1.60	-61.2	0.7983	3
tr52	corridor	1	0	279	0.800	-63.8	1.4060	6
tr53	corridor	1	0	279	1.25	-53.3	0.4244	3
tr54	corridor	1	0	279	2.50	-68.3	1.3808	3
tr55	corridor	1	1	279	1.00	-64.0	0.1682	3
tr56	corridor	1	1	279	1.10	-72.4	2.3105	3
tr57	corridor	1	1	279	1.20	-68.8	0.6001	3
tr58	corridor	1	1	279	2.40	-74.2	0.1210	3
tr59	corridor	1	1	279	1.60	-78.1	0.3509	3
tr60	corridor	1	1	279	0.800	-76.2	0.1234	3
tr61	corridor	1	1	279	1.25	-69.3	1.0934	3
tr62	corridor	1	1	279	2.50	-75.3	0.0473	3
tr35	1-100-2-L	1	1	62.1	1.60	-63.5	0.9205	3

Trace	Receiver	Bulkheads	Hatches	Distance	Frequency	Receive	Standard	Samples
				(ft)	(GHz)	(dBm)	Dev (dB)	
tr36	1-100-2-L	1	1	62.1	0.800	-63.7	0.6293	2
tr37	1-100-2-L	1	1	62.1	1.25	-56.2	1.9001	3
tr38	1-100-2-L	1	1	62.1	2.50	-74.7	0.3842	3
tr39	1-100-4-A	2	2	76.9	1.00	-77.3	0.5244	3
tr40	1-100-4-A	2	2	76.9	1.10	-69.2	2.3058	3
Tr41	1-100-4-A	2	2	76.9	1.20	-62.9	0.3387	3
tr42	1-100-4-A	2	2	76.9	2.40	-76.5	0.0693	3
tr43	1-100-4-A	2	2	76.9	1.60	-77.2	0.5565	3
tr44	1-100-4-A	2	2	76.9	0.800	-78.5	0.0404	3
tr45	1-100-4-A	2	2	76.9	1.25	-75.3	1.2309	3
tr46	1-100-4-A	2	2	76.9	2.50	-77.3	0.0924	3
tr47	corridor	1	0	279	1.01	-49.1	0.3672	3
tr48	corridor	1	0	279	1.11	-57.1	0.4285	3
tr49	corridor	1	0	279	1.21	-50.7	0.4258	3
tr50	corridor	1	0	279	2.41	-53.7	0.5248	3
tr51	corridor	1	0	279	1.60	-61.2	0.7983	3
tr52	corridor	1	0	279	0.800	-63.8	1.4060	6
tr53	corridor	1	0	279	1.25	-53.3	0.4244	3
tr54	corridor	1	0	279	2.50	-68.3	1.3808	3
tr55	corridor	1	1	279	1.00	-64.0	0.1682	3
tr56	corridor	1	1	279	1.10	-72.4	2.3105	3
tr57	corridor	1	1	279	1.20	-68.8	0.6001	3
tr58	corridor	1	1	279	2.40	-74.2	0.1210	3
tr59	corridor	1	1	279	1.60	-78.1	0.3509	3
tr60	corridor	1	1	279	0.800	-76.2	0.1234	3
tr61	corridor	1	1	279	1.25	-69.3	1.0934	3
tr62	corridor	1	1	279	2.50	-75.3	0.0473	3

USS Ross

The *Ross* is a *Burke*-class destroyer, the Navy's newest destroyer class. These tests were across the bulkhead between Main Engine Room (MER) One and the Machine Shop (Fig. 18). The transmitter was placed on a table in the Machine Shop (antenna height approximately 4 feet). Four measurements were taken at all frequencies tested—three in MER 1 and one along the forward wall of the Machine Shop. Though the bulkhead between MER 1 and the Machine Shop contained no hatches, two hatches existed through which the signal could propagate. The designation of the inboard hatch is 2-188-2 and that of the outboard hatch is 2-188-4.

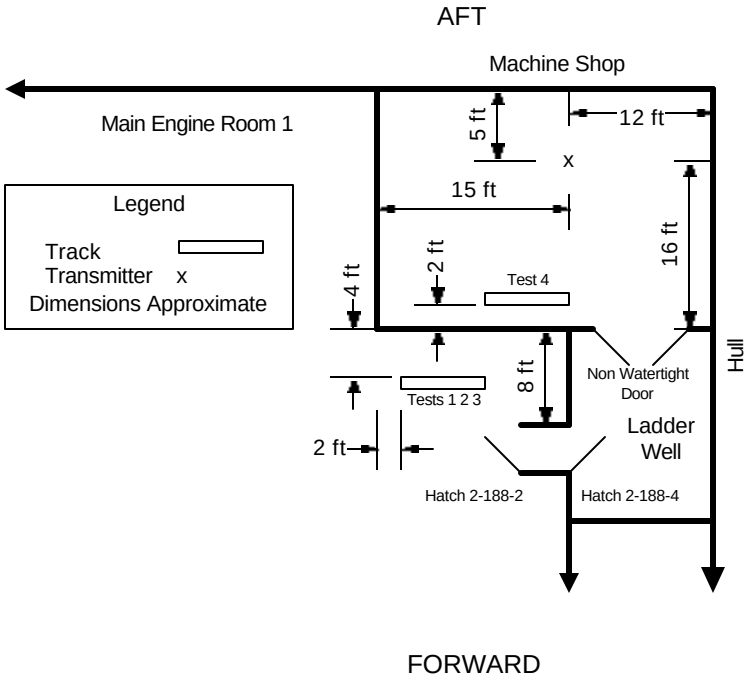

Figure 18 Test Layout Aboard *USS Ross.*

The raw data is presented as plots that show received signal versus sample number. The received signal is the power, in dBm, recorded by the data logging system of the receiver.

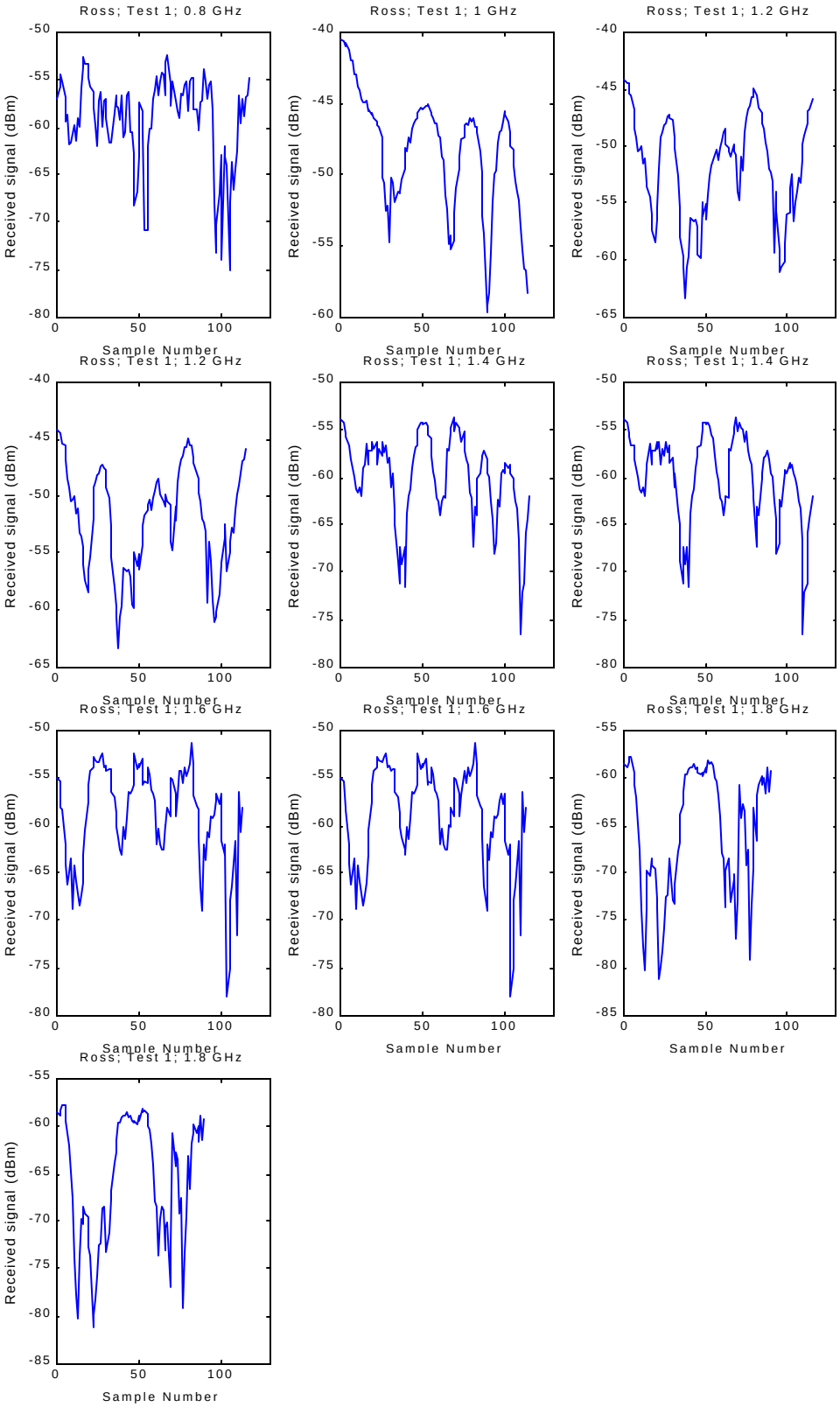
Ross; Test 1; 0.8 GHz
Ross; Test 1; 1 GHz
Ross; Test 1; 1.2 GHz
Ross; Test 1; 1.2 GHz
Ross; Test 1; 1.4 GHz
Ross; Test 1; 1.4 GHz
Ross; Test 1; 1.6 GHz
Ross; Test 1; 1.6 GHz
Ross; Test 1; 1.8 GHz
Ross; Test 1; 1.8 GHz
Received signal (dBm)
Sample Number

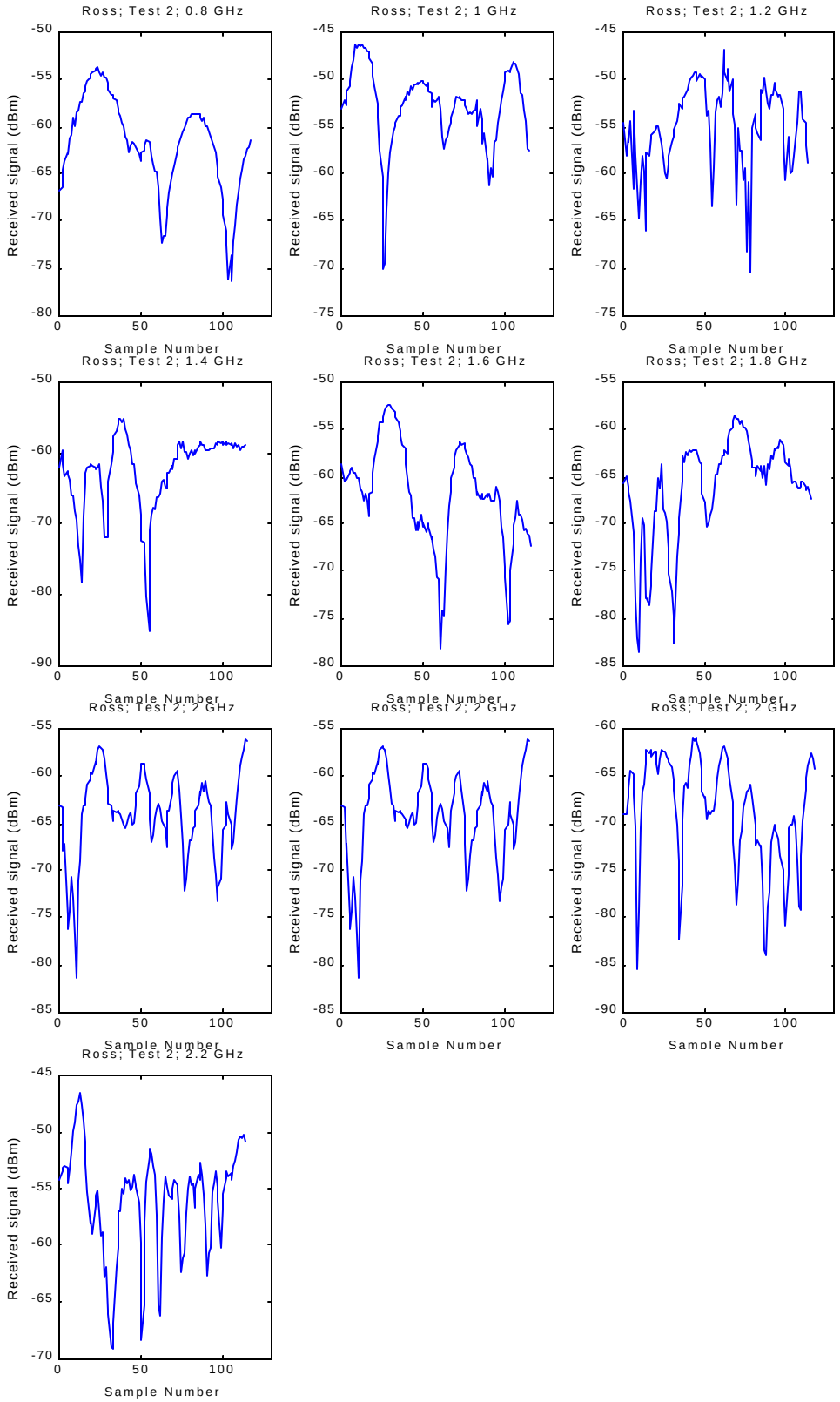
Ross; Test 2; 0.8 GHz
Ross; Test 2; 1 GHz
Ross; Test 2; 1.2 GHz
Ross; Test 2; 1.4 GHz
Ross; Test 2; 1.6 GHz
Ross; Test 2; 1.8 GHz
Ross; Test 2; 2 GHz
Ross; Test 2; 2 GHz
Ross; Test 2; 2 GHz
Ross; Test 2; 2.2 GHz
Received signal (dBm)
Sample Number

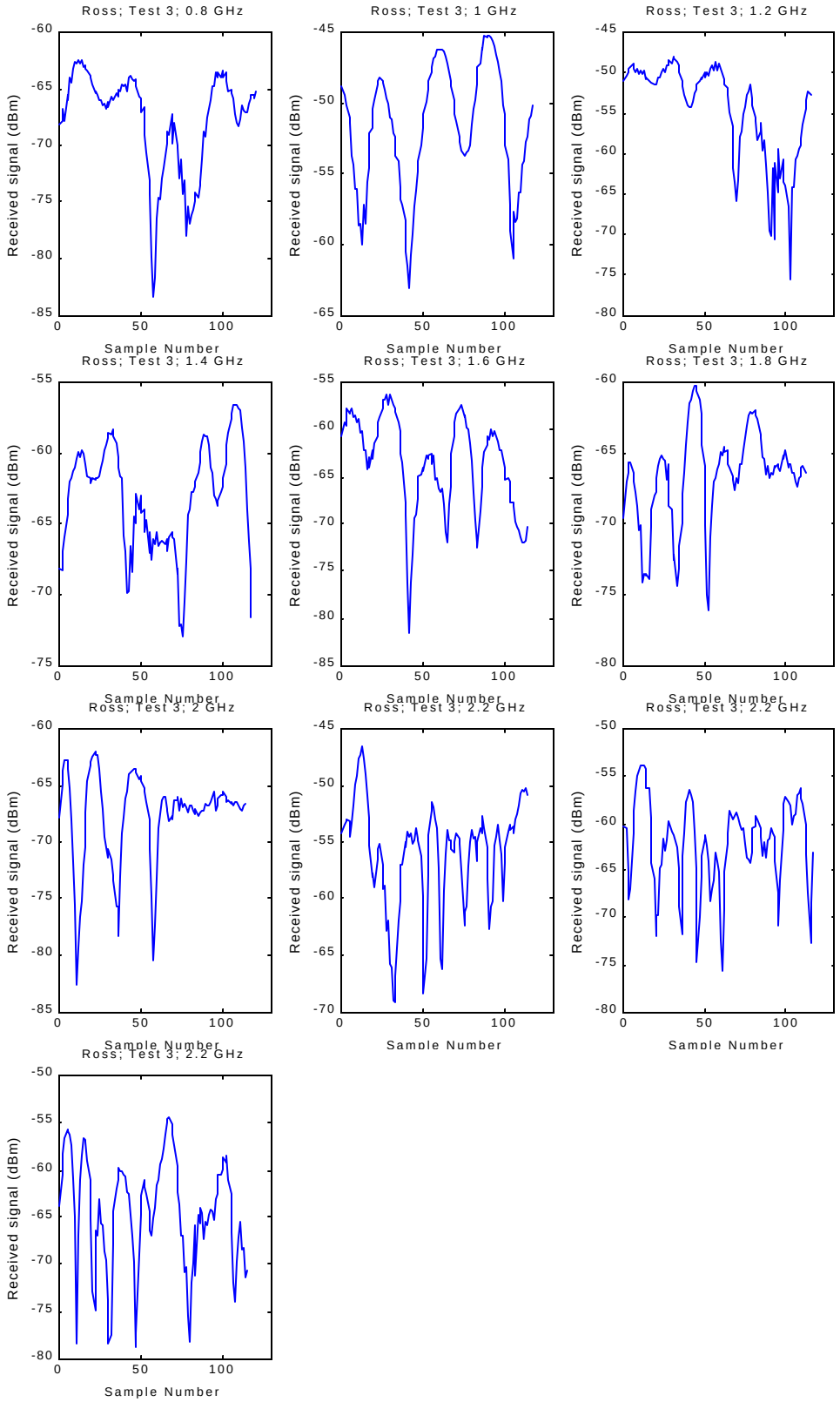
Ross; Test 3; 0.8 GHz
Ross; Test 3; 1 GHz
Ross; Test 3; 1.2 GHz
Ross; Test 3; 1.4 GHz
Ross; Test 3; 1.6 GHz
Ross; Test 3; 1.8 GHz
Ross; Test 3; 2 GHz
Ross; Test 3; 2.2 GHz
Ross; Test 3; 2.2 GHz
Ross; Test 3; 2.2 GHz
Received signal (dBm)
Sample Number

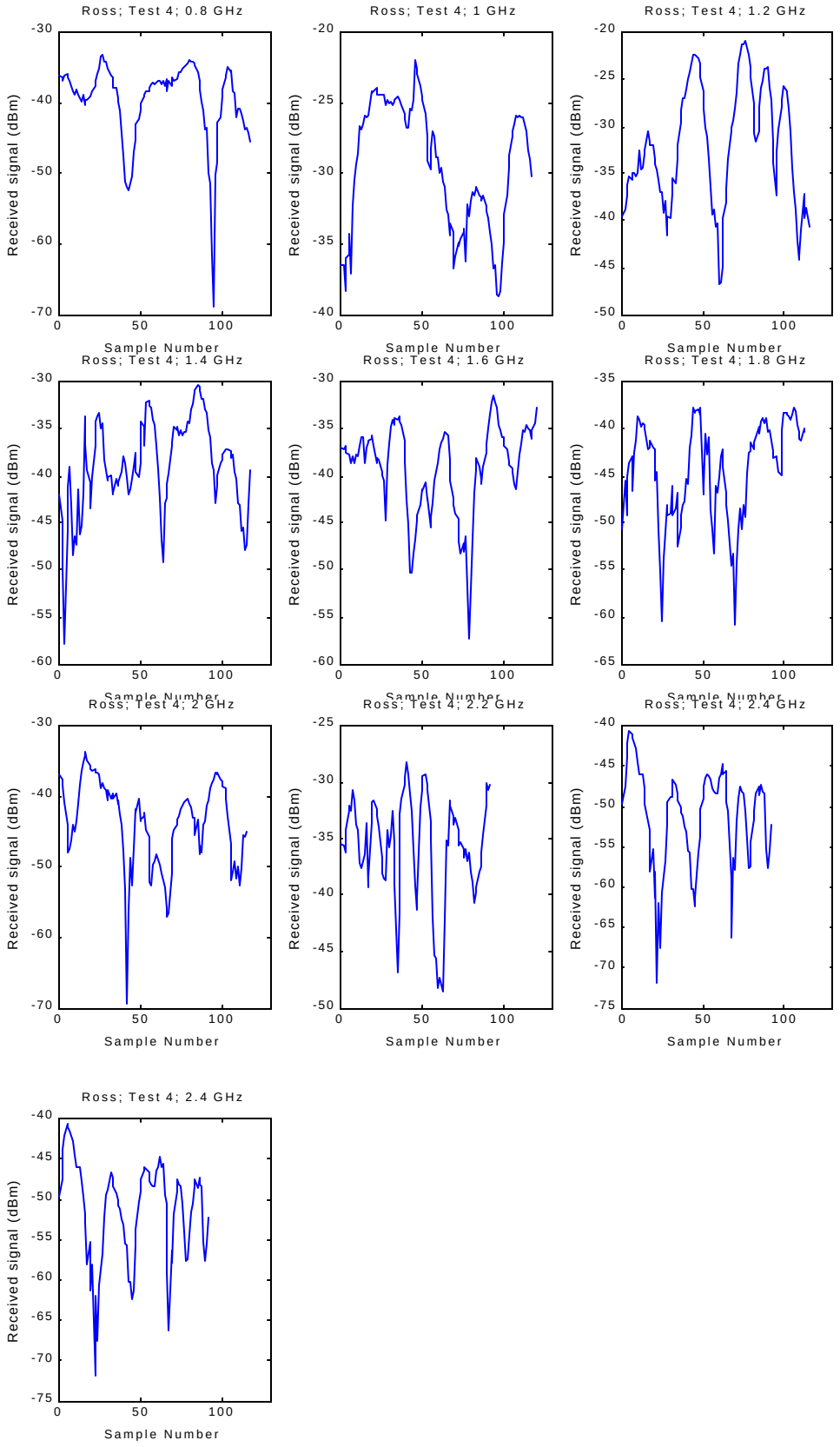
Ross; Test 4; 0.8 GHz
Ross; Test 4; 1 GHz
Ross; Test 4; 1.2 GHz
Ross; Test 4; 1.4 GHz
Ross; Test 4; 1.6 GHz
Ross; Test 4; 1.8 GHz
Ross; Test 4; 2 GHz
Ross; Test 4; 2.2 GHz
Ross; Test 4; 2.4 GHz
Ross; Test 4; 2.4 GHz
Received signal (dBm)
Sample Number

The first test was performed with the receiver in MER 1 with both hatches open. The received signal was measured at frequency intervals of 200 MHz from 800 MHz to 2.4 GHz. 2.5 GHz was also tested. The receiver was at a height of 38 inches for all tests.

Table 2 Results from Test 1 Aboard *USS Ross*.

Frequency (GHz)	Max Power (dBm)	Ave Power (dBm)	Min Power (dBm)	Power STD (dBm)	Number Data Points	Max Error (dBm)	*K* Factor	*K* MSE
0.800	-52.5	-57.5	-75.1	4.6	117	0.43	1.9	0.000524
1.000	-40.4	-46.7	-59.6	4.2	114	0.39	1.8	0.001486
1.200	-44.1	-50.0	-63.3	4.5	115	0.42	0.0	0.000382
1.400	-53.5	-58.3	-76.7	4.6	115	0.43	1.6	0.000545
1.600	-51.2	-56.9	-78.0	5.1	113	0.48	1.1	0.000812
1.800	-57.8	-62.3	-81.3	6.6	90	0.70	0.0	0.013662
2.000	-56.0	-62.2	-81.4	4.6	115	0.43	1.4	0.000809
2.200	-46.6	-54.0	-69.2	4.6	114	0.43	2.0	0.001343
2.400	-40.7	-48.2	-72.0	6.1	92	0.64	0.0	0.001030
2.500	-46.2	-52.2	-72.4	4.8	116	0.45	1.4	0.000346

Most of the channels measured during this test showed an MSE greater than 0.0005. This could be due to several factors. The number of measurement data points may not have been high enough to create a smooth cumulative distribution function.

It could also mean that the antenna passed through diffraction pattern or shadowing effects in addition to the multipath variation. That is, it moves out from behind an object into a region of stronger signal. In this situation, the fact that the received signal power changed suggests that the *K* factor also changed: a proportionately large amount of power in one path was blocked enough to cause a received signal power change. Consequently, it can be inferred that the actual *K* in any location is highly variable with position, and can vary with any change in the geometry of the channel.

The second test was performed with the receiver in the same location as the first, but hatch 2-188-4, the outboard hatch, was shut.

Table 3 Results from Test 2 Aboard *USS Ross.*

Frequency (GHz)	Max Power (dBm)	Ave Power (dBm)	Min Power (dBm)	Power STD (dBm)	Number Data Points	Max Error (dBm)	*K* Factor	*K* MSE
0.800	-53.6	-59.6	-76.3	5.1	117	0.47	0.0	0.000878
1.000	-46.2	-51.3	-70.1	4.2	115	0.39	2.1	0.000819
1.200	-46.9	-53.3	-70.4	4.3	114	0.41	1.4	0.000441
1.400	-54.9	-60.5	-85.2	5.4	114	0.51	1.7	0.001728
1.600	-52.4	-59.2	-78.2	5.3	116	0.49	0.0	0.001900
1.800	-58.4	-64.0	-83.5	5.4	115	0.51	1.5	0.000773
2.000	-60.8	-66.0	-85.5	5.7	118	0.52	0.8	0.002027
2.200	-53.8	-60.2	-75.7	4.6	117	0.42	1.1	0.000511
2.400	-48.5	-54.7	-78.4	5.4	115	0.50	0.0	0.001560
2.500	-50.7	-56.6	-80.8	6.7	115	0.63	0.0	0.001563

The third test was again performed with the receiver in the same location. This time, however, both hatches were shut.

Table 4 Results from Test 3 Aboard *USS Ross.*

Frequency (GHz)	Max Power (dBm)	Ave Power (dBm)	Min Power (dBm)	Power STD (dBm)	Number Data Points	Max Error (dBm)	*K* Factor	*K* MSE
0.800	-62.5	-66.2	-83.3	4.4	121	0.40	2.2	0.0
1.000	-45.2	-50.0	-63.0	4.4	117	0.40	0.9	0.000798
1.200	-48.0	-52.1	-75.4	6.0	115	0.56	1.5	0.007298
1.400	-56.5	-61.7	-73.0	3.7	118	0.34	1.2	0.000464
1.600	-56.1	-61.4	-81.7	5.1	114	0.48	1.1	0.000994
1.800	-60.3	-65.5	-76.1	3.3	112	0.32	2.8	0.002558
2.000	-61.9	-66.4	-82.6	4.0	114	0.38	2.7	0.002530
2.200	-54.4	-61.4	-78.8	5.8	115	0.54	0.0	0.001603
2.400	-47.9	-53.7	-74.8	5.7	117	0.53	0.0	0.001298
2.500	-53.0	-58.3	-78.1	6.7	117	0.62	0.0	0.002931

The fourth test was performed with the receiver in the machine shop, along the forward bulkhead. This is to provide a reference measurement from which to compare the other measurements. From this comparison, the effect of the bulkhead can be found.

Table 5 Results from Test 4 Aboard *USS Ross.*

Frequency (GHz)	Max Power (dBm)	Ave Power (dBm)	Min Power (dBm)	Power STD (dBm)	Number Data Points	Max Error (dBm)	*K* Factor	*K* MSE
0.800	-33.2	-37.8	-68.9	5.6	117	0.52	2.0	0.001557
1.000	-22.0	-27.6	-38.8	4.4	117	0.41	0.0	0.002177
1.200	-20.9	-28.1	-46.8	6.4	115	0.60	0.0	0.007203
1.400	-30.2	-36.6	-57.9	4.9	117	0.45	0.0	0.000692
1.600	-31.5	-37.4	-57.3	4.8	120	0.43	1.7	0.000320
1.800	-37.6	-42.2	-60.8	5.2	113	0.49	1.2	0.002977
2.000	-33.7	-40.7	-69.3	6.0	115	0.56	0.0	0.000911
2.200	-28.2	-33.9	-48.5	4.6	92	0.48	1.4	0.000238
2.400	-22.5	-28.7	-47.3	5.3	117	0.49	0.9	0.000684
2.500	-21.6	-26.7	-48.9	5.9	115	0.55	1.2	0.001941

By comparing tests 1, 2, and 3 to test 4, the effect of the bulkhead between MER 1 and the machine room can be determined.

Table 6 Test 1 Compared to Test 4.

Frequency (GHz)	Power Loss (dBm)	Power St. Dev. (dBm)	Error Val (dBm)
0.80	19.7	5.15	0.95
1.00	19.1	4.31	0.80
1.20	21.9	5.58	1.03
1.40	21.7	4.71	0.87
1.60	19.5	4.94	0.92
1.80	20.2	5.86	1.18
2.00	21.5	5.39	1.00
2.20	20.1	4.62	0.92
2.40	19.5	5.69	1.13
2.50	25.5	5.38	1.00

Average Loss (dBm) 20.9

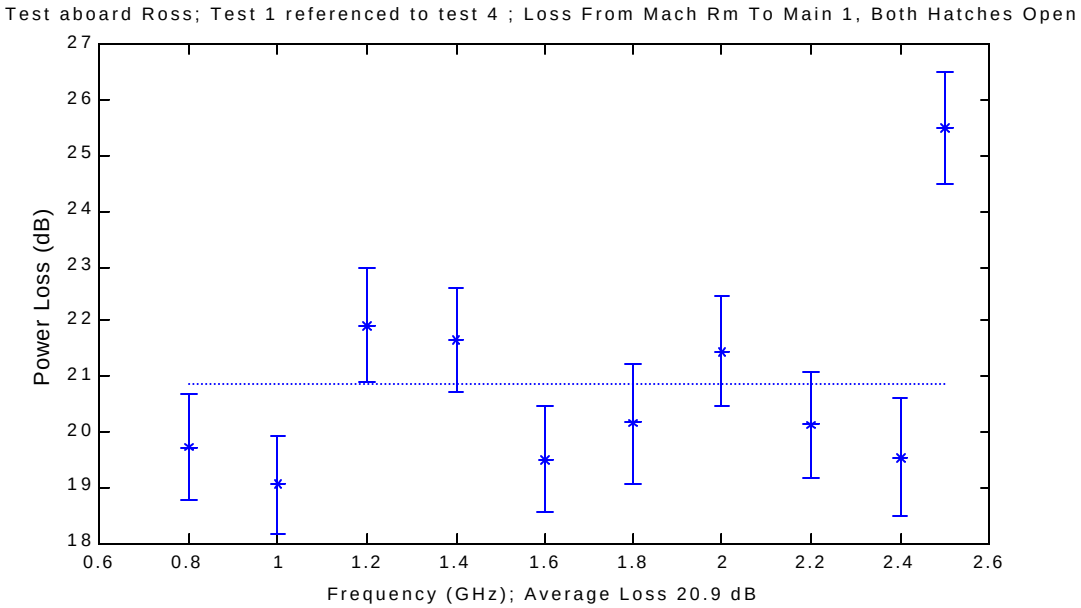

Figure 19 Attenuation Due to MER Bulkhead With Hatches Open.

The difference between tests 1 and 4 is approximately 21 dB (Fig. 19). That is, moving the receiver to the other side of the bulkhead from the machine room causes 21 dB attenuation.

Table 7 Test 2 Compared to Test 4.

Frequency (GHz)	Power Loss (dBm)	Power St. Dev. (dBm)	Error Val (dBm)
0.80	21.8	5.35	0.99
1.00	23.7	4.31	0.80
1.20	25.3	5.50	1.01
1.40	23.9	5.14	0.96
1.60	21.8	5.04	0.93
1.80	21.8	5.32	1.00
2.00	25.2	5.85	1.08
2.20	26.3	4.61	0.91
2.40	26.0	5.34	0.99
2.50	29.8	6.33	1.18

Average Loss (dBm) 24.6

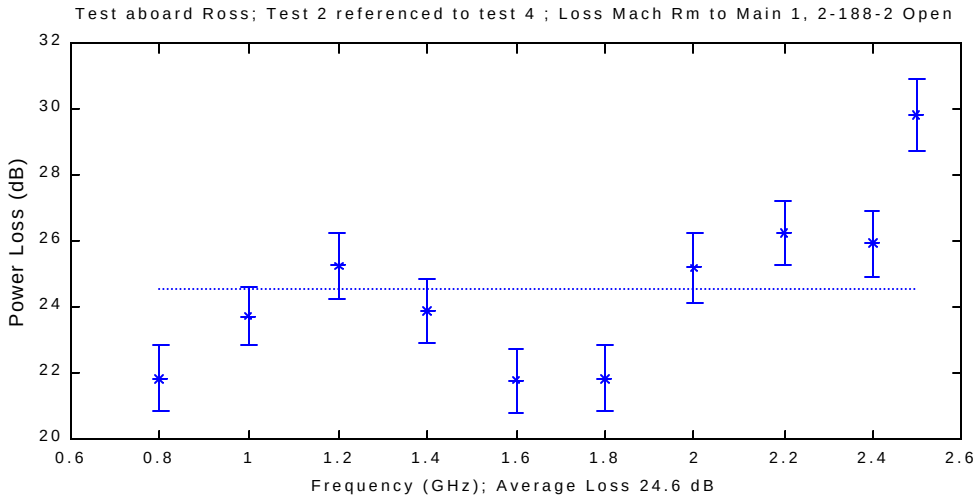

Figure 20 Attenuation Due to MER Bulkhead With 2-188-2 Open and 2-188-4 Shut.

When hatch 2-188-4 was shut, but 2-188-2 remained open, the attenuation experienced across the bulkhead was 24.6 dB (Fig. 20).

Table 8 Test 3 Compared to Test 4.

Frequency (GHz)	Power Loss (dBm)	Power St. Dev. (dBm)	Error Val (dBm)
0.80	28.5	5.04	0.92
1.00	22.4	4.41	0.82
1.20	24.0	6.22	1.16
1.40	25.0	4.33	0.79
1.60	24.0	4.92	0.91
1.80	23.3	4.37	0.80
2.00	25.7	5.14	0.94
2.20	27.5	5.33	1.03
2.40	25.0	5.50	1.02
2.50	31.5	6.31	1.17

Average Loss (dBm) 25.7

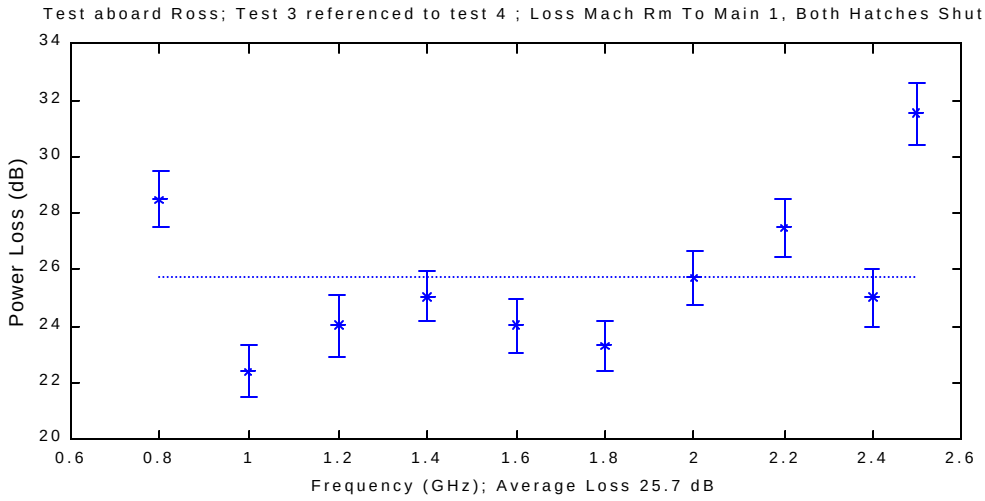

Figure 21 Attenuation Due to MER Bulkhead With Hatches Shut.

When both hatches were shut, the attenuation caused by the bulkhead was 25.7 dB (Fig. 21).

The loss in signal due to each hatch can be calculated by comparing the signal power with that hatch open to the signal power with it shut.

Table 9 Test 2 Compared to Test 1.

Frequency (GHz)	Power Loss (dBm)	Power St. Dev. (dBm)	Error Val (dBm)
0.80	2.1	4.84	0.89
1.00	4.7	4.18	0.78
1.20	3.3	4.44	0.83
1.40	2.2	5.01	0.93
1.60	2.3	5.22	0.98
1.80	1.7	5.98	1.20
2.00	3.8	5.18	0.95
2.20	6.1	4.59	0.85
2.40	6.4	5.73	1.14
2.50	4.3	5.83	1.07

Average Loss (dBm) 3.69

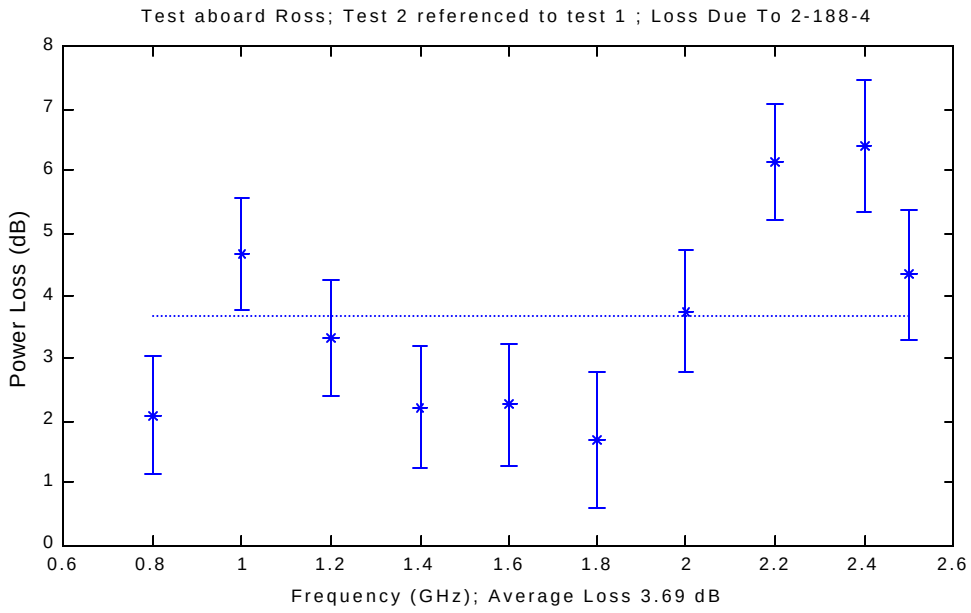

Figure 22 Loss Due to Shutting Hatch 2-188-4.

The power loss caused by shutting hatch 2-188-4 was 3.69 dB (Fig. 22).

Table 10 Test 3 Compared to Test 1.

Frequency (GHz)	Power Loss (dBm)	Power St. Dev. (dBm)	Error Val (dBm)
0.80	8.7	4.51	0.83
1.00	3.3	4.28	0.80
1.20	2.1	5.32	0.98
1.40	3.4	4.17	0.77
1.60	4.5	5.10	0.96
1.80	3.1	5.06	1.01
2.00	4.3	4.35	0.81
2.20	7.3	5.25	0.97
2.40	5.5	5.90	1.17
2.50	6.0	5.81	1.06

Average Loss (dBm) 4.83

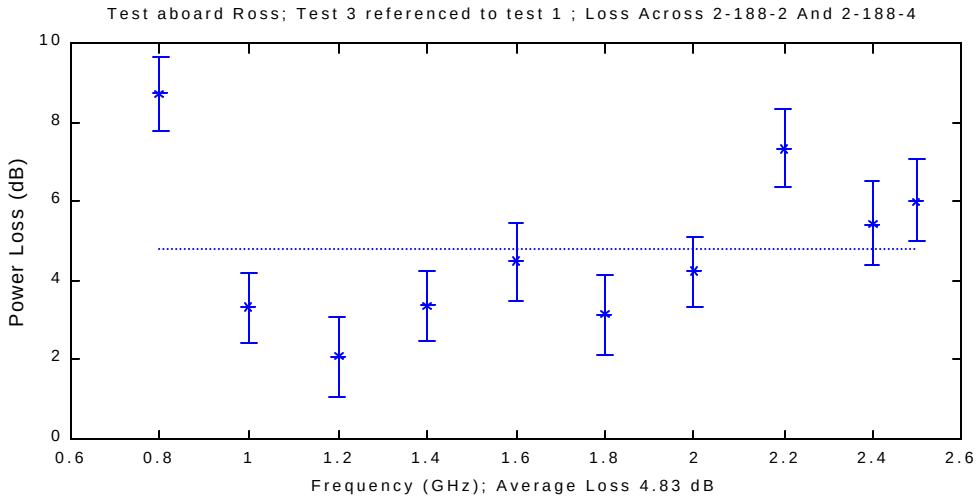

Figure 23 Loss Due to Shutting Hatches 2-188-2 and 2-188-4.

The signal loss caused by shutting both hatches was 4.83 dB (Fig. 23).

Table 11 Test 3 Compared to Test 2.

Frequency (GHz)	Power Loss (dBm)	Power St. Dev. (dBm)	Error Val (dBm)
0.80	6.6	4.74	0.87
1.00	-1.3	4.28	0.79
1.20	-1.2	5.24	0.97
1.40	1.2	4.64	0.85
1.60	2.2	5.20	0.97
1.80	1.5	4.52	0.82
2.00	0.5	4.93	0.90
2.20	1.2	5.24	0.97
2.40	-0.9	5.54	1.03
2.50	1.7	6.69	1.24

Average Loss (dBm) 1.14

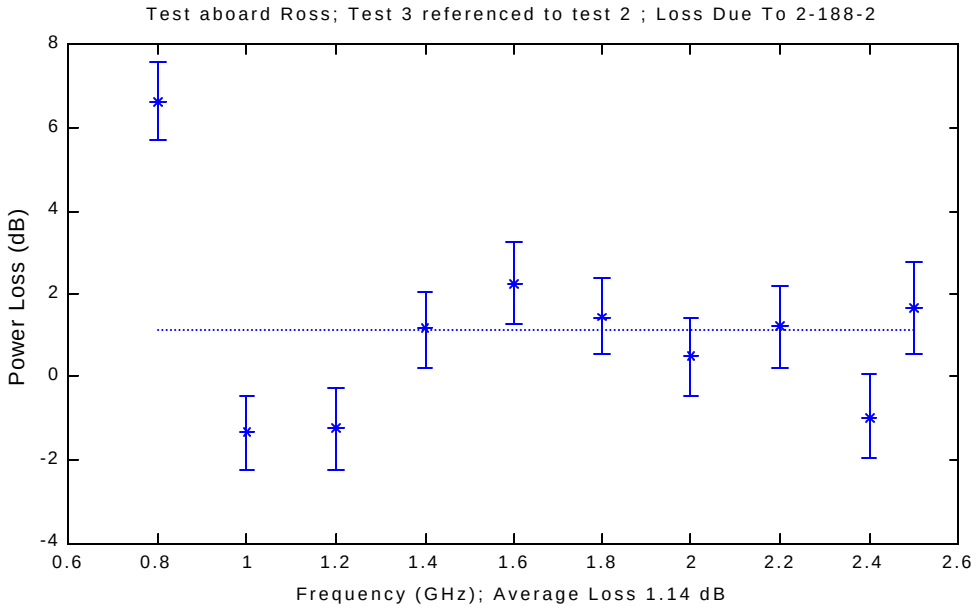

Figure 24 Loss Due To Shutting Hatch 2-188-2.

Shutting hatch 2-188-4 caused an average of 3.7 dB drop in received power. However, shutting hatch 2-188-2 caused only an additional 1.1 dB drop (Fig. 24). This provides three key pieces of information about the channel.

The drop in signal corresponding to shutting the hatch shows that energy was propagating through the ladderwell and into the engine room, which is not surprising. With the hatch open, the electromagnetic waves propagating along this path required only reflection, scattering, and diffraction to be redirected around corners, and did not need to penetrate any objects between the transmitter and receiver. Adding an obstacle, shutting hatch 2-188-4, blocked some of the energy in this path.

Secondly, the additional drop in power when the second hatch was shut shows that there was still energy propagating along that path. If the first hatch were to block all electromagnetic waves, it would be expected that the second couldn't block any waves. These tests show that energy does propagate through closed hatches.

Thirdly, since the drop in power due to the second hatch was smaller than that associated with the first hatch, it shows that there is another propagation path. The hatches are identical, therefore it is expected that if the only propagation path were through the ladderwell, shutting the second hatch should induce as much attenuation as the first. The fact that it doesn't shows that there is additional energy propagating along another path.

USS Leyte Gulf

Only one test was performed on the *Leyte Gulf*. The *Leyte Gulf* is a *Ticonderoga*-class cruiser, the Navy's newest class. The transmitter and receiver were both located in one of the engine rooms. The transmitter was placed on the deck next to an engine instrument panel (Fig. 25). The receiver was placed on the other side of the gas turbine engines (Fig. 26). The antenna height of the receiver was 38 inches.

The engines blocked the line of sight propagation path between the transmitter and receiver. However, there was a large amount of open space surrounding the engine equipment, which should allow good multipath propagation between the transmitter and receiver. The test was performed from 800 MHz to 2.5 GHz in 100 MHz steps.

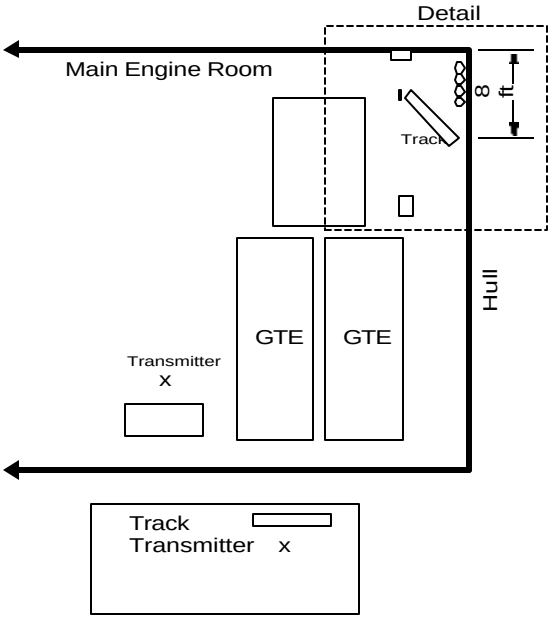

Figure 25 Test Layout Aboard *USS Leyte Gulf*.

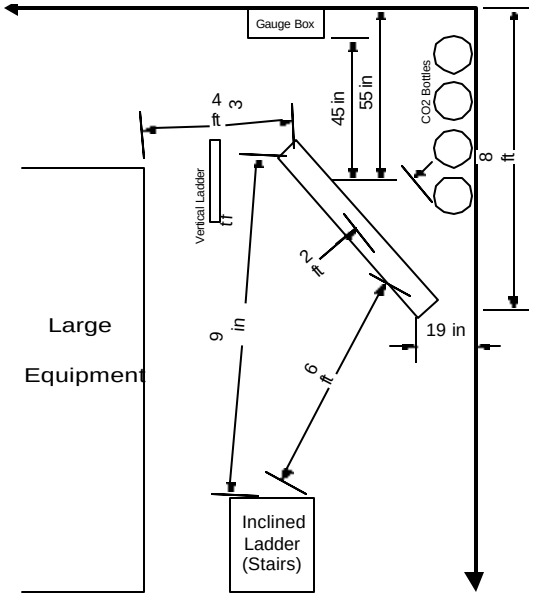

Figure 26 Detail of Receiver Area.

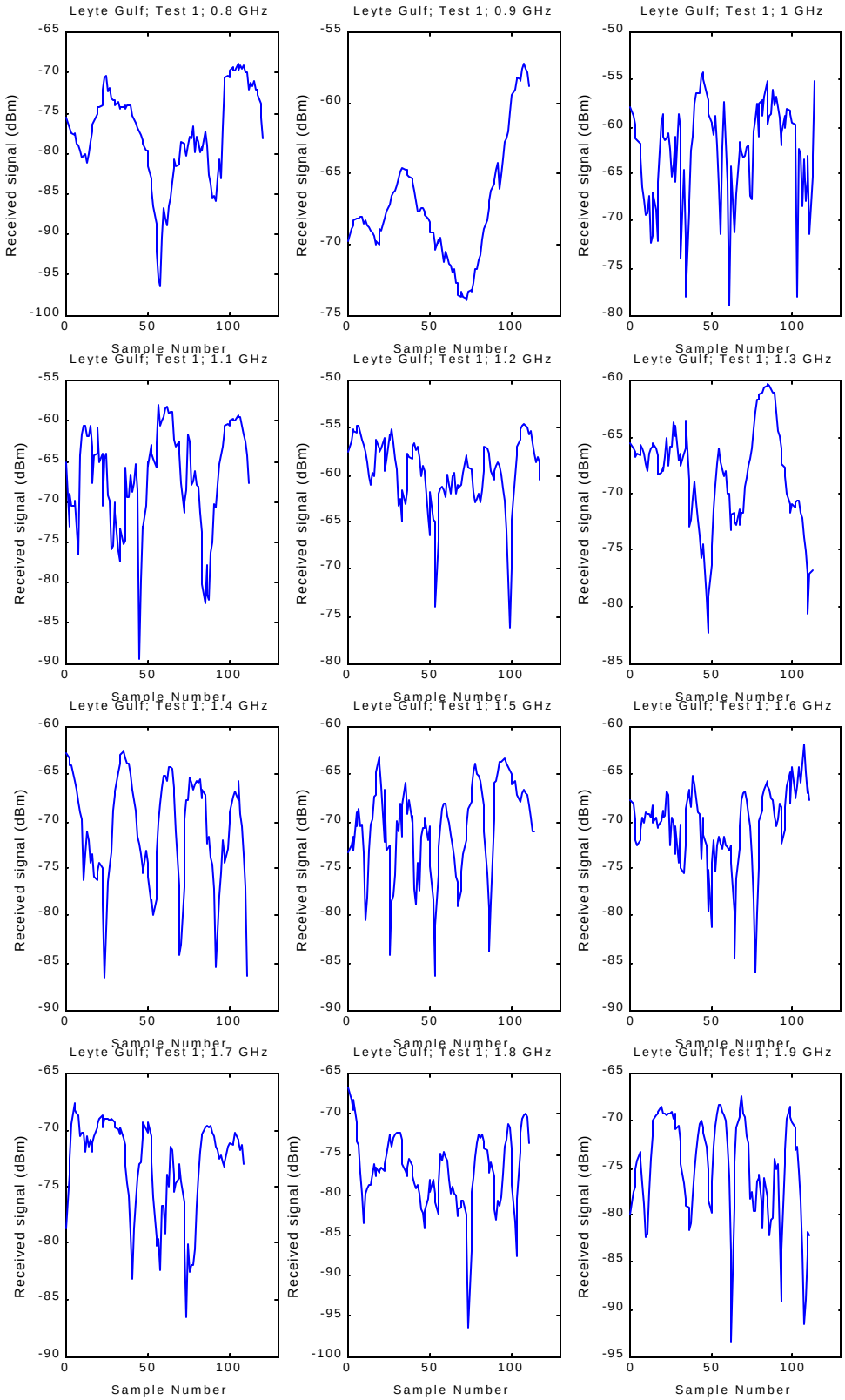
Leyte Gulf; Test 1; 0.8 GHz
Leyte Gulf; Test 1; 0.9 GHz
Leyte Gulf; Test 1; 1 GHz
Leyte Gulf; Test 1; 1.1 GHz
Leyte Gulf; Test 1; 1.2 GHz
Leyte Gulf; Test 1; 1.3 GHz
Leyte Gulf; Test 1; 1.4 GHz
Leyte Gulf; Test 1; 1.5 GHz
Leyte Gulf; Test 1; 1.6 GHz
Leyte Gulf; Test 1; 1.7 GHz
Leyte Gulf; Test 1; 1.8 GHz
Leyte Gulf; Test 1; 1.9 GHz
Received signal (dBm)
Sample Number

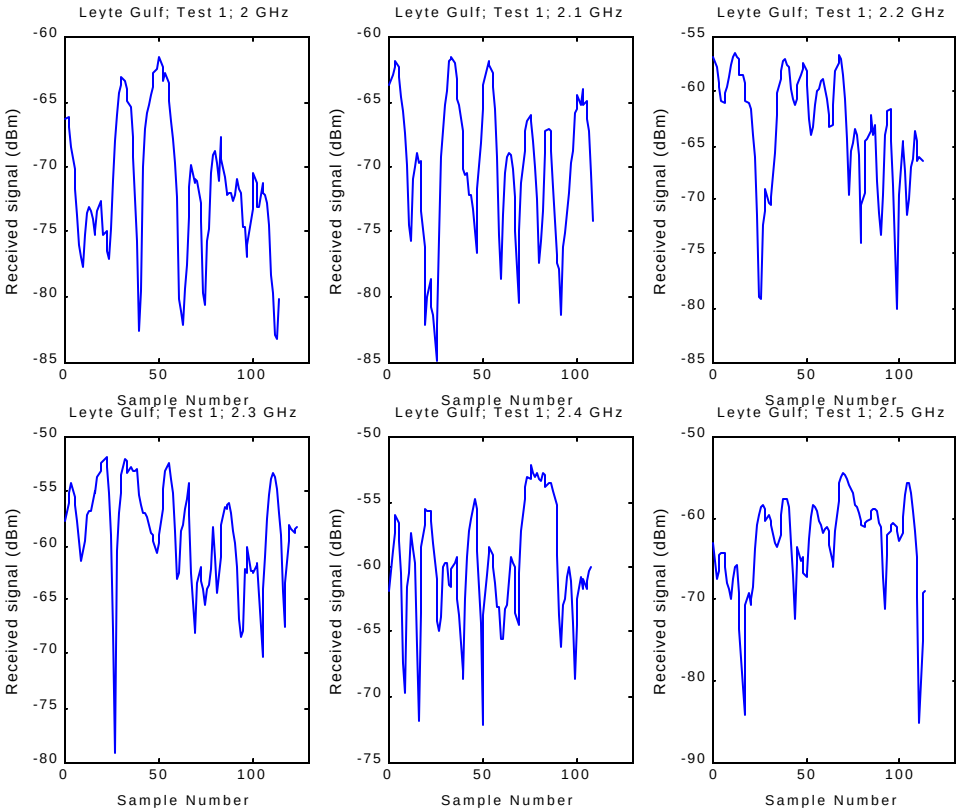
Leyte Gulf; Test 1; 2 GHz
Leyte Gulf; Test 1; 2.1 GHz
Leyte Gulf; Test 1; 2.2 GHz
Leyte Gulf; Test 1; 2.3 GHz
Leyte Gulf; Test 1; 2.4 GHz
Leyte Gulf; Test 1; 2.5 GHz
Received signal (dBm)
Sample Number

Table 12 Results From Test Aboard *USS Leyte Gulf.*

Frequency (GHz)	Max Power (dBm)	Ave Power (dBm)	Min Power (dBm)	Power STD (dBm)	Number Data Points	Max Error (dBm)	*K* Factor	*K* MSE
0.800	-68.9	-74.8	-96.4	5.7	121	0.52	0.0	0.001844
0.900	-57.2	-64.9	-73.9	4.2	111	0.40	0.0	0.011482
1.000	-54.3	-60.4	-79.0	5.3	114	0.50	0.9	0.000440
1.100	-57.9	-63.8	-89.5	6.4	112	0.60	0.0	0.002608
1.200	-54.5	-58.6	-76.3	3.8	118	0.35	2.4	0.000583
1.300	-60.4	-66.4	-82.3	4.7	112	0.44	0.0	0.001335
1.400	-62.6	-68.2	-86.6	5.7	111	0.54	0.0	0.002841
1.500	-63.1	-68.5	-86.4	5.0	114	0.46	1.0	0.000449
1.600	-61.9	-68.9	-85.9	4.1	111	0.39	2.2	0.000221
1.700	-67.6	-71.6	-86.6	4.0	109	0.38	2.3	0.002806
1.800	-66.7	-75.0	-96.3	4.5	111	0.43	0.0	0.000904
1.900	-67.4	-72.6	-93.4	5.5	111	0.52	0.0	0.003255
2.000	-61.4	-68.7	-83.2	5.2	114	0.49	0.0	0.004334
2.100	-61.6	-67.1	-84.9	5.6	109	0.54	0.0	0.002176
2.200	-56.4	-61.1	-80.2	5.4	112	0.51	1.2	0.002019
2.300	-51.8	-56.8	-79.2	4.7	124	0.42	1.3	0.000764
2.400	-52.1	-57.9	-72.1	4.4	108	0.43	0.0	0.001903
2.500	-54.5	-60.6	-85.2	5.6	114	0.52	1.1	0.000397

As there was only one measurement taken aboard the *Leyte Gulf*, no information about attenuation can be calculated. The mean square errors from the *K* estimations are almost all over 0.0005, the accepted measure of a good fit Ricean curve. This could be due to diffraction patterns or shadowing effects of objects in the communication path, or to the small number of data points in each measurement.

USS Carr

The *Carr* is a *Perry*-class frigate, the Navy's newest frigate class. Five tests were performed aboard the *Carr* (Fig. 27). The transmitter was placed on the deck in the Central Control Station (CCS) for all tests. The transmitter antenna height was 19 inches. It was positioned approximately in the center of the room, 30 inches from the propulsion control panel. During the tests, the receiver was positioned along the after bulkhead of CCS for one test, in the passageway between CCS and the Main Engine Room for two tests, and in the engine room for the final two. The receiver height was 38 inches for all tests. There was also another hatch into CCS, on the port side. This hatch led to another passageway, which connected directly to the one between CCS and the engine room. To allow crew access to CCS, this hatch remained open throughout the testing procedure.

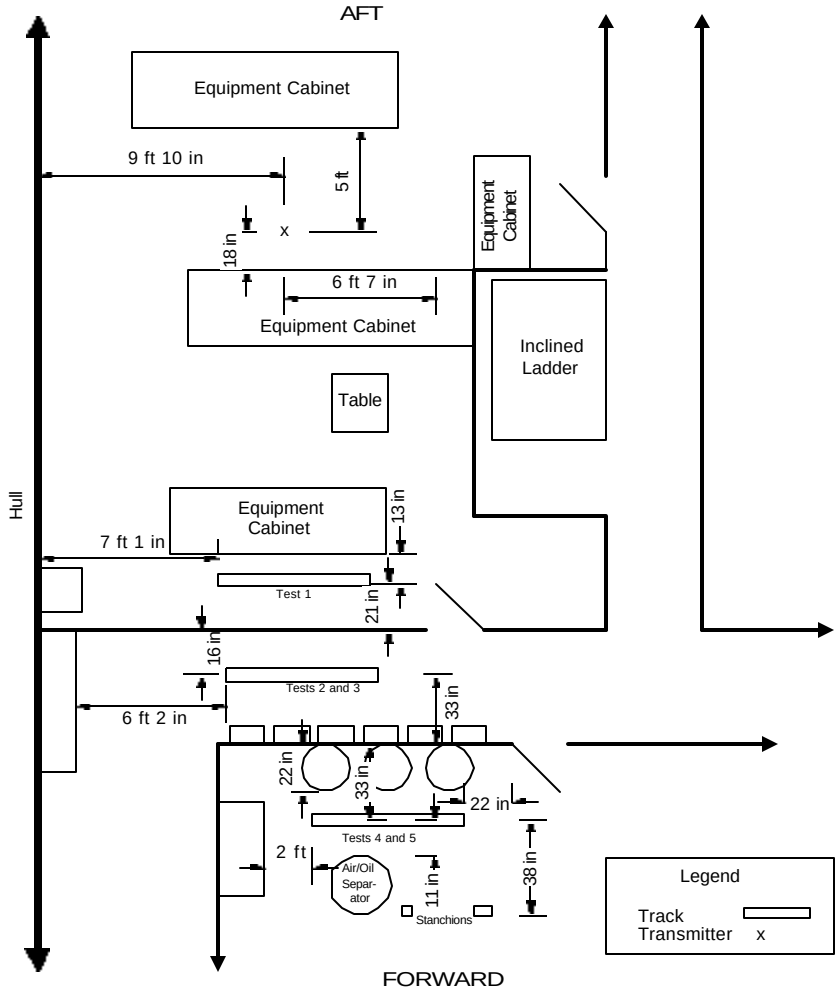

Figure 27 Test Layout Aboard *USS Carr*.

The first test was done with the receiver in CCS with the transmitter. There were two large cabinets of controls blocking the line-of-sight path between them. Once again, measurements were taken at increments of 100 MHz from 800 MHz to 2.5 GHz.

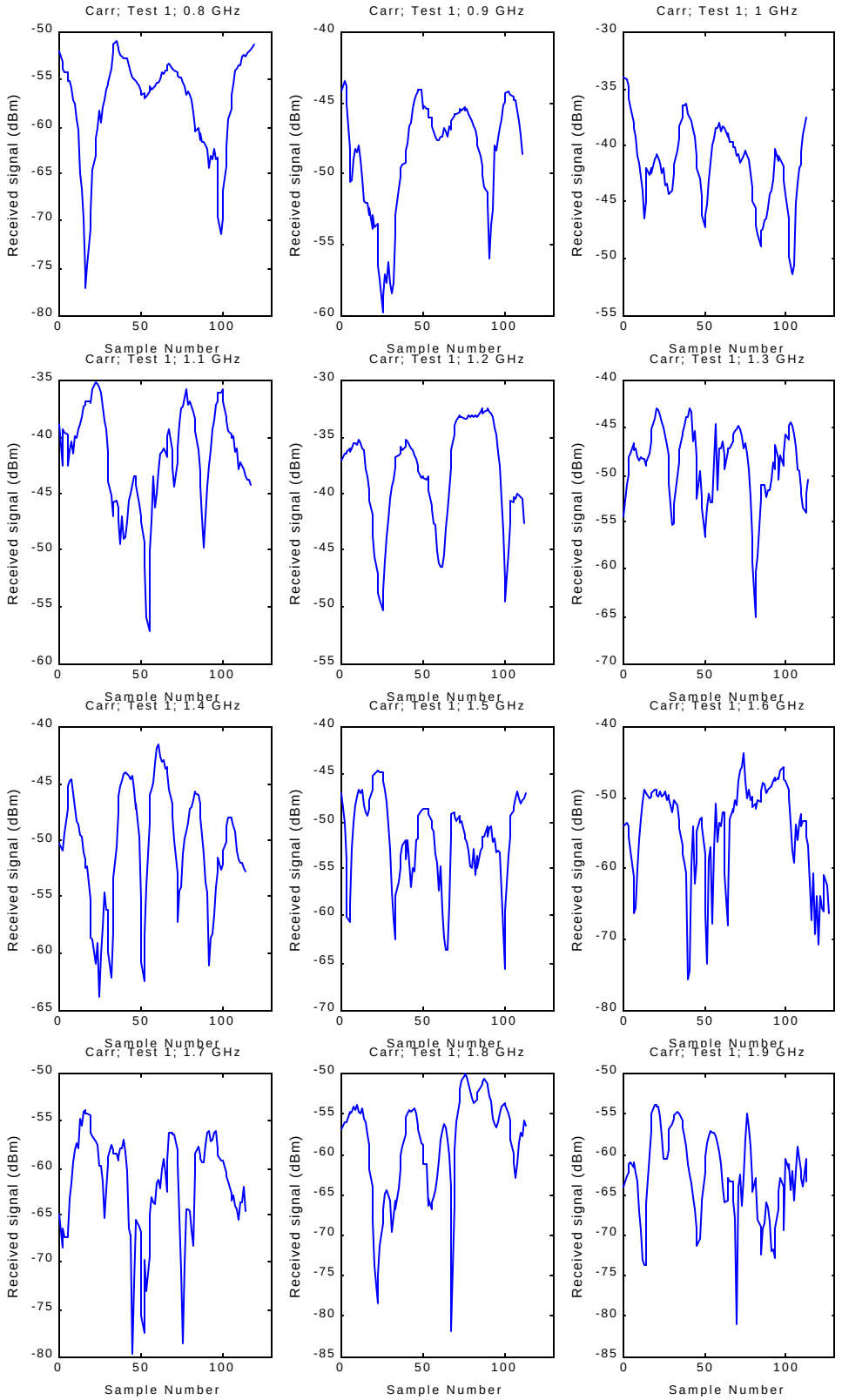
Carr; Test 1; 0.8 GHz
Carr; Test 1; 0.9 GHz
Carr; Test 1; 1 GHz
Carr; Test 1; 1.1 GHz
Carr; Test 1; 1.2 GHz
Carr; Test 1; 1.3 GHz
Carr; Test 1; 1.4 GHz
Carr; Test 1; 1.5 GHz
Carr; Test 1; 1.6 GHz
Carr; Test 1; 1.7 GHz
Carr; Test 1; 1.8 GHz
Carr; Test 1; 1.9 GHz
Received signal (dBm)
Sample Number

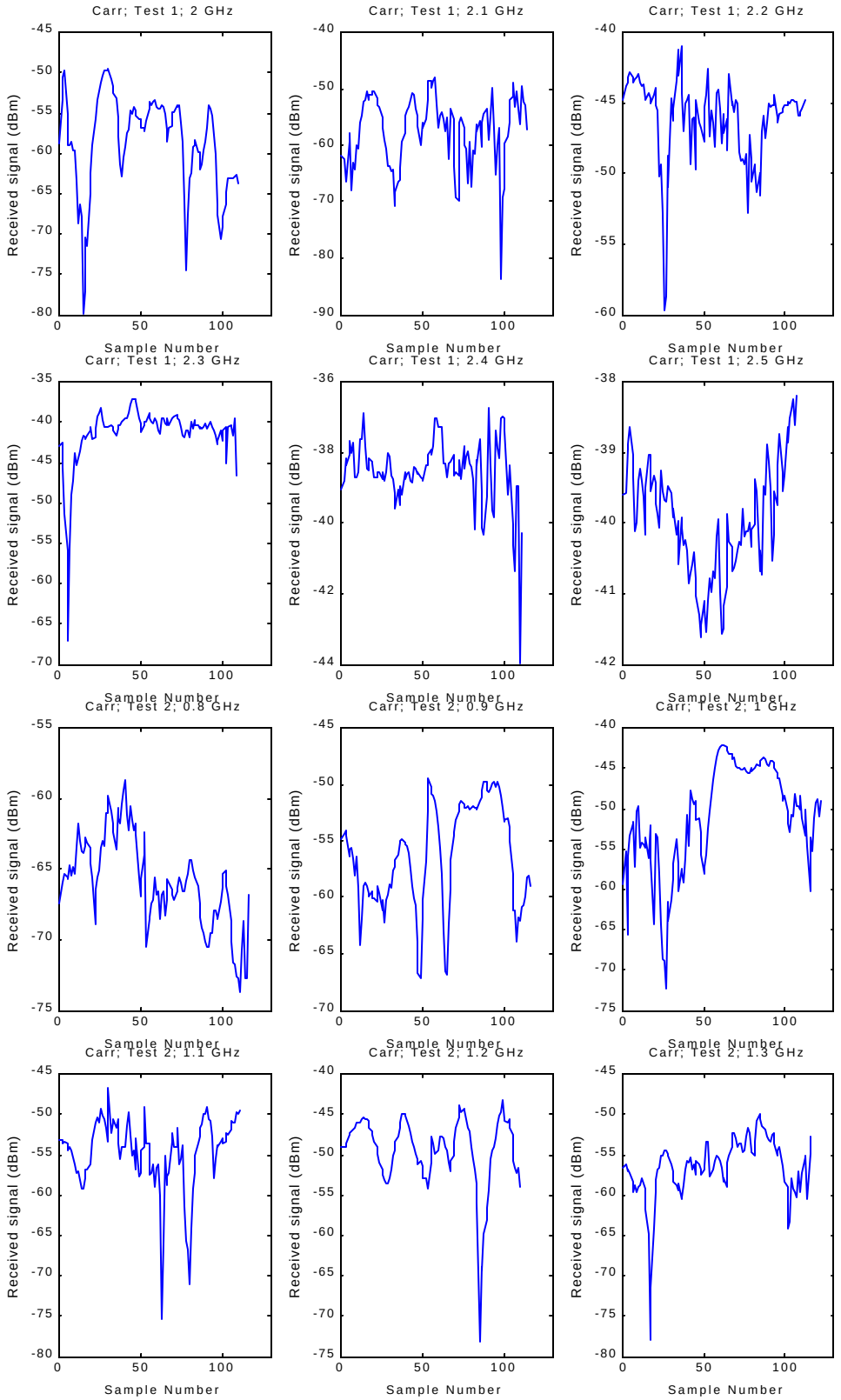
Carr; Test 1; 2 GHz
Carr; Test 1; 2.1 GHz
Carr; Test 1; 2.2 GHz
Carr; Test 1; 2.3 GHz
Carr; Test 1; 2.4 GHz
Carr; Test 1; 2.5 GHz
Carr; Test 2; 0.8 GHz
Carr; Test 2; 0.9 GHz
Carr; Test 2; 1 GHz
Carr; Test 2; 1.1 GHz
Carr; Test 2; 1.2 GHz
Carr; Test 2; 1.3 GHz
Received signal (dBm)
Sample Number

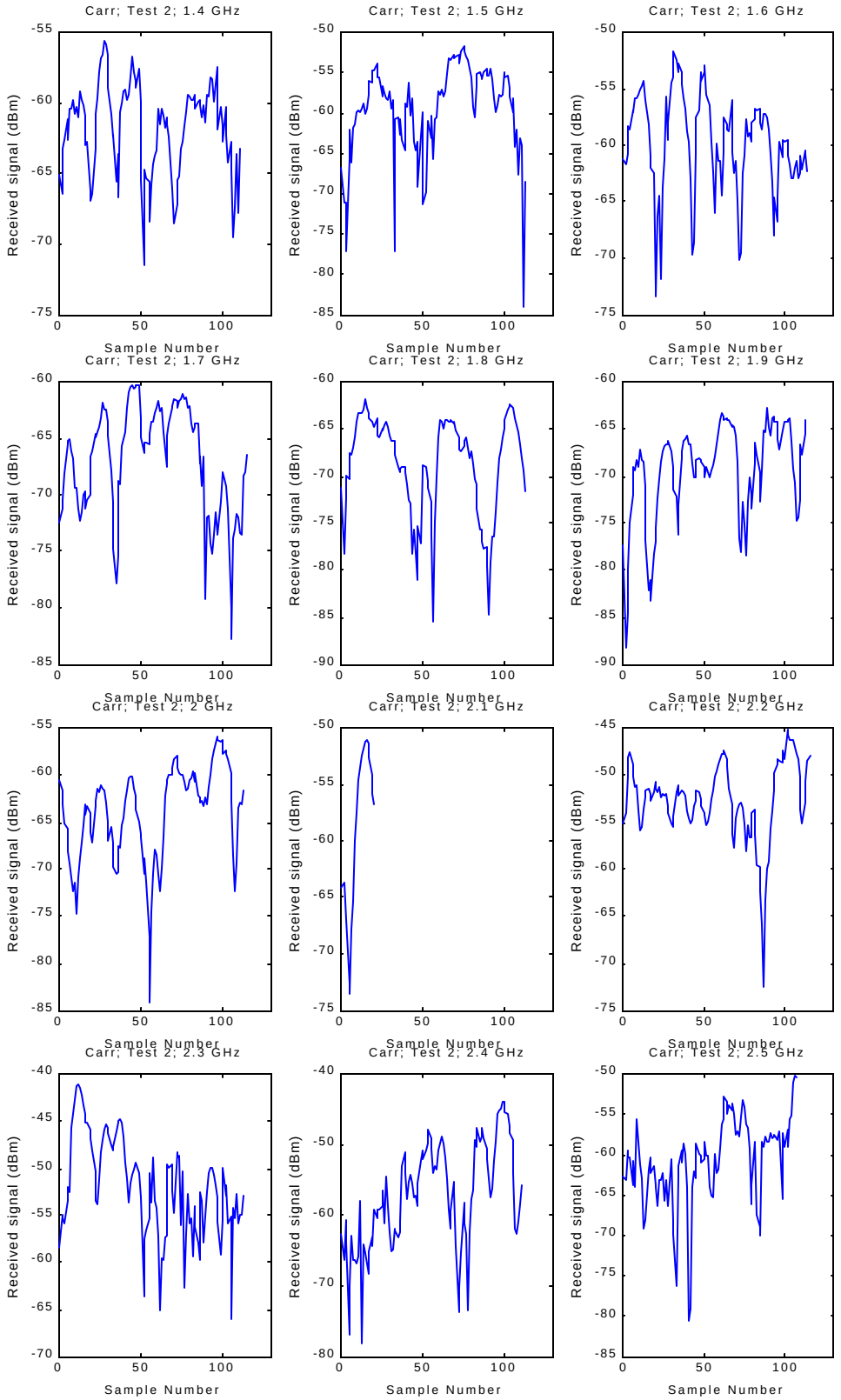
Carr; Test 2; 1.4 GHz
Carr; Test 2; 1.5 GHz
Carr; Test 2; 1.6 GHz
Carr; Test 2; 1.7 GHz
Carr; Test 2; 1.8 GHz
Carr; Test 2; 1.9 GHz
Carr; Test 2; 2 GHz
Carr; Test 2; 2.1 GHz
Carr; Test 2; 2.2 GHz
Carr; Test 2; 2.3 GHz
Carr; Test 2; 2.4 GHz
Carr; Test 2; 2.5 GHz
Received signal (dBm)
Sample Number

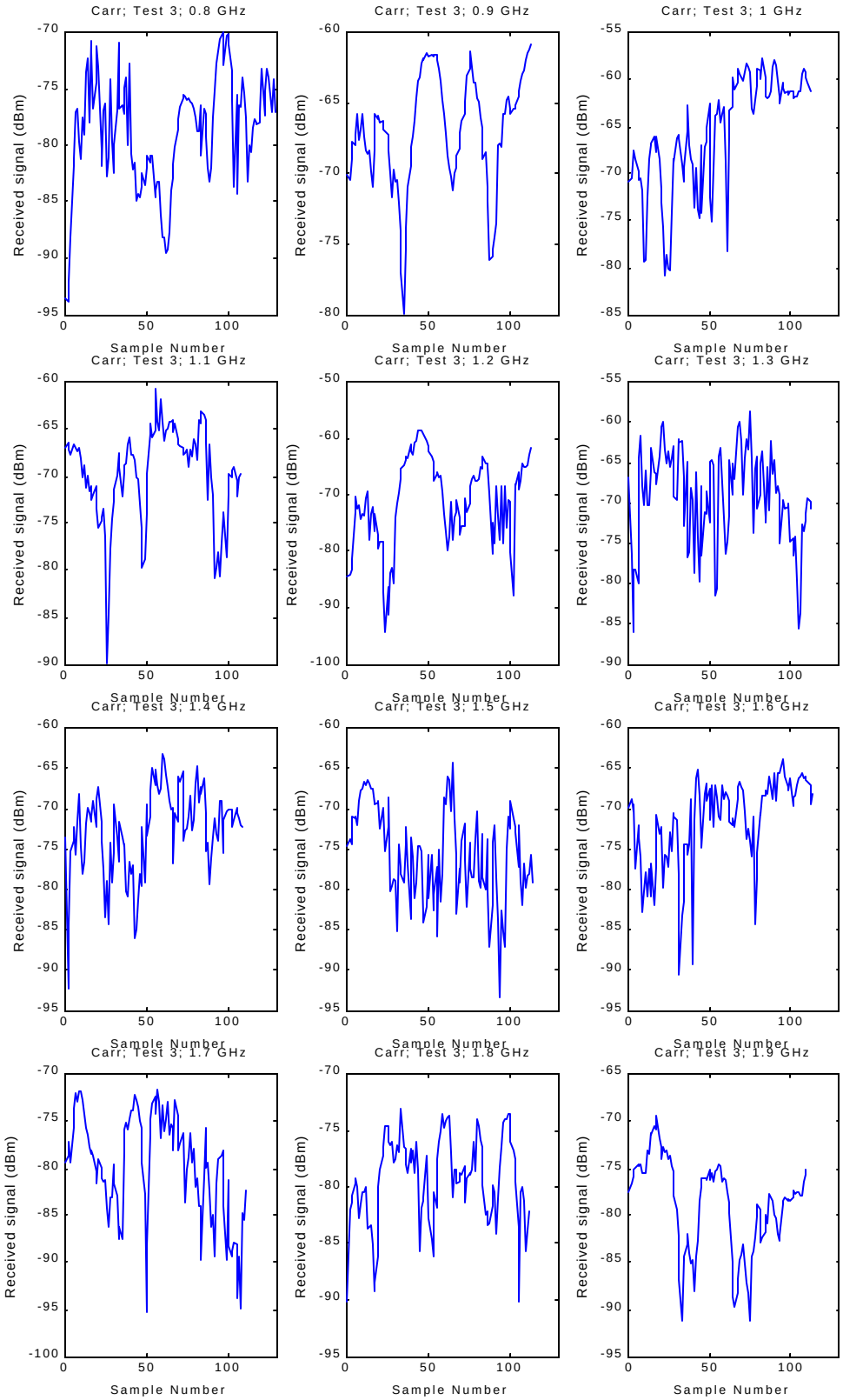
Carr; Test 3; 0.8 GHz
Carr; Test 3; 0.9 GHz
Carr; Test 3; 1 GHz
Carr; Test 3; 1.1 GHz
Carr; Test 3; 1.2 GHz
Carr; Test 3; 1.3 GHz
Carr; Test 3; 1.4 GHz
Carr; Test 3; 1.5 GHz
Carr; Test 3; 1.6 GHz
Carr; Test 3; 1.7 GHz
Carr; Test 3; 1.8 GHz
Carr; Test 3; 1.9 GHz
Received signal (dBm)
Sample Number

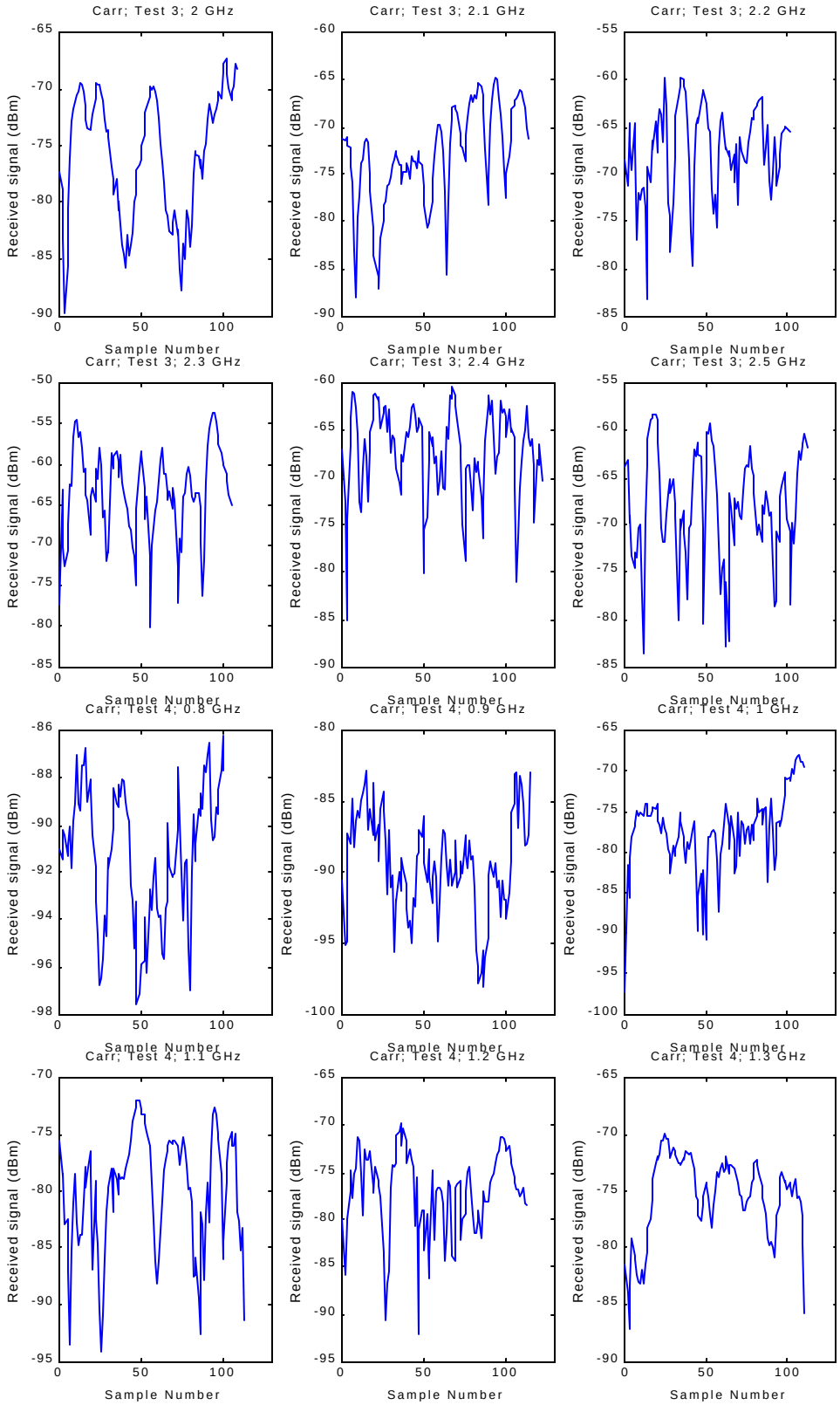
Carr; Test 3; 2 GHz
Carr; Test 3; 2.1 GHz
Carr; Test 3; 2.2 GHz
Carr; Test 3; 2.3 GHz
Carr; Test 3; 2.4 GHz
Carr; Test 3; 2.5 GHz
Carr; Test 4; 0.8 GHz
Carr; Test 4; 0.9 GHz
Carr; Test 4; 1 GHz
Carr; Test 4; 1.1 GHz
Carr; Test 4; 1.2 GHz
Carr; Test 4; 1.3 GHz
Received signal (dBm)
Sample Number

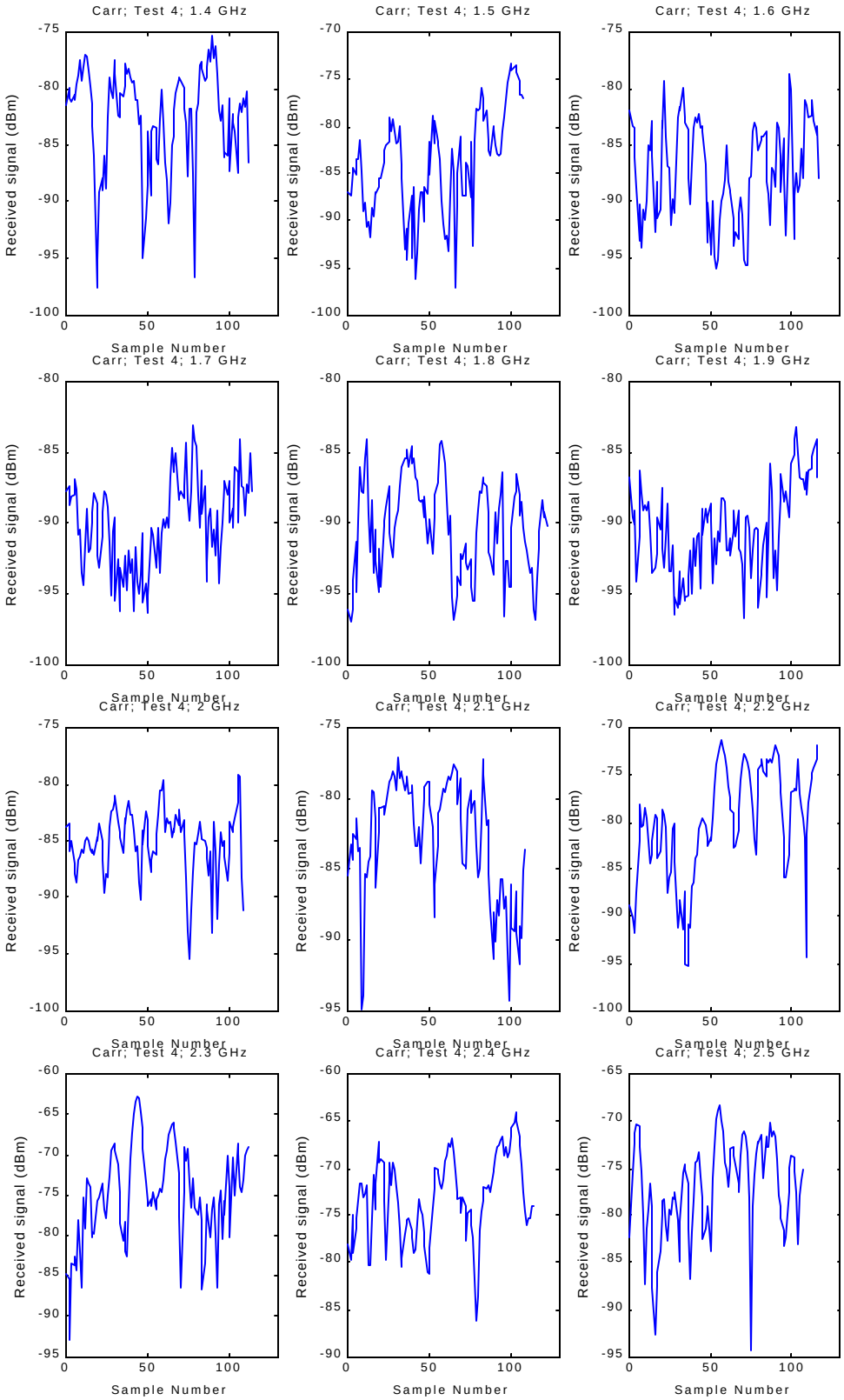
Carr; Test 4; 1.4 GHz
Carr; Test 4; 1.5 GHz
Carr; Test 4; 1.6 GHz
Carr; Test 4; 1.7 GHz
Carr; Test 4; 1.8 GHz
Carr; Test 4; 1.9 GHz
Carr; Test 4; 2 GHz
Carr; Test 4; 2.1 GHz
Carr; Test 4; 2.2 GHz
Carr; Test 4; 2.3 GHz
Carr; Test 4; 2.4 GHz
Carr; Test 4; 2.5 GHz
Received signal (dBm)
Sample Number

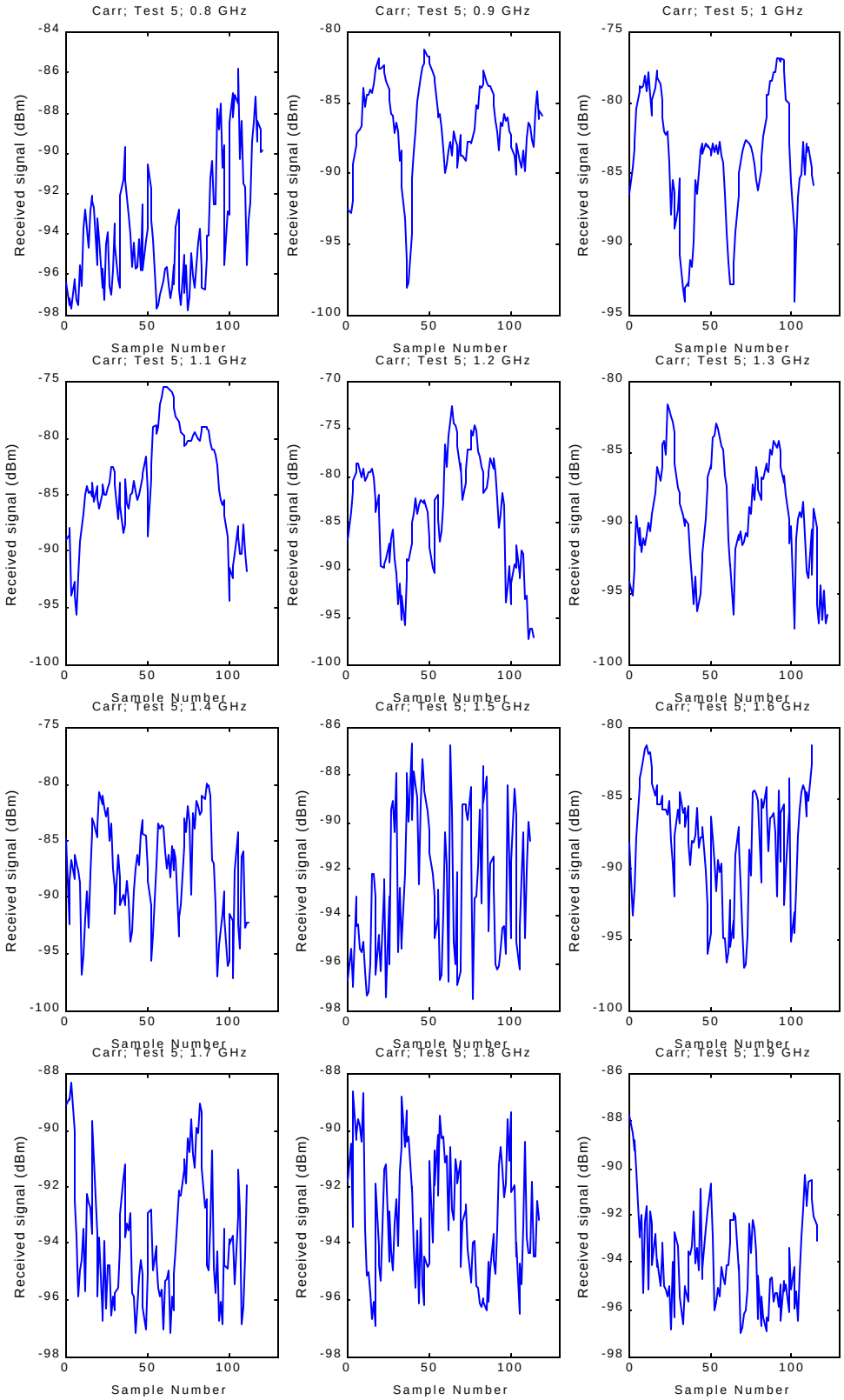
Carr; Test 5; 0.8 GHz
Carr; Test 5; 0.9 GHz
Carr; Test 5; 1 GHz
Carr; Test 5; 1.1 GHz
Carr; Test 5; 1.2 GHz
Carr; Test 5; 1.3 GHz
Carr; Test 5; 1.4 GHz
Carr; Test 5; 1.5 GHz
Carr; Test 5; 1.6 GHz
Carr; Test 5; 1.7 GHz
Carr; Test 5; 1.8 GHz
Carr; Test 5; 1.9 GHz
Received signal (dBm)
Sample Number

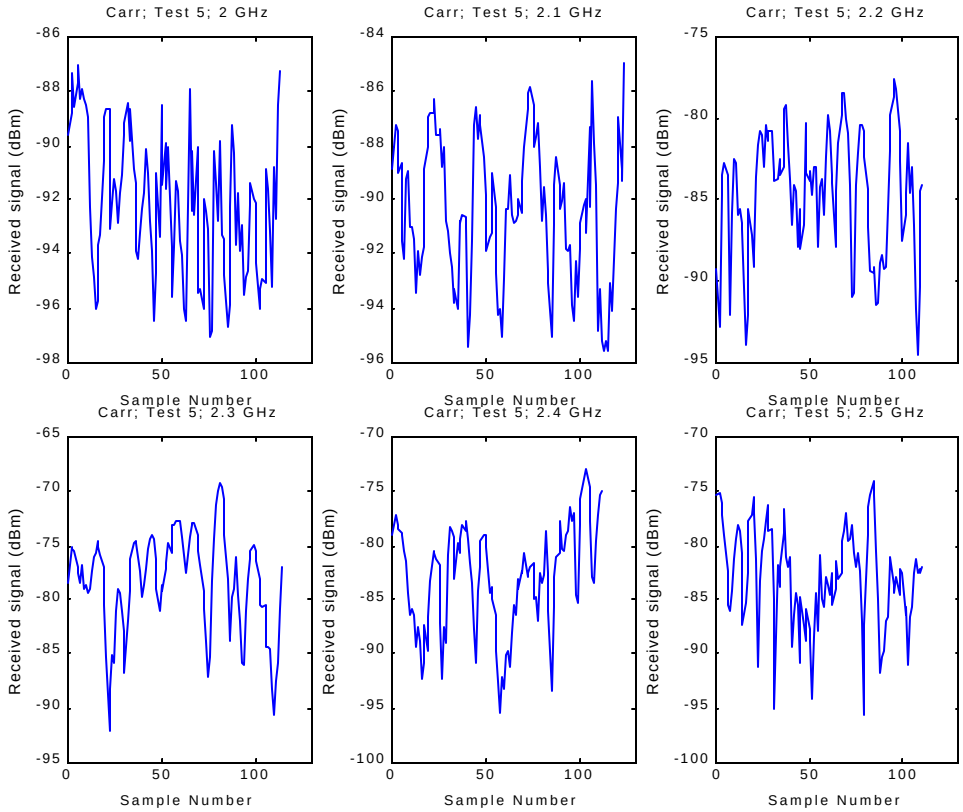

Table 13 Results from Test 1 Aboard *USS Carr*.

Frequency (GHz)	Max Power (dBm)	Ave Power (dBm)	Min Power (dBm)	Power STD (dBm)	Number Data Points	Max Error (dBm)	*K* Factor	*K* MSE
0.800	-50.9	-55.5	-77.1	5.6	119	0.51	1.6	0.002322
0.900	-43.4	-47.3	-59.8	4.0	111	0.38	2.0	0.002618
1.000	-34.1	-40.5	-51.5	3.6	112	0.34	2.1	0.000894
1.100	-35.1	-40.0	-57.2	4.4	117	0.41	1.3	0.000772
1.200	-32.5	-36.6	-50.3	4.6	112	0.44	1.4	0.003260
1.300	-42.9	-47.5	-65.0	4.0	114	0.37	1.9	0.000349
1.400	-41.6	-48.0	-63.8	5.4	114	0.50	0.0	0.000825
1.500	-44.5	-50.1	-65.8	4.6	113	0.43	1.3	0.000262
1.600	-43.6	-51.3	-75.8	6.9	126	0.61	0.0	0.001796
1.700	-53.8	-59.5	-79.8	5.3	114	0.50	1.1	0.000720
1.800	-50.0	-55.7	-81.8	6.2	113	0.59	0.9	0.001670
1.900	-53.8	-60.1	-81.1	5.3	113	0.50	0.0	0.001416
2.000	-49.3	-55.8	-79.8	6.1	110	0.58	0.0	0.000854
2.100	-48.0	-54.5	-83.6	6.1	114	0.57	0.0	0.000808
2.200	-41.0	-45.5	-59.7	2.9	112	0.28	3.7	0.001103
2.300	-37.1	-40.6	-67.1	3.8	109	0.37	5.2	0.002364
2.400	-36.7	-38.4	-44.0	1.0	111	0.09	12.3	0.000915
2.500	-38.2	-39.9	-41.6	0.8	107	0.08	10.1	0.000423

The second test aboard the *Carr* was performed with the receiver in the passageway between CCS and the engine room. For this test, the after CCS Hatch was open. It should be noted that the measurement at 2.1 GHz in this test recorded only 21 data points.

Table 14 Results from Test 2 Aboard *USS Carr*.

Frequency (GHz)	Max Power (dBm)	Ave Power (dBm)	Min Power (dBm)	Power STD (dBm)	Number Data Points	Max Error (dBm)	*K* Factor	*K* MSE
0.800	-58.6	-64.7	-73.7	3.2	116	0.30	2.3	0.002143
0.900	-49.5	-54.4	-67.1	4.5	116	0.42	0.0	0.002266
1.000	-42.0	-47.7	-72.3	6.5	122	0.59	0.0	0.004490
1.100	-46.7	-53.2	-75.3	4.4	111	0.42	2.3	0.000313
1.200	-43.1	-48.0	-73.0	4.4	110	0.42	2.2	0.000382
1.300	-49.8	-55.5	-77.9	3.8	116	0.35	2.6	0.000481
1.400	-55.5	-60.8	-71.4	3.2	111	0.30	2.5	0.000587
1.500	-51.7	-57.3	-84.1	5.6	113	0.52	1.4	0.000410
1.600	-51.7	-58.0	-73.3	4.4	114	0.41	1.3	0.000560
1.700	-60.3	-65.0	-82.8	4.8	115	0.45	1.2	0.001728
1.800	-61.9	-66.6	-85.4	5.3	113	0.49	1.4	0.002412
1.900	-62.7	-67.5	-88.2	5.1	113	0.48	1.6	0.001200
2.000	-55.8	-61.9	-84.2	5.0	113	0.47	1.1	0.000483
2.100	-51.0	-55.3	-73.5	7.4	21	1.62	0.0	0.016831
2.200	-45.2	-51.1	-72.5	4.1	115	0.38	2.0	0.001378
2.300	-41.1	-49.0	-66.0	5.2	113	0.49	0.0	0.002176
2.400	-43.9	-52.4	-78.0	7.4	111	0.70	0.0	0.006679
2.500	-50.2	-58.3	-80.6	5.3	107	0.51	0.0	0.000505

The small number of data points recorded during the measurement at 2.1 GHz led to a large error value and *K* factor MSE.

The receiver was left in place for the third test, but the after CCS hatch was shut.

Table 15 Results from Test 3 Aboard *USS Carr*.

Frequency (GHz)	Max Power (dBm)	Ave Power (dBm)	Min Power (dBm)	Power STD (dBm)	Number Data Points	Max Error (dBm)	*K* Factor	*K* MSE
0.800	-70.0	-76.4	-93.8	5.0	129	0.44	0.0	0.000719
0.900	-60.9	-65.5	-79.9	4.0	113	0.37	1.6	0.001008
1.000	-57.8	-62.9	-80.8	5.9	112	0.56	0.0	0.003935
1.100	-60.7	-67.8	-89.8	5.0	108	0.48	1.5	0.000210
1.200	-58.5	-66.4	-94.2	7.7	113	0.72	0.0	0.004938
1.300	-58.7	-66.2	-85.9	5.9	113	0.55	0.0	0.000932
1.400	-63.2	-70.4	-92.4	5.2	109	0.49	0.0	0.000228
1.500	-64.2	-72.5	-93.3	5.6	114	0.52	0.0	0.001731
1.600	-63.7	-69.3	-90.4	5.3	114	0.50	1.3	0.001000
1.700	-71.7	-77.1	-95.3	5.5	111	0.53	0.0	0.001319
1.800	-73.0	-77.9	-90.3	3.8	112	0.36	1.4	0.000546
1.900	-69.5	-76.7	-91.1	4.8	110	0.46	0.0	0.000586
2.000	-67.4	-73.2	-89.8	5.5	109	0.53	0.0	0.003040
2.100	-64.9	-70.7	-88.0	5.2	114	0.48	0.0	0.001172
2.200	-59.8	-65.5	-83.2	4.6	101	0.45	1.3	0.000206
2.300	-53.7	-60.8	-80.1	5.6	105	0.54	0.0	0.001024
2.400	-60.3	-65.4	-85.2	4.6	122	0.42	1.5	0.000502
2.500	-58.2	-65.1	-83.5	5.7	112	0.54	0.0	0.001921

The fourth test was performed with the receiver in the engine room and with the engine room hatch open. The CCS hatch remained shut.

Table 16 Results from Test 4 Aboard *USS Carr*.

Frequency (GHz)	Max Power (dBm)	Ave Power (dBm)	Min Power (dBm)	Power STD (dBm)	Number Data Points	Max Error (dBm)	*K* Factor	*K* MSE
0.800	-70.0	-76.4	-93.8	5.0	129	0.44	1.7	0.000439
0.900	-60.9	-65.5	-79.9	4.0	113	0.37	0.0	0.001561
1.000	-57.8	-62.9	-80.8	5.9	112	0.56	0.0	0.002512
1.100	-60.7	-67.8	-89.8	5.0	108	0.48	0.0	0.000629
1.200	-58.5	-66.4	-94.2	7.7	113	0.72	1.6	0.000236
1.300	-58.7	-66.2	-85.9	5.9	113	0.55	2.1	0.000743
1.400	-63.2	-70.4	-92.4	5.2	109	0.49	1.8	0.000396
1.500	-64.2	-72.5	-93.3	5.6	114	0.52	0.0	0.002376
1.600	-63.7	-69.3	-90.4	5.3	114	0.50	0.0	0.001702
1.700	-71.7	-77.1	-95.3	5.5	111	0.53	2.6	0.001846
1.800	-73.0	-77.9	-90.3	3.8	112	0.36	0.0	0.001035
1.900	-69.5	-76.7	-91.1	4.8	110	0.46	2.5	0.002638
2.000	-67.4	-73.2	-89.8	5.5	109	0.53	3.4	0.000362
2.100	-64.9	-70.7	-88.0	5.2	114	0.48	1.6	0.001662
2.200	-59.8	-65.5	-83.2	4.6	101	0.45	0.0	0.002525
2.300	-53.7	-60.8	-80.1	5.6	105	0.54	0.0	0.002379
2.400	-60.3	-65.4	-85.2	4.6	122	0.42	0.0	0.000518
2.500	-58.2	-65.1	-83.5	5.7	112	0.54	0.0	0.000232

Finally, for the fifth test, the receiver remained in the same place, but the engine room hatch was shut.

Table 17 Results from Test 5 Aboard *USS Carr*.

Frequency (GHz)	Max Power (dBm)	Ave Power (dBm)	Min Power (dBm)	Power STD (dBm)	Number Data Points	Max Error (dBm)	*K* Factor	*K* MSE
0.800	-86.2	-90.4	-97.6	2.8	101	0.28	2.9	0.012107
0.900	-82.7	-88.1	-98.0	3.5	115	0.32	2.5	0.000863
1.000	-67.9	-75.2	-97.3	4.9	111	0.46	0.0	0.001802
1.100	-72.0	-77.7	-94.1	5.1	113	0.48	0.0	0.001734
1.200	-69.9	-75.5	-92.2	4.3	113	0.41	0.0	0.002306
1.300	-69.9	-74.3	-87.1	3.7	111	0.35	0.0	0.001272
1.400	-75.3	-80.9	-97.6	4.5	112	0.43	0.0	0.000634
1.500	-73.2	-80.9	-97.0	5.4	108	0.52	0.0	0.006077
1.600	-78.7	-85.3	-96.0	4.3	117	0.40	1.3	0.000946
1.700	-83.1	-89.0	-96.4	3.1	114	0.29	3.8	0.007445
1.800	-84.0	-89.1	-96.9	3.3	122	0.30	3.3	0.003880
1.900	-83.1	-89.4	-96.8	3.1	116	0.29	4.4	0.004731
2.000	-79.1	-84.3	-95.4	2.8	109	0.27	2.7	0.003218
2.100	-77.0	-81.3	-94.9	4.2	109	0.40	2.9	0.001953
2.200	-71.3	-77.2	-95.4	5.8	116	0.54	1.7	0.000556
2.300	-62.9	-71.6	-93.0	5.8	112	0.54	1.4	0.000422
2.400	-64.0	-71.1	-86.2	4.4	114	0.41	0.0	0.000480
2.500	-68.4	-74.8	-94.3	5.1	107	0.49	0.0	0.000653

To determine the effects of the CCS and engine room bulkheads and the hatches in each, we compare the results from different tests. The effect of moving the receiver from CCS to the passageway is the difference between tests 1 and 2.

Table 18 Test 2 Compared to Test 1.

Frequency (GHz)	Power Loss (dBm)	Power St. Dev. (dBm)	Error Val (dBm)
0.80	9.2	4.57	0.81
0.90	7.1	4.26	0.80
1.00	7.2	5.29	0.92
1.10	13.2	4.42	0.83
1.20	11.5	4.53	0.86
1.30	7.9	3.90	0.73
1.40	12.8	4.42	0.80
1.50	7.2	5.11	0.96
1.60	6.8	5.85	1.03
1.70	5.5	5.08	0.95
1.80	10.9	5.77	1.08
1.90	7.4	5.17	0.97
2.00	6.1	5.55	1.05
2.10	0.8	6.34	2.19
2.20	5.7	3.59	0.66
2.30	8.4	4.56	0.85
2.40	14.0	5.28	0.79
2.50	18.4	3.78	0.59

Average Loss (dBm) 8.89

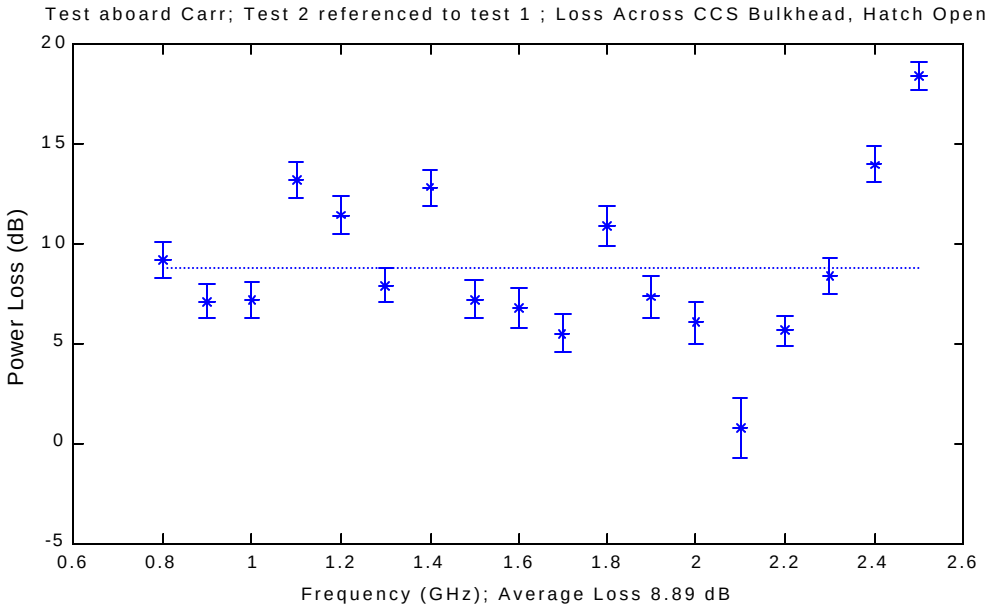

Figure 28 Attenuation Due to CCS Bulkhead With Hatch Open.

This shows that there was approximately 10 dB of loss associated with moving the receiver from CCS to the outside of CCS (Fig. 28). This is less attenuation than

encountered aboard the *Ross*. This may be because the propagation path varied greatly between measurements aboard the *Ross*, due to the hatch being far removed from the direct path to the transmitter, whereas the paths on the *Carr* were only slightly different, due to the hatch being close to the direct path to the transmitter.

When the hatch was closed, an obstacle was placed in this path. While it has already been shown that electromagnetic energy does pass through shut hatches, this arrangement was very similar to that performed aboard the *Ross*—the most direct path from the transmitter to the receiver had a bulkhead attenuating the signal, whereas there was another path, which relied on multipath propagation but was unobstructed. Therefore, it is to be expected that the difference between tests 1 and 3 on the *Carr* should be very close to the difference between tests 4 and 1 on the *Ross*. This is, in fact, the case.

Table 19 Test 3 Compared to Test 1.

Frequency (GHz)	Power Loss (dBm)	Power St. Dev. (dBm)	Error Val (dBm)
0.80	20.8	5.29	0.95
0.90	18.2	4.00	0.76
1.00	22.5	4.88	0.90
1.10	27.8	4.71	0.89
1.20	29.8	6.33	1.16
1.30	18.6	5.03	0.93
1.40	22.4	5.27	1.00
1.50	22.5	5.11	0.96
1.60	18.1	6.19	1.11
1.70	17.7	5.43	1.02
1.80	22.2	5.18	0.95
1.90	16.6	5.06	0.96
2.00	17.3	5.79	1.10
2.10	16.1	5.67	1.06
2.20	20.0	3.79	0.73
2.30	20.2	4.76	0.91
2.40	27.0	3.43	0.51
2.50	25.2	4.12	0.62

Average Loss (dBm) 21.3

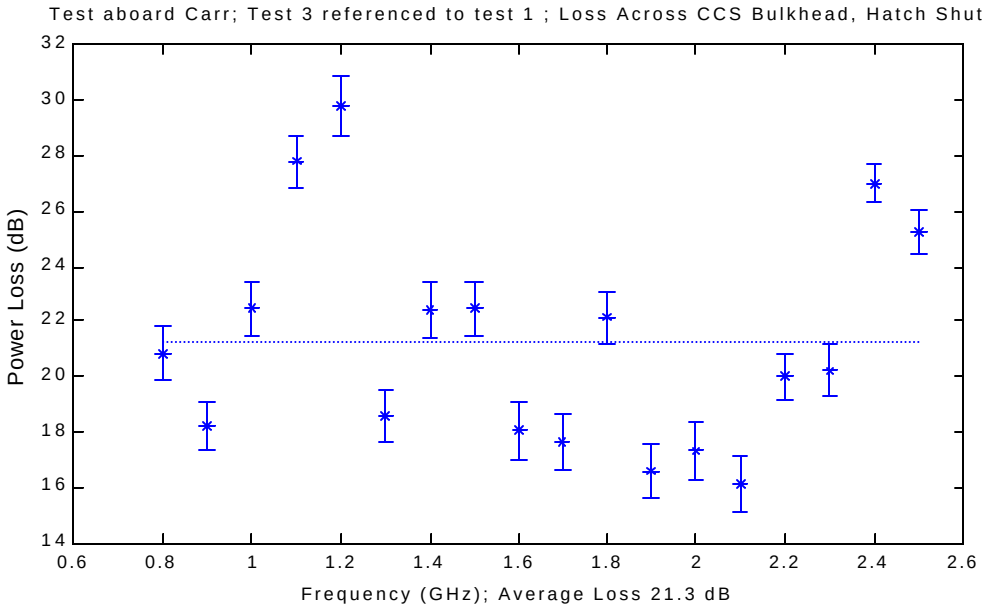

Figure 29 Attenuation Due to CCS Bulkhead With Hatch Closed.

The average attenuation due to the bulkhead on the *Carr* was 21.3 dB (Fig. 29), whereas it was 20.9 dB on the *Ross*. Therefore, in these two cases, placing the receiver such that the electromagnetic waves have an open, but not direct, path from the transmitter yields a signal power approximately 20 dB lower than that received within the same compartment as the transmitter.

Table 20 Test 3 Compared to Test 2.

Frequency (GHz)	Power Loss (dBm)	Power St. Dev. (dBm)	Error Val (dBm)
0.80	11.7	4.23	0.73
0.90	11.1	4.24	0.79
1.00	15.3	6.21	1.14
1.10	14.6	4.70	0.90
1.20	18.3	6.27	1.14
1.30	10.7	4.94	0.91
1.40	9.6	4.28	0.80
1.50	15.3	5.56	1.04
1.60	11.3	4.89	0.91
1.70	12.1	5.18	0.97
1.80	11.3	4.59	0.85
1.90	9.3	4.95	0.94
2.00	11.3	5.25	1.00
2.10	15.4	5.58	2.10
2.20	14.3	4.33	0.84
2.30	11.8	5.36	1.03
2.40	13.0	6.12	1.12
2.50	6.8	5.51	1.05

Average Loss (dBm) 12.4

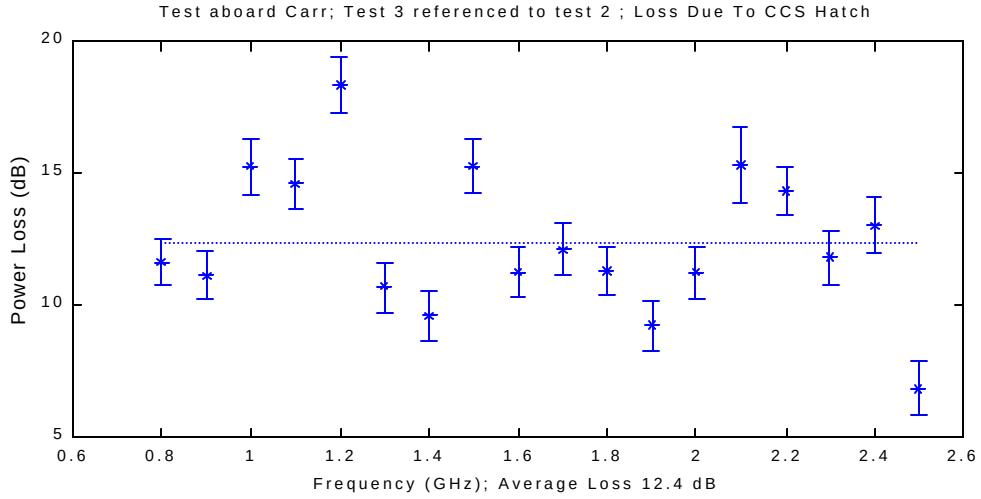

Figure 30 Loss Due to Shutting CCS Hatch.

Shutting the CCS Hatch caused 12.4 dB loss in signal power at the receiver (Fig. 30).

When the receiver was moved again from the passageway to the engine room without shutting the hatch, it could be expected that the power loss would be similar to that encountered when the receiver was moved from CCS into the passageway. The results were similar, but slightly different.

Table 21 Test 4 Compared to Test 3.

Frequency (GHz)	Power Loss (dBm)	Power St. Dev. (dBm)	Error Val (dBm)
0.80	14.0	4.18	0.72
0.90	22.6	3.73	0.70
1.00	12.2	5.41	1.02
1.10	10.0	5.04	0.96
1.20	9.1	6.22	1.13
1.30	8.1	4.91	0.90
1.40	10.6	4.85	0.92
1.50	8.4	5.49	1.04
1.60	16.0	4.84	0.90
1.70	11.9	4.45	0.81
1.80	11.2	3.57	0.66
1.90	12.6	4.03	0.75
2.00	11.2	4.37	0.80
2.10	10.6	4.72	0.89
2.20	11.7	5.28	0.99
2.30	10.7	5.67	1.09
2.40	5.7	4.53	0.83
2.50	9.7	5.41	1.03

Average Loss (dBm) 11.5

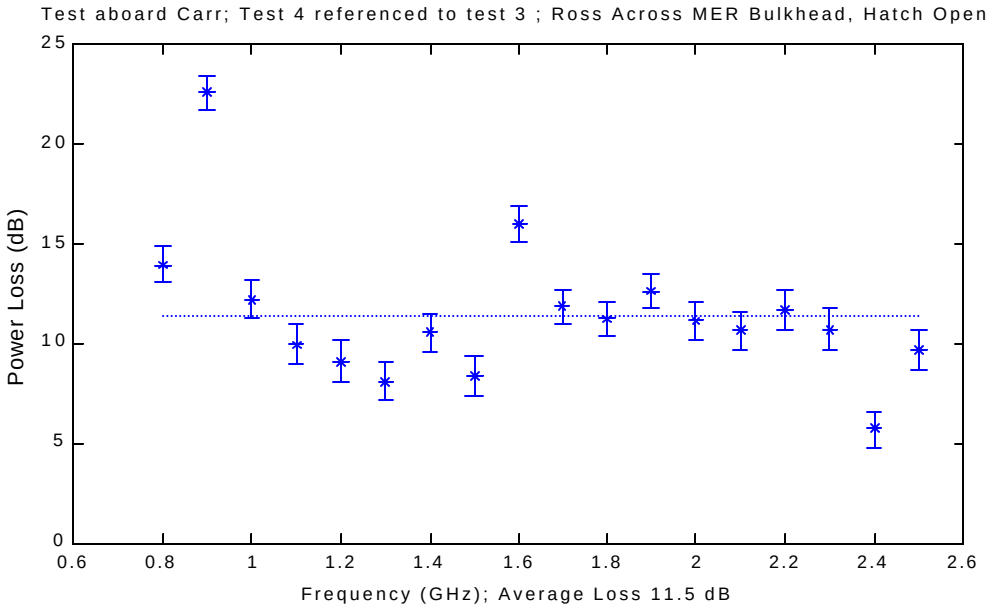

Figure 31 Attenuation Due to Engine Room Bulkhead With Hatch Open.

The power loss associated with moving from CCS to the passageway was 8.9 dB. However, the loss due to moving the receiver into the engine room was 11.5 dB (Fig. 31), a difference of 2.6 dB. This can be accounted for by the geometry of the surrounding equipment. In the passageway, the receiver was located in front of another bulkhead, which provided a surface that could reflect electromagnetic waves back towards the antenna. In the engine room, however, there was only empty space or irregularly shaped equipment behind the receiver. Also, the open CCS hatch did not block the path from CCS to the receiver in the passageway, whereas the open engine room hatch was positioned directly between the passageway and the receiver.

For test five, the receiver remained in the engine room, but the hatch was shut.

Table 22 Test 5 Compared to Test 3.

Frequency (GHz)	Power Loss (dBm)	Power St. Dev. (dBm)	Error Val (dBm)
0.80	16.1	4.16	0.72
0.90	20.2	3.60	0.67
1.00	19.1	5.23	0.98
1.10	13.9	4.87	0.93
1.20	14.4	6.85	1.28
1.30	21.6	4.99	0.91
1.40	15.2	4.79	0.91
1.50	19.1	4.49	0.81
1.60	17.2	4.70	0.87
1.70	16.0	4.23	0.74
1.80	14.6	3.07	0.56
1.90	16.6	3.67	0.65
2.00	18.2	4.26	0.77
2.10	19.0	4.03	0.71
2.20	17.7	4.17	0.81
2.30	15.6	5.09	0.97
2.40	15.1	4.79	0.89
2.50	15.7	5.16	0.97

Average Loss (dBm) 17.0

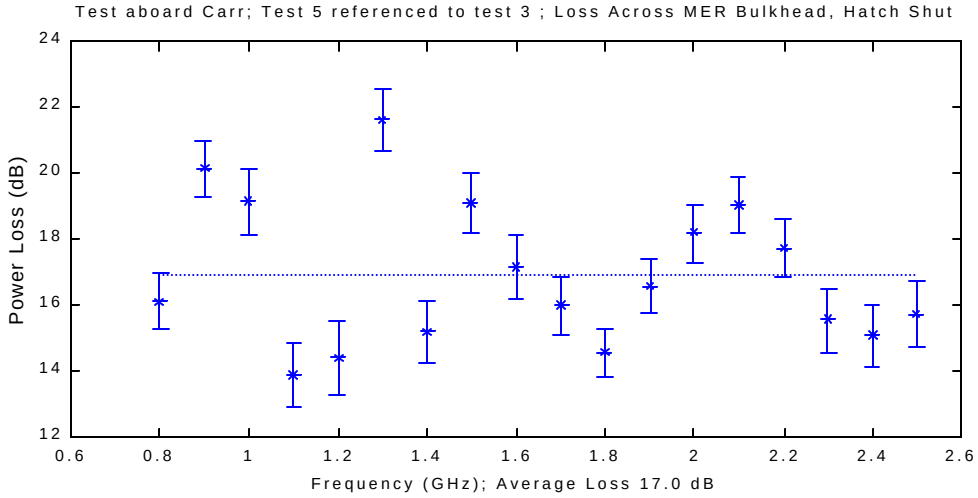

Figure 32. Attenuation Due to MER Bulkhead With Hatch Shut.

The signal loss across the engine room bulkhead was 17.0 dB with the hatch shut (Fig. 32).

Comparing test five to test four shows the attenuation associated with shutting the hatch.

Table 23 Test 5 Compared to Test 4.

Frequency (GHz)	Power Loss (dBm)	Power St. Dev. (dBm)	Error Val (dBm)
0.80	2.2	2.96	0.56
0.90	-2.5	3.34	0.62
1.00	6.9	4.66	0.88
1.10	3.9	4.92	0.93
1.20	5.3	5.21	0.97
1.30	13.5	3.83	0.71
1.40	4.6	4.46	0.84
1.50	10.8	4.36	0.81
1.60	1.2	4.15	0.77
1.70	4.1	2.69	0.50
1.80	3.3	2.81	0.50
1.90	4.0	2.60	0.47
2.00	7.0	2.70	0.51
2.10	8.4	3.42	0.63
2.20	6.0	4.94	0.90
2.30	4.8	5.21	0.98
2.40	9.4	4.68	0.88
2.50	6.1	4.81	0.92

Average Loss (dBm) 5.50

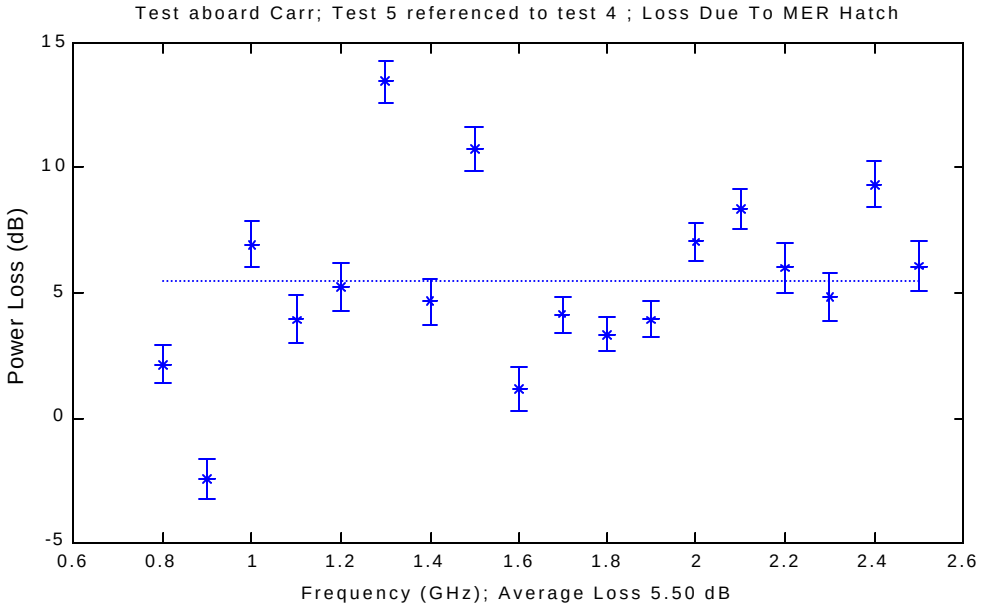

Figure 33 Loss Due to Shutting Engine Room Hatch.

When the engine room hatch was shut, there was a 5.5 dB drop in signal power (Fig. 33).

To investigate the general effect of the channel on frequency, the difference between measured attenuation at each frequency and the average attenuation of each attenuation calculation was found for each attenuation calculation. These differences between measured and average attenuation were then averaged over all measurements, to yield the *average difference between measured attenuation and local area average attenuation for all tests aboard USS Carr*. Additionally, the error values associated with each of these measurements were added to determine the error value of this average. As is shown in Figure 34, the associated error in the measurement is larger than the difference between average measured attenuation at each frequency. Therefore, it appears that the channel affects all frequencies nearly equally.

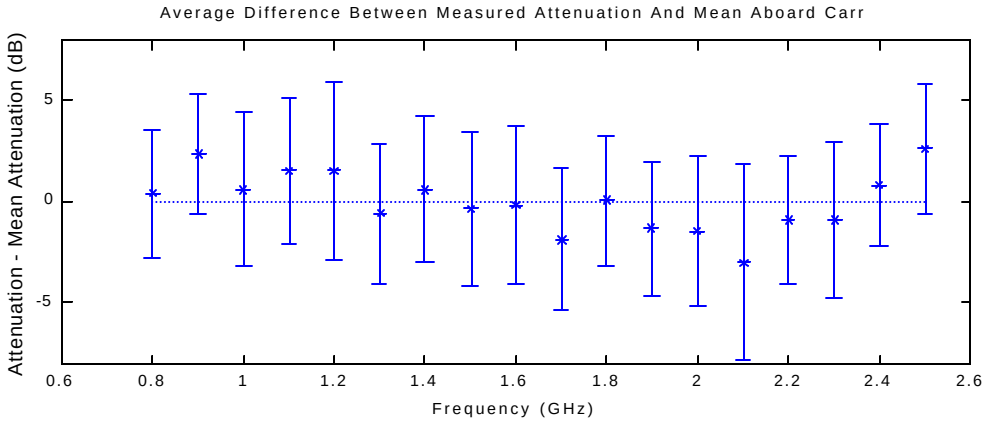

Figure 34 Average Effect of Channel On Each Frequency Aboard *Carr*.

USS Oscar Austin

The *Oscar Austin* is a *Burke*-class destroyer, the same class as the *USS Ross*. Two tests were attempted aboard this ship, though only one was completed. The receiver was placed on a table in CCS. The receiver was placed one deck directly below the transmitter in MER 2 (Fig. 35). The antenna height of the receiver was 38 inches.

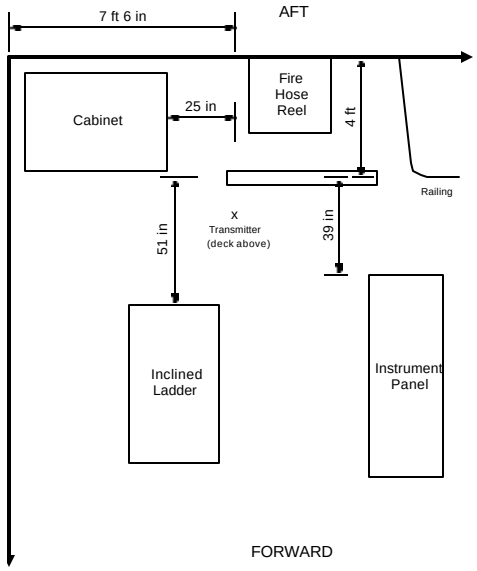

Figure 35 Test Layout Aboard *USS Oscar Austin*.

The deck between the transmitter and receiver had no breaks in it. Additionally, whip antennas, which were used for this test, are similar to dipole antennas, which transmit no waves vertically (Fig. 36) [17]. Even so, the receiver measured the signal one deck below. This demonstrated that multipath propagation allows signals to propagate between decks as well as between compartments. This test was performed at 100 MHz increments from 900 MHz to 2.5 GHz.

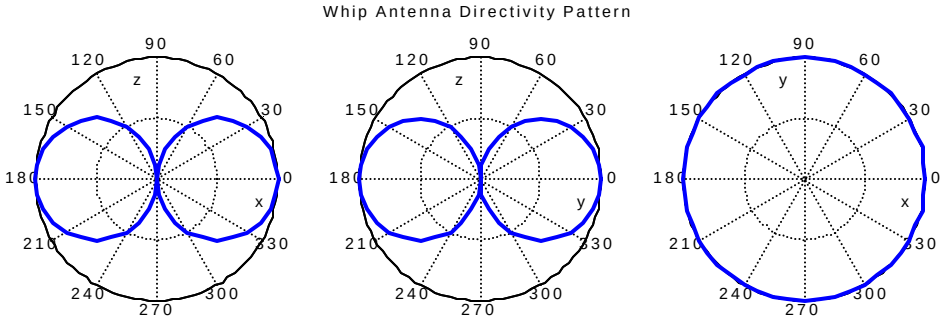

Figure 36 Whip Antenna Directivity Pattern, x and y horizontal, z vertical direction.

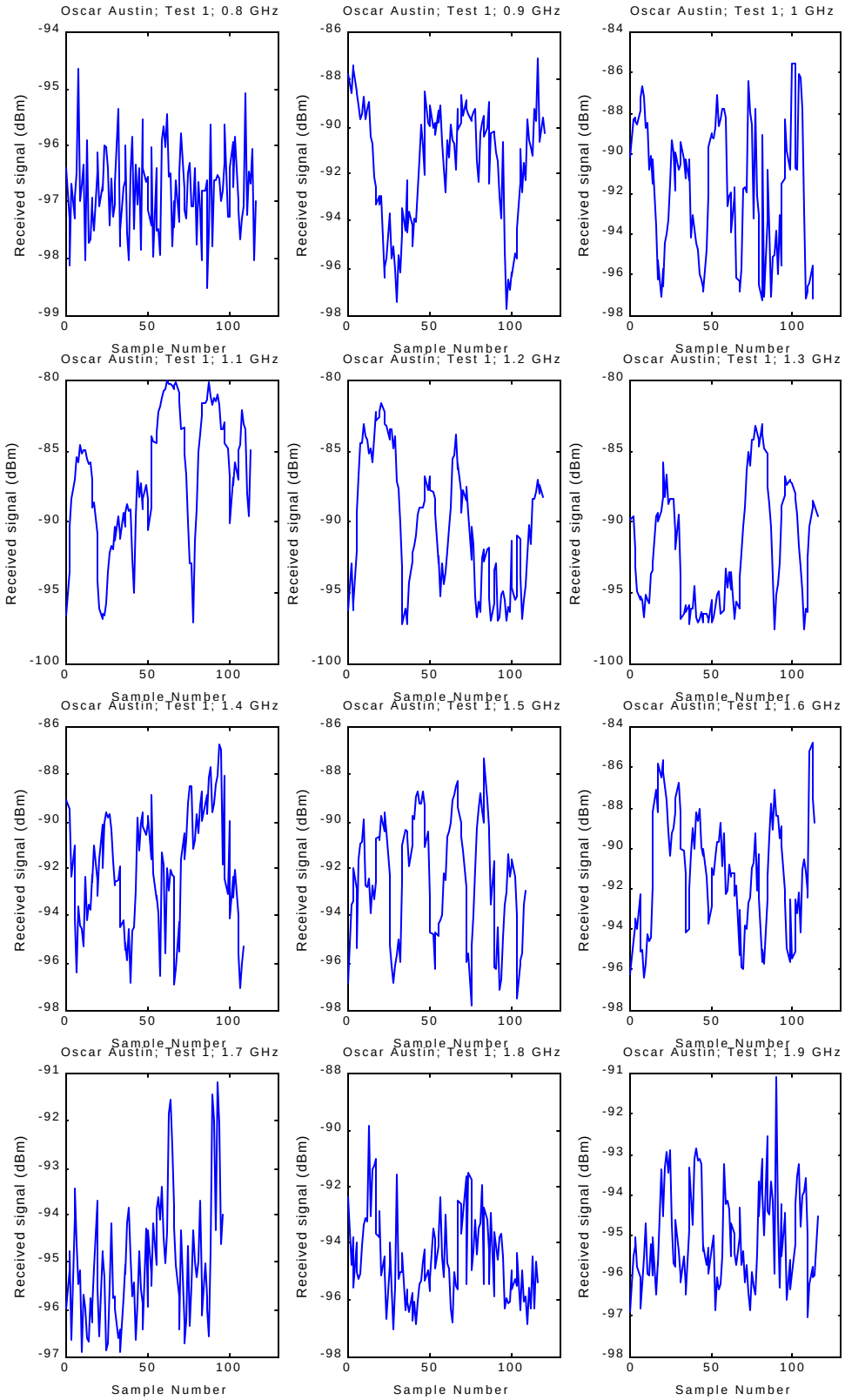
Oscar Austin; Test 1; 0.8 GHz
Oscar Austin; Test 1; 0.9 GHz
Oscar Austin; Test 1; 1 GHz
Oscar Austin; Test 1; 1.1 GHz
Oscar Austin; Test 1; 1.2 GHz
Oscar Austin; Test 1; 1.3 GHz
Oscar Austin; Test 1; 1.4 GHz
Oscar Austin; Test 1; 1.5 GHz
Oscar Austin; Test 1; 1.6 GHz
Oscar Austin; Test 1; 1.7 GHz
Oscar Austin; Test 1; 1.8 GHz
Oscar Austin; Test 1; 1.9 GHz
Received signal (dBm)
Sample Number

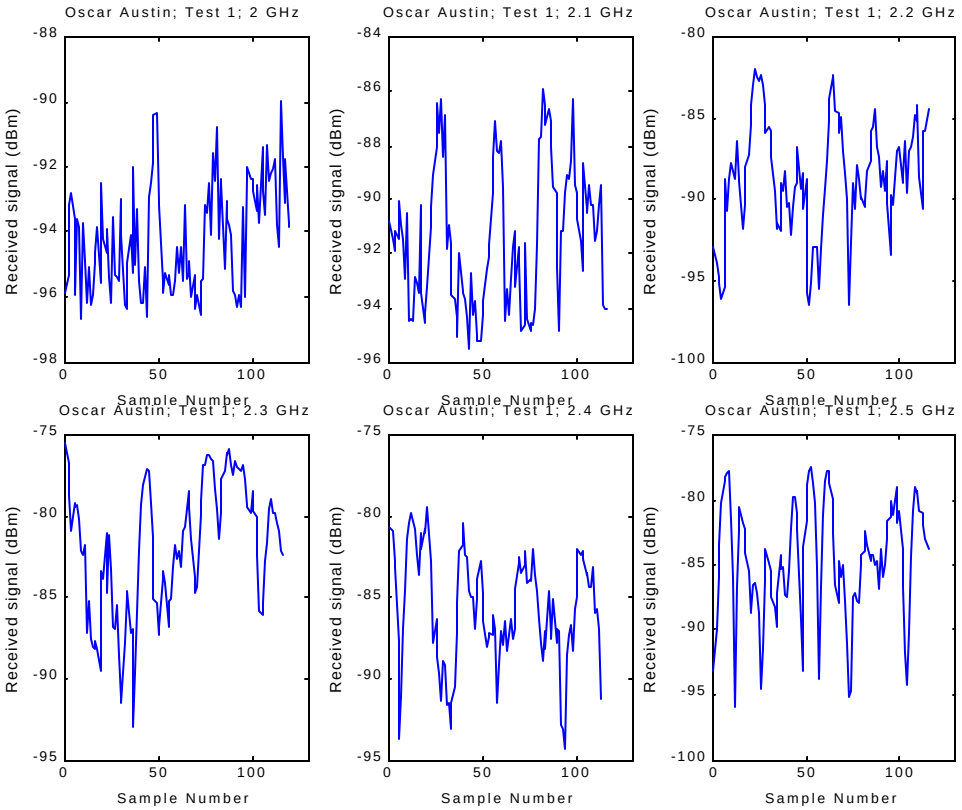
Oscar Austin; Test 1; 2 GHz
Oscar Austin; Test 1; 2.1 GHz
Oscar Austin; Test 1; 2.2 GHz
Oscar Austin; Test 1; 2.3 GHz
Oscar Austin; Test 1; 2.4 GHz
Oscar Austin; Test 1; 2.5 GHz
Received signal (dBm)
Sample Number

Table 24 Results from Test Aboard *USS Oscar Austin*.

Frequency (GHz)	Max Power (dBm)	Ave Power (dBm)	Min Power (dBm)	Power STD (dBm)	Number Data Points	Max Error (dBm)	*K* Factor	*K* MSE
0.900	-87.1	-90.9	-97.7	2.5	120	0.23	2.8	0.001399
1.000	-85.6	-90.7	-97.3	3.3	113	0.31	0.0	0.003146
1.100	-80.0	-84.7	-97.0	4.6	113	0.43	0.0	0.002101
1.200	-81.6	-88.0	-97.2	4.5	119	0.41	0.0	0.005926
1.300	-83.0	-89.8	-97.6	4.3	115	0.40	0.0	0.010813
1.400	-86.7	-91.3	-97.1	2.5	109	0.24	3.1	0.001594
1.500	-87.3	-91.7	-97.8	2.6	109	0.24	2.7	0.001430
1.600	-84.7	-90.3	-96.5	2.8	114	0.26	2.8	0.002993
1.700	-91.2	-94.8	-96.9	1.3	96	0.13	7.8	0.004954
1.800	-89.8	-94.3	-97.0	1.5	116	0.14	6.1	0.003619
1.900	-91.1	-94.9	-97.0	1.2	115	0.11	7.4	0.002999
2.000	-90.0	-93.8	-96.7	1.6	120	0.15	5.1	0.005356
2.100	-85.8	-90.6	-95.5	2.6	116	0.24	3.1	0.007122
2.200	-82.0	-87.3	-96.4	3.4	115	0.32	0.0	0.001521
2.300	-75.5	-80.3	-92.9	4.1	116	0.38	1.1	0.000700
2.400	-79.3	-84.5	-94.3	3.4	113	0.32	1.1	0.000896
2.500	-77.5	-82.7	-95.9	4.4	115	0.41	0.0	0.000629

The test aboard the *Oscar Austin* showed that wireless signals can be used to communicate across decks. Since only one measurement was taken, the attenuation caused by the deck cannot be calculated.

Summary of Narrowband Results

The narrowband tests provided useful information about the channel aboard US Navy ships. The tests show that the *K* factor is highly dependent upon location. Additionally, the tests aboard *USS Carr* indicate that the channel affects all frequencies nearly equally.

Further analysis of these results appears in chapter 5.

ex-USS America

Loss Across 1-100-2	17.0 dB
Loss Across 1-100-4	14.4 dB
Loss Across 1-59-0	15.0 dB

USS Ross

Loss Across Machine Room/Engine Room bulkhead	20.9 dB
Loss Due to Shutting Hatch 2-188-4	3.69 dB
Loss Due to Shutting Hatch 2-188-2	1.14 dB

Energy was propagating around bulkhead through the ladderwell, as evidenced by the fact that shutting hatch 2-188-4 caused signal loss.

Shutting hatch 2-188-4 did not block all energy, because shutting hatch 2-188-2 caused further signal loss.

Energy was propagating through other paths than the ladderwell, as evidenced by the different signal loss caused by the two hatches.

USS Leyte Gulf

Communication is possible within a compartment, even when the direct path from the transmitter to receiver is blocked.

USS Carr

Loss Across After CCS Bulkhead With Hatch Open	8.89 dB
Loss Across After CCS Bulkhead With Hatch Shut	21.3 dB
Loss Across Forward Engine Room Bulkhead With Hatch Open	11.5 dB
Loss Due To Shutting Engine Room Hatch	5.50 dB

The test across the CCS bulkhead was very similar to the test aboard the *Ross*, and the results were also very similar.

The loss across a bulkhead with a hatch very near the line of sight is approximately 10 dB.

USS Oscar Austin

Communication is possible between decks.

This communication between decks is made possible by the multipath environment, as evidenced by the fact that the antennas used in the test were oriented such that there was no direct-path propagation from the transmitter to the receiver.

3. Ultra-Wideband Testing

Ultra-wideband communication is a new technology that greatly simplifies channel sounding and characterization. Time Domain Corporation graciously allowed the Naval Academy to borrow two PulsON Application Demonstrators [18], which showcase Time Domain's new communication technology. This equipment allowed a more complete study of the shipboard wireless channel.

The narrowband testing discussed in the previous chapter provided information about the strength of the signal only. From this information, only the channel effect on the magnitude of the signal could be determined. Additionally, in order to gather information about different frequencies, a measurement was required at each frequency.

The UWB system, however, provided a channel sounding—a recording of the received signal from which channel effects could be calculated—any time it was communicating, which could be saved for later analysis. This gave information about the channel's time delay and frequency characteristics. Therefore, whenever the system was communicating, it could record a complete profile of the channel at the click of a button.

Pulse Communication

Traditional communications systems transmit continuous waves. The information is modulated onto a radio frequency carrier wave. The spectrum of the resulting signal is highly concentrated around the frequency of the carrier. UWB communication systems, however, have nothing to do with continuous waves. Instead, the information is modulated with very short (.5 nanoseconds), precisely timed pulses. Unlike continuous waves, which contain one discrete frequency, these pulses have spectral content across all frequencies from about 1 GHz to 3 GHz (Fig. 37) [19].

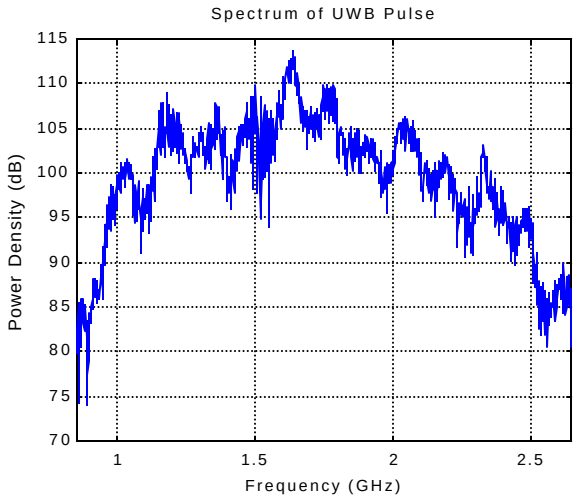

Figure 37 Spectrum of Ultra-Wideband Pulse.

As each of these pulses travels through the channel, it experiences the same multipath effects that a continuous wave would experience. However, because the pulse is of such short duration—0.5 ns—the multiple copies that arrive from different paths are easily distinguishable. The received signal shows the time delay profile of the channel. Figure 38 shows a time delay profile measured aboard *America*. Each received pulse identifies a different path that the energy took from the transmitter to the receiver. Much information about the channel can be extracted from this time delay profile.

Mean Excess Time Delay: Excess time delay, τ, is defined as the amount of time it takes a reflected pulse to reach the receiver after the first pulse in the time delay profile arrives. Mean excess time delay, μ_τ,is the average amount of time it takes for the received power to arrive at the receiver [1 p. 160]. That is, when P_k and τ_k are the power and time delay of pulse k, respectively, μ_τ is

$$m_t = \frac{\sum_k P_k \cdot t_k}{\sum_k P_k}$$

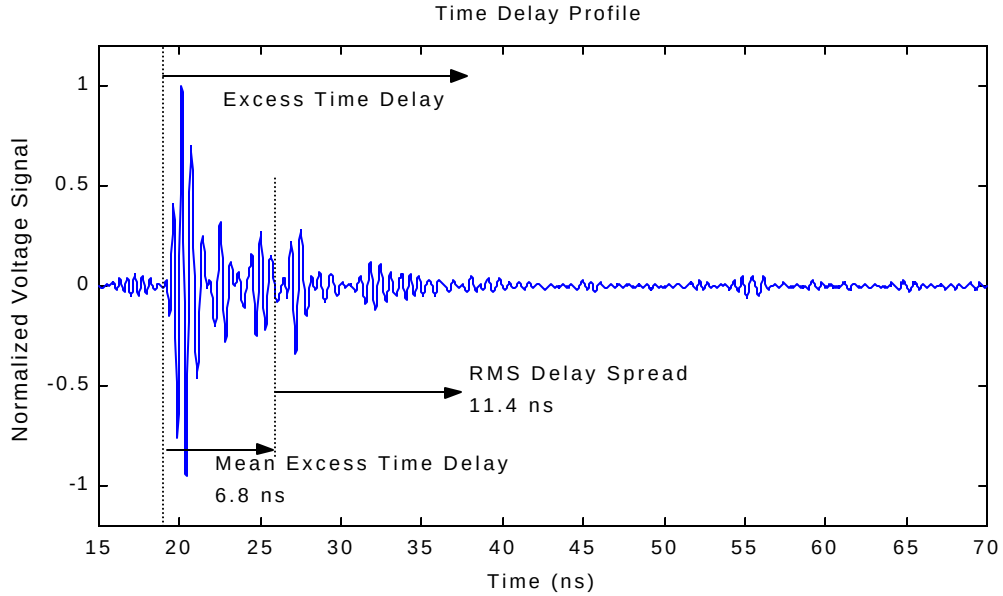

Figure 38 Excess Time Delay, Mean Excess Time Delay, and RMS Delay Spread.

RMS Delay Spread: The RMS delay spread, σ_τ, is the standard deviation of the excess time delay. It is a measure of how much the signal spread out due to the different paths within the channel [1 p. 160].

$$s_t = \sqrt{\frac{\sum_k P_k \cdot (t_k - m_t)^2}{\sum_k P_k}}$$

The RMS delay spread can be used to calculate (approximately) the bandwidth that can be transmitted through the channel. In order for a signal to be understandable, each frequency in its spectrum must be affected nearly equally. If the effect varies too greatly across the frequency range, the signal cannot be understood without the use of an equalizer to counter the effects of the channel. The bandwidth across which the frequency correlation function is 0.9 is approximately:

$$B_c \approx \frac{1}{50\sigma_t}$$

For a frequency correlation of .5, this approximation becomes:

$$B_c \approx \frac{1}{5\sigma_t}$$

Path Loss Exponent: As electromagnetic energy propagates, its signal strength decays as a power law with distance traveled [1 p. 73]. The exponent of this decay, however, depends on the channel. In free space, for example, this exponent is 2 [15 p. 104]. Relating the received power to the distance between the transmitter and receiver at multiple points allows this exponent to be calculated.

$$P = P_o\left(\frac{d}{d_o}\right)^{-n}$$

Frequency Response: Finally, the time delay profile can be analyzed to determine the frequency response of the channel. Since the frequency spectrum of the input signal is known, and that of the received signal can be calculated, the difference between the two is the attenuation of the channel as a function of frequency.

Test Results-Loss Across Hatch 1-101-2

The ultra-wideband tests were performed aboard the *ex-USS America*. One test was performed across hatch 1-101-2 (Fig. 39). A measurement was taken with the hatch open and one with it shut. These measurements were compared to determine the effect of the closed hatch on the signal.

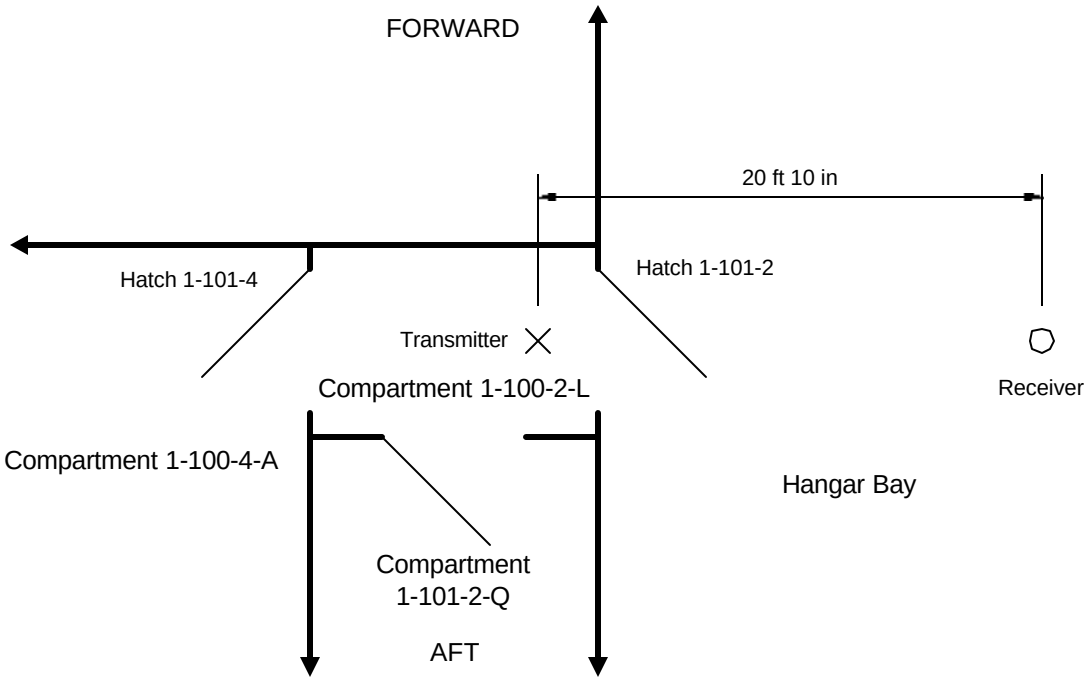

Figure 39 Test Layout aboard *ex-USS America*.

The transmitter was placed in compartment 1-100-2-L, centered on hatch 1-101-2. The receiver was also centered on hatch 1-101-2, and was placed 20 ft, 10 in from the transmitter. The system was started, hatch 1-101-2 was shut, and the time delay profile of the channel was recorded. From this profile, the mean excess time delay, the RMS delay spread, and the frequency content of the signal were determined.

Hatch 1-101-2 Shut:

μ_τ: 138.6 ns
σ_τ: 108.1 ns

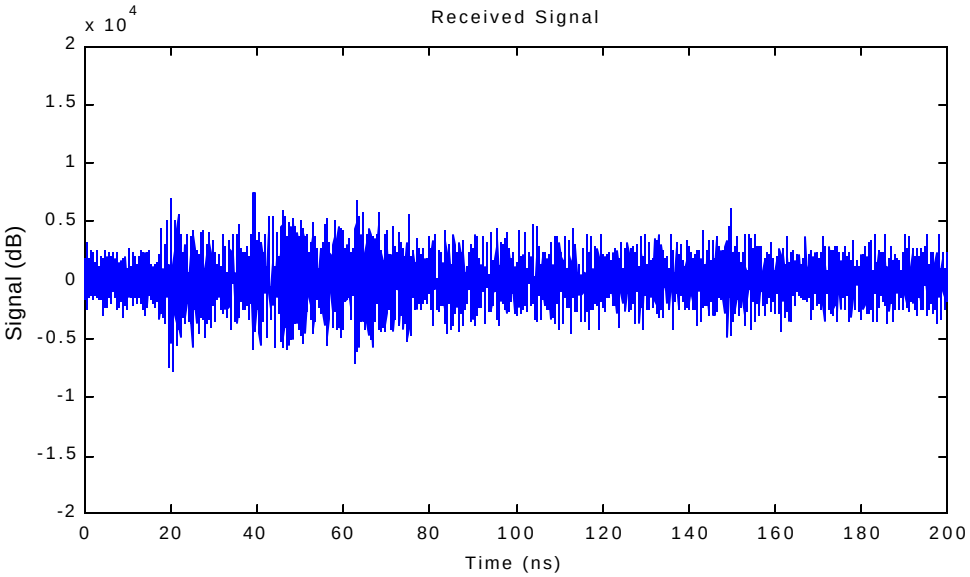

Figure 40 Signal Received With Hatch 1-101-2 Shut.

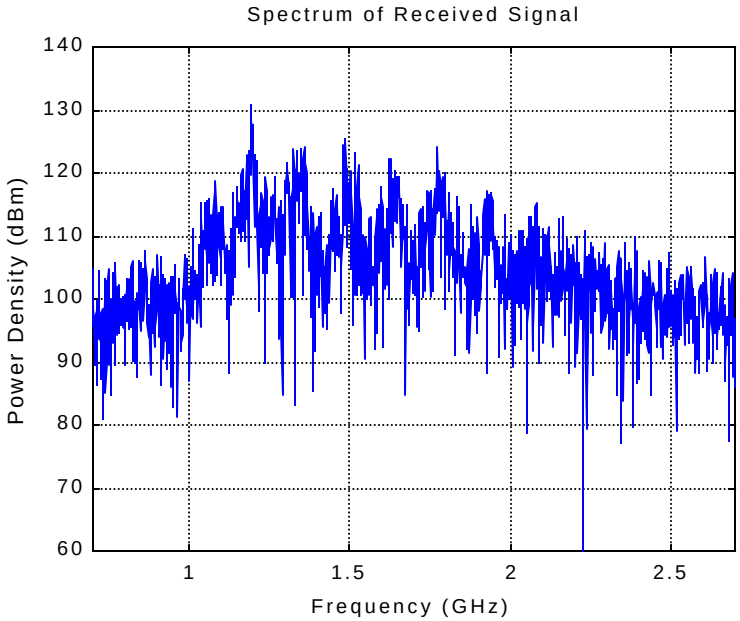

Figure 41 Spectrum of Signal Received With Hatch 1-101-2 Shut.

The time delay profile was recorded (Fig. 40), and was later used to determine the spectrum of the received signal (Fig. 41). Once the time delay profile was recorded with the hatch shut, the hatch was opened. The time delay profile was recorded again.

Hatch 1-101-2 Open:

μ_τ: 68.8 ns
σ_τ: 92.5 ns

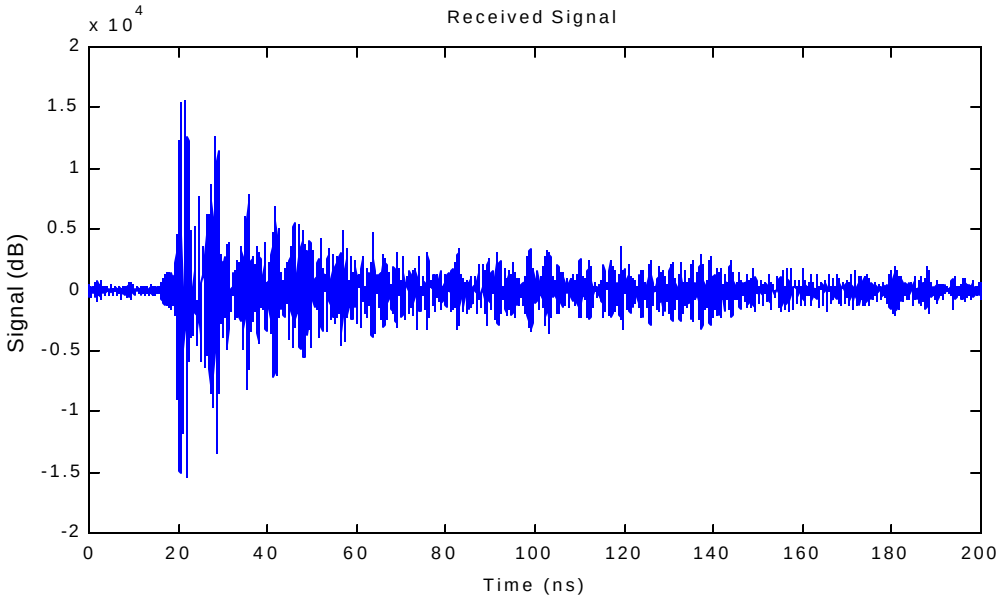

Figure 42 Signal Received With Hatch 1-101-2 Open.

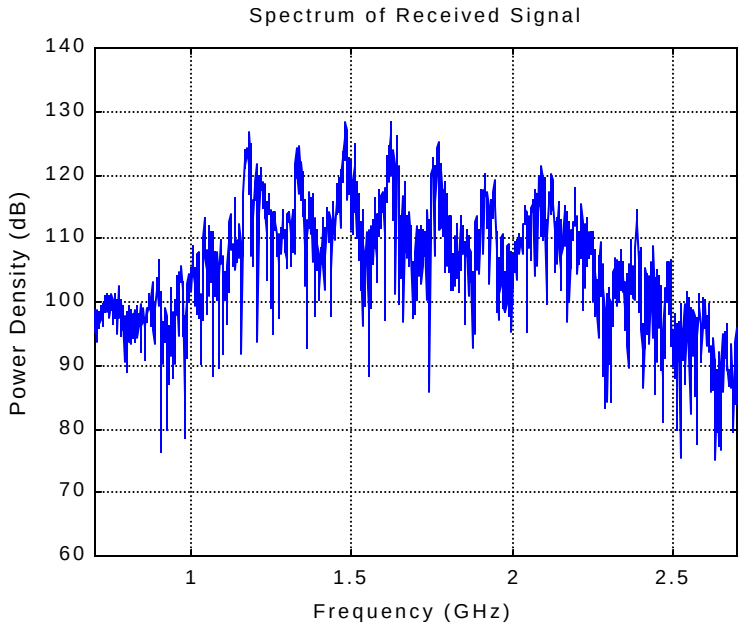

Figure 43 Spectrum of Signal Received With Hatch 1-101-2 Open.

Again, the time delay profile was recorded (Fig. 42) and used to calculate the spectrum of the received signal (Fig. 43). When the hatch was shut, the RMS delay

spread was 108.1 ns. Therefore, any system intended for communication across bulkheads that requires a frequency correlation of at least 0.9 must contain less than approximately 190 kHz of bandwidth. If more bandwidth were needed, the receiver would need to be equipped with an equalizer to recover the signal from the effects of the channel.

Information about the propagation paths could also be extracted from the change in RMS delay spread. This showed that the shorter propagation paths—those that passed through the open hatch—were blocked when the hatch is shut. The longer paths, which did not pass through the open hatch, were not blocked.

In order to calculate the loss in signal caused by the closed hatch, the power spectrum of the signal through the shut hatch was subtracted from that of the signal through the open hatch. From this frequency response, the average attenuation caused by the hatch was calculated. For comparison, the UWB attenuation is plotted with the attenuation calculated from the narrowband tests (Fig. 44).

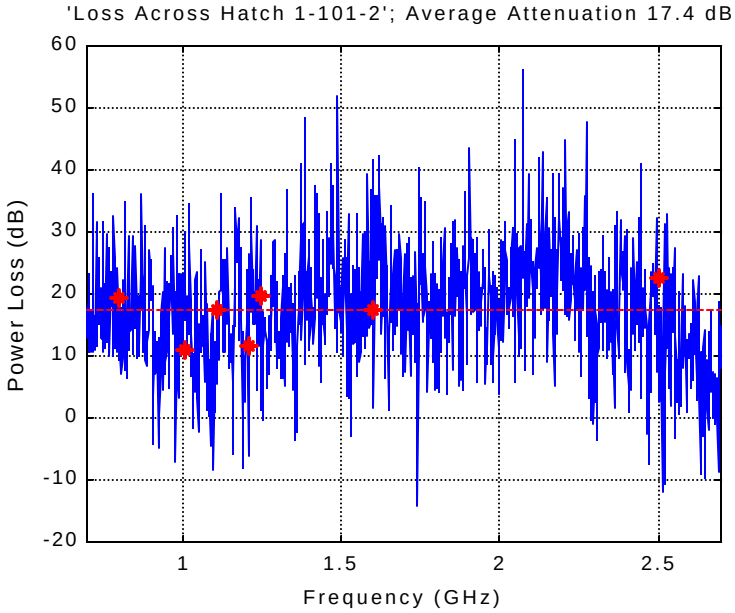

Figure 44 Attenuation Due To Hatch 1-101-2 Aboard *ex-USS America*.

The average value of the attenuation across hatch 1-101-2, as calculated from the UWB measurements, was 17.43 dB, which is very close to the value obtained from the narrowband testing, 17.01 dB. Plotting the results from both tests on the same axes shows the correlation: the attenuation measured using the narrowband equipment lies on the attenuation curve measured by the ultra-wideband equipment.

Test Results-Characterization of One Compartment

The UWB equipment was also used to characterize a single compartment. Compartment 1-21-1-Q was located farther forward of the hangar bay, and provided a simple geometry to characterize.

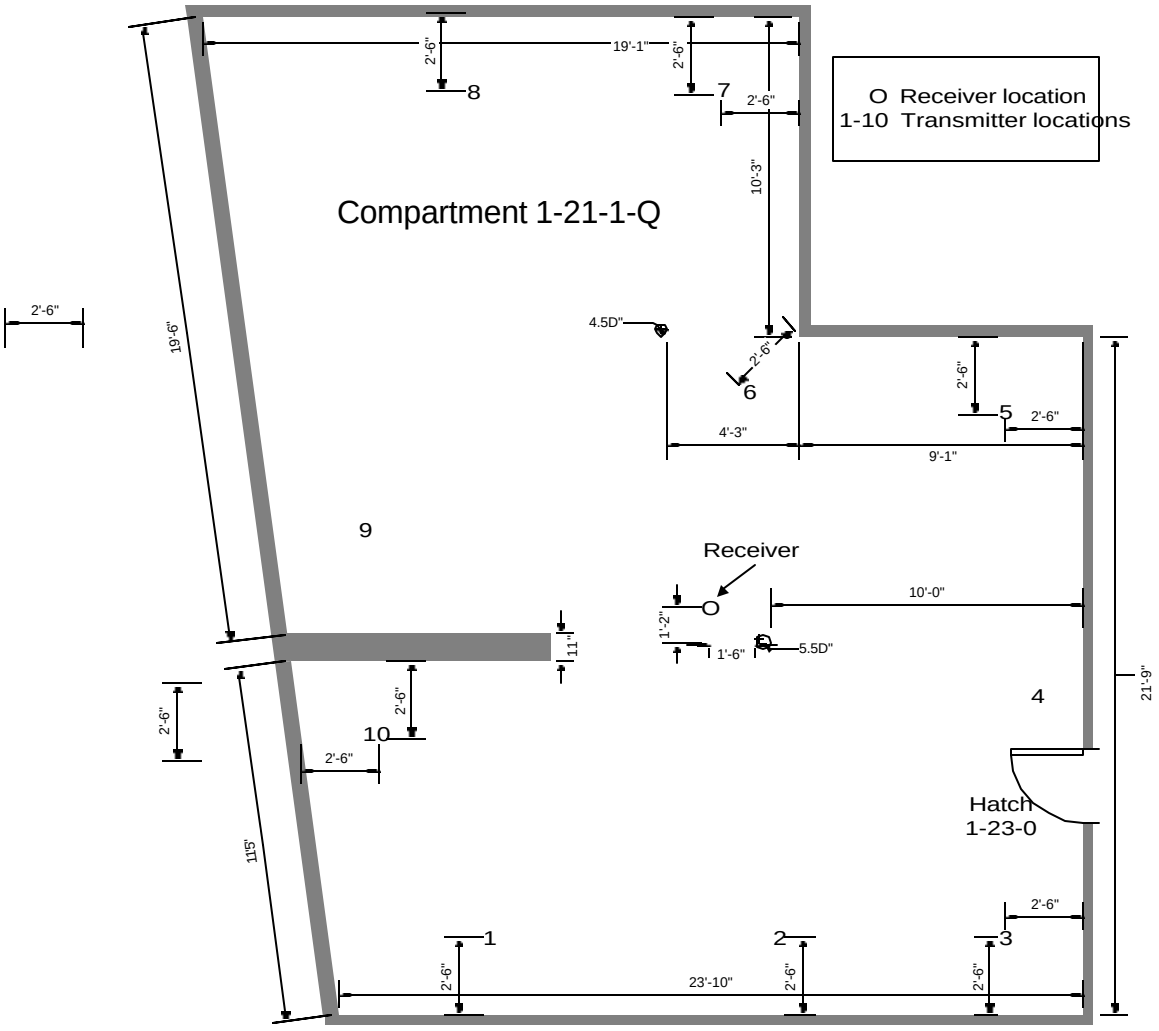

Figure 45 Test Layout In Compartment 1-21-1-Q Aboard *ex-USS America*.

The test was performed by placing the receiver approximately in the center of the compartment, and taking channel soundings with the transmitter in different locations around the room. In the figure 45, the receiver is denoted by a circle, and the different transmitter locations by numbers. Two soundings were recorded at each location. From these channel soundings, the mean excess time delay, μ_τ, and the RMS delay spread, σ_τ, were calculated. The path loss exponent within the compartment was also calculated by comparing the strength versus the distance of each measurement.

Table 25 Results from Compartment Characterization Aboard *ex-USS America*.

Sample	Location	μ_τ (ns)	σ_τ (ns)
1	1	39.0	21.7
2	1	38.6	21.6
3	2	81.7	86.4
4	2	80.6	86.7
5	3	88.2	87.9
6	3	91.4	88.7
7	4	69.8	84.0
8	4	73.6	83.9
9	5	70.5	85.9
10	5	66.5	82.3
11	6	91.2	86.8
12	6	101	93.7
13	7	87.6	91.3
14	7	85.9	90.0
15	8	125	106
16	8	118	101
17	9	94.2	91.0
18	9	98.8	92.6
19	10	87.2	85.2
20	10	88.0	86.9
Ave:		83.9	82.7

This test shows that, on average, the mean excess time delay within compartment 1-21-1-Q was 83.9 ns, and that the standard deviation of the arrival time of this energy was 82.7 ns.

Because the signal strength decays as a power law with distance, plotting the amplitude of the largest peak versus distance on a logarithmic scale allowed the path loss exponent to be estimated by finding the best-fit line (Fig. 46). From all 20 scans taken in this compartment, the path loss exponent was estimated to be 1.65, which is typical for indoor communications with no obstruction between the transmitter and receiver [15 p.102].

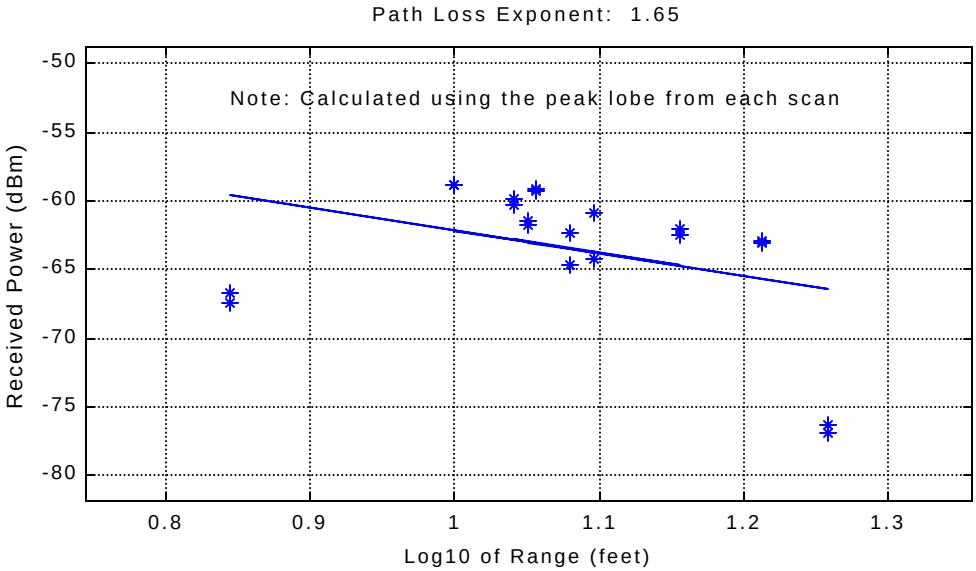

Figure 46 Plot of Signal Power versus Distance.

4. Computer Simulation

To better understand the mechanism by which the radio waves passed through bulkheads, computer simulations were run. These simulations used Maxwell3D, a product of Ansoft Corporation, which is a finite-element electromagnetic field modeler [20]. The software supported the modeling of time-varying electromagnetic fields and solved for displacement and eddy currents. For a more in-depth description of the modeling process, see appendix H.

Derivation of Effect of Steel on Signal

The effect of a steel bulkhead on a transmitted signal was calculated with the skin depth equation. Skin depth, $\ddot{a}$, provides a measure of the distance an electromagnetic wave penetrates into a material. For every distance $\ddot{a}$ a signal propagates into a conductor, its power drops by a factor of 1 / *e*—that is, it experiences 4.3 dB attenuation [21 p. 219]. For a material with conductivity s, permeability m, and a wave with frequency *f*,

$$d = \sqrt{\frac{2}{2p f \cdot m \cdot s}}$$

Often, the permeability of a material is listed in terms of its relative permeability, m_r, according to the relationship $m = m_r \cdot m_0 = m_r \cdot 4p \cdot 10^{-7}$ T·m·A^{-1}. A typical value for the relative permeability of steel is m_r = 350 [22 p. 76]. Similarly, conductivity is often listed by its reciprocal, resistivity $\tilde{n}$. A typical value of resistivity for steel, $r = 45 \cdot 10^{-8}$ ohm-meters, corresponds to a conductivity of $s = 2.2 \cdot 10^{6}$ (ohm-meter)$^{-1}$ [22 p. 73].

Using these values to solve for the skin depth yields:

$$d = \sqrt{\frac{2}{2p \cdot 800 \cdot 10^{6} \cdot \left(350 \cdot 4p \cdot 10^{-7}\right) \cdot \left(2.2 \cdot 10^{6}\right)}} = .64 \text{ mm} = 25 \cdot 10^{-6} \text{ in}$$

Model

In order to set up an electromagnetic wave within the simulation, an antenna was included in the model. The antenna was half of a current loop made from copper and driven with an 800 MHz alternating current of 1 amp, which entered the antenna through the boundary of the simulation space. The time-varying current caused an electromagnetic wave to be created, which propagated away from the antenna.

The simulation space was a region 30 in by 30 in by 225 in. A steel plate was placed 150 inches away from the antenna in order to simulate a bulkhead. The plate was .5 inches thick. At this thickness, the value of attenuation that can be expected when the wave propagates through the steel is

$$A_{ex} = 4.3 \text{ dB} \cdot \frac{.5 \text{ in.}}{25 \cdot 10^{-6} \text{ in.}} = 4.3 \text{ dB} \cdot 20 \cdot 10^{3} = 85 \cdot 10^{3} \text{ dB}$$

That is, the signal is attenuated 85 thousand dB, effectively blocking the signal entirely. Consequently, the steel used in this simulation is assumed to be a perfect conductor.

Two scenarios were created—one with a solid steel plate (Fig. 47), and one with a .2 inch wide rubber slit in the plate to simulate a hatch seal (Fig. 48). In order to compare the power contained in the electromagnetic wave on either side of the plate, two imaginary surfaces were also entered into the simulation—one on each side of the bulkhead. The power flowing through each surface would be calculated after the simulation was complete, and the results compared.

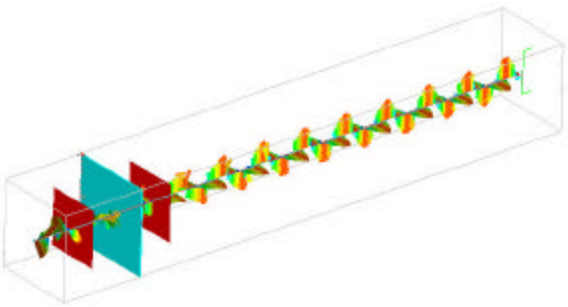

Figure 47 Solid Bulkhead Simulation.

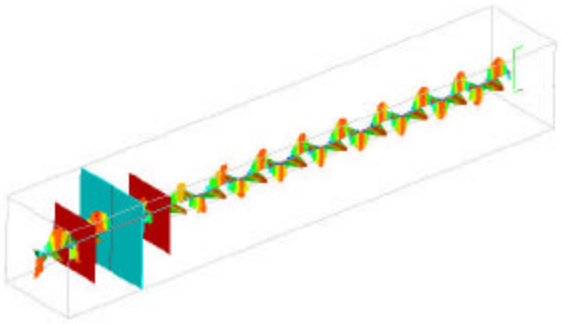

Figure 48 Slit Bulkhead Simulation.

Simulation Boundaries

Before the software was started, an environmental variable was created in the operating system. This variable, use_abc_boundary, was set to 1. When Maxwell3D was started, this environmental variable told the software to not simulate reflections off of the sides of the simulation space when solving the problem. Five of the six sides of the simulation space were chosen to be an impedance boundary. The final side, the side through which the antenna was driven, contained two current sources. These sources supplied 1 A, and were offset in phase 180°, so that the top terminal "pushed" 1 A into the antenna while the bottom terminal "pulled" 1 A from the antenna (Fig 49).

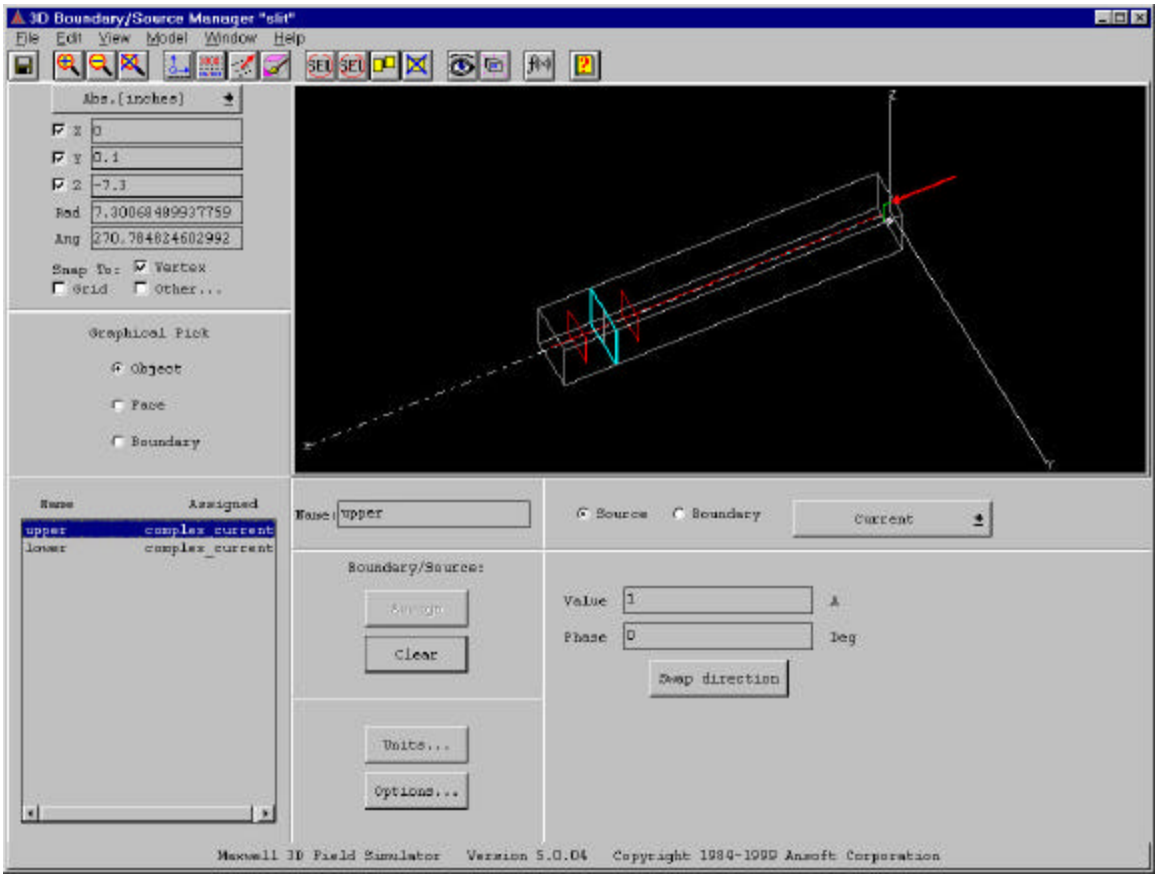

Figure 49 Source Editor—Current Entering Antenna.

Simulation Setup

The frequency of the applied current had to be defined before the simulation was run. The simulation was run at 800 MHz. The wavelength at this frequency is 14.9 in.

This software used finite-element modeling, wherein the magnetic intensity field (H field) was calculated at points throughout the simulation space. This set of points,

referred to as a "mesh", must be fine enough allow several points per wavelength. The initial mesh was created with approximately three points per wavelength by instructing the program to seed the space with points every 5 in.

Since the program solves Maxwell's field equations in an iterative manner, a number of passes are required. This number of passes must be defined. Between iterations, the mesh is refined—in regions with high field gradients, for example—in order to generate a more accurate solution. If the mesh grows too large, the computer will not be able to store all the calculations, and the simulation will fail. Therefore, the number of iterations to perform must be chosen so as to generate an accurate solution without overworking the computer. The number of iterations was chosen as two. The computer consistently failed every time a third iteration was attempted.

Simulation Results

Two simulations were run. Once completed, the power in the electromagnetic wave was measured by finding the power through surfaces placed at the end of the solution space. This required the calculation of the Poynting vector, which tells the amount of power and the direction of propagation of an electromagnetic wave. In turn, this required the calculation of the electric field vector from the H field vector solved for by the computer. These calculations are described in appendix H.

The power through these surfaces was calculated in this manner for both simulations. These values of power were then compared to calculate the amount of attenuation caused by the bulkhead and the slit. Because these values of power are in watts rather than decibels, the attenuation is

$$A = 10 \cdot \log_{10} \frac{P_{near}}{P_{far}}$$

The results of the simulation are:

Table 26 Simulation Results

Simulation	Power Near side	Power Far side	Attenuation
Slit bulkhead (Fig. 50)	6.28	.00739	29.3
Solid bulkhead (Fig. 51)	5.75	0	

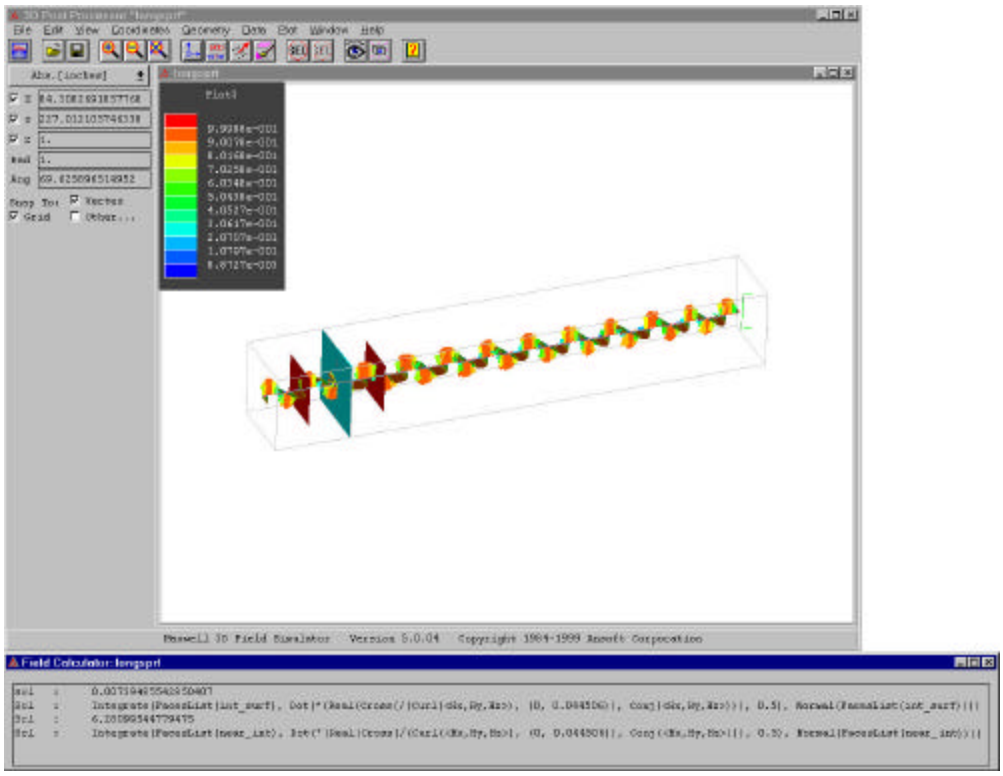

Figure 50 Results of Slit Bulkhead Simulation.

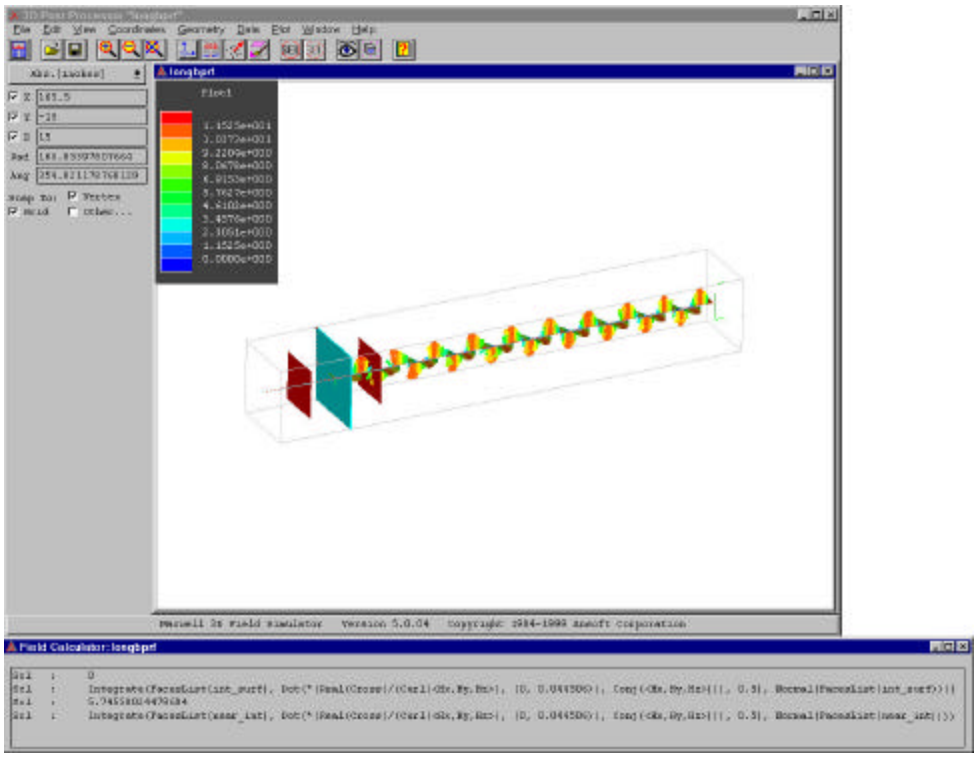

Figure 51 Results of Solid Bulkhead Simulation.

These results correlate with the measurements taken aboard ships. The bulkhead attenuation measured aboard ships was as high as 25 dB. The simulation shows 29 dB attenuation. The slightly lower attenuation measured aboard ships could be explained by the higher number of propagation paths through the bulkhead, which would increase the amount of energy that can propagate through the bulkhead.

5. Conclusions

Narrowband Test Results

The narrowband testing aboard Navy ships was designed to measure the path loss associated with transmission across bulkheads, including various configurations of hatches. The narrowband tests also showed that communication can occur from deck to deck even when the antennas are not oriented for direct path communication. This is due to the multipath effect allowing the signal to be reflected, scattered, and diffracted towards the receiver.

The path losses of different communication scenarios are:

Transmission across one bulkhead, open hatch nearly in direct path:

Carr, CCS to passageway: 8.89 dB
Carr, passageway to MER: 11.46 dB

Approximately 10 dB

Transmission across one bulkhead, open hatch not in direct path:

Ross, machinery room to MER: 20.87 dB
Carr, CCS to passageway: 21.28 dB

Approximately 20 dB

Loss due to closed hatches almost in direct-path from transmitter to receiver:

ex-USS America, Hatch 1-100-2: 17.01 dB
ex-USS America, Hatch 1-59-0: 14.99 dB
USS Carr, CCS Hatch: 12.39 dB

The lower value for the loss across the CCS hatch aboard *Carr* may be due to the fact that when this hatch was closed there was another hatch, which was not in the direct-path from the transmitter to receiver, that was left open. Whereas the tests aboard *America* involved no other open hatches, the test aboard *Carr* did. Comparing the two values obtained from tests aboard *America*, the measurement across hatch 1-59-0 should be slightly more accurate because it involves no change of the receiver's location, whereas the one across hatch 1-100-2 does. The loss due to a closed hatch that lies almost in the direct-path between the transmitter and the receiver is approximately 15 dB.

Approximately 15 dB

Transmission across one bulkhead, no open hatches:

Ross, machinery room to MER, 2-188-2 open, 2-188-4 shut: 24.56 dB
Carr, passageway to MER: 16.96 dB

The apparent disparity between these two measurements could be attributed to the fact that the bulkhead on the *Ross* was blocking a fairly strong direct-path signal from the transmitter, whereas the bulkhead being measured across on the *Carr* was not blocking a direct-path signal. Additionally, it stands to reason that the attenuation associated with a bulkhead with no open hatches should be higher than that of a bulkhead with open hatches. Furthermore, the loss across one bulkhead with an open hatch nearly in the direct path was shown to be approximately 10 dB, and the loss due to such a hatch approximately 15 dB. Therefore, the value obtained aboard the *Ross*, approximately 25 dB, is supported by other measurements.

First Bulkhead: Approximately 25 dB

Loss due to closed hatches, not near direct-path from transmitter to receiver:

Ross, 2-188-2: 1.14 dB
Ross, 2-188-4: 3.69 dB
Carr, MER Hatch: 5.50 dB

The different results for seemingly similar tests can be explained by the very nature of the test—these hatches are not near the direct-path from the transmitter to the receiver. Therefore the amount of signal loss associated with shutting one of these hatches is a function not only of the amount of energy propagating through the hatch, but also of the amount of energy finding its way to the receiver via other paths. Whereas the engine room hatch aboard *Carr* was located near the receiver, and presumably was in the path of a large proportion of the energy detected by the receiver, the two hatches aboard *Ross* were not as near to the receiver.

Furthermore, hatch 2-188-4 aboard the *Ross* caused 3.69 dB attenuation, whereas hatch 2-188-2—an identical hatch in almost exactly the same location—caused 1.14 dB signal loss. This can be explained by the fact that these hatches were a part of one possible propagation path from the transmitter to the receiver. While they may each have had the same effect on the energy traveling via that path, they had no effect on energy traveling by other paths. Therefore, closing the second hatch had, proportionately, less effect on the signal strength at the receiver.

Therefore, the effect of a hatch not near the direct-path does not seem to be predictable. However, a rough estimate can be made using the results obtained describing a bulkhead with no hatches (25 dB) and a bulkhead with an open hatch not near the direct-path (20 dB), which seem to indicate 5 dB attenuation associated with a hatch not near the direct-path from the transmitter to the receiver.

Ultra-Wideband Test Results

The ultra-wideband tests performed aboard the *ex-USS America* showed approximately the same attenuation across hatch 1-100-2 as the narrowband tests. The UWB equipment measured 17.43 dB whereas the narrowband equipment measured 17.01 dB attenuation. This lent confidence to the measurements obtained by both systems.

The UWB equipment was used to find the path loss exponent within one compartment. The value obtained, 1.65, is typical for indoor communications with no obstruction between the transmitter and receiver. The free space path loss exponent is 2. This measured path loss is less than that of free space due to the effect of the bulkheads, overhead (ceiling), and deck reflecting energy back toward the receiver, resulting in higher energy reception.

The RMS delay spread was measured as 82.7 ns within a compartment, and as 108.1 ns across one hatch. The maximum bandwidth a signal can have, therefore, to communicate across hatches is approximately 190 kHz for a frequency correlation of 0.9. If the system requires a larger bandwidth, the use of equalizers to recover the signal from the effects of the channel may be required.

Computer Simulation Results

The results of the computer simulation showed approximately the same attenuation as that measured aboard ships. The attenuation of a steel plate bulkhead with a rubber slit, modeling a hatch seal, was 29.3 dB, whereas this attenuation has only been measured as high as 25 dB. The lower attenuation measured in real systems could be due to the presence of more than one propagation path allowing more energy to cross the bulkhead.

Future Work

The advent of Bluetooth, a new set of wireless communication devices designed to automatically set up networks [23], will allow wireless systems to be implemented with great ease. This technology, which operates at 2.4 GHz and is intentionally designed to be inexpensive, could be exploited to create any number of wireless devices to support the operation of a ship. A study should be done to determine the performance of Bluetooth-enabled devices in a shipboard environment. Particularly, the ability of such devices to set up a network that can communicate across sealed bulkheads should be investigated.

References

[1] Theodore S. Rappaport, *Wireless Communications: Principles & Practice* Upper Saddle River, NJ: Prentice Hall, PTR, 1996.

[2] Vinko Erceg, A.J. Rustako, R.S. Roman. "Diffraction Around Corners and Its Effects on the Microcell Coverage Area in Urban and Suburban Environments at 900 MHz, 2 GHz, and 6 GHz." *IEEE Transactions on Vehicular Technology,* Vol. 43, No. 3, August 94, pp. 762-766.

[3] Theodore S. Rappaport, Scott Y. Seidel, Rajendra Singh, "900 MHz Multipath Propagation Measurements for US Digital Cellular Radiotelephone," *IEEE Transactions on Vehicular Technology*, Vol. 39, No. 2, May 1990, pp. 132-139.

[4] Lambertus J.W. van Loon, "Mobile In-Home UHF Radio Propagation For Short Range Devices," *IEEE Antennas and Propagation Magazine*, Vol. 41, No. 2, 1999, pp. 37-40.

[5] Gerard J.M. Janssen, Patrick A. Stigter, Ramjee Prasad, "Wideband Indoor Channel Measurements and BER Analysis of Frequency Selective Multipath Channels at 2.4, 4.75, and 11.5 GHz," *IEEE Transactions on Communications*, Vol. 44, No. 10, October 1996, pp. 1272-1288.

[6] Scott Y. Seidel, Theodore S. Rappaport, "914 MHz Path Loss Prediction Models for Indoor Wireless Communications in Multifloored Buildings" *IEEE Transactions on Antennas and Propagation*, Vol. 40, No. 2, February 1992, pp. 207-217.

[7] Scott Y. Seidel, Theodore S. Rappaport, "Site-Specific Propagation Prediction for Wireless In-Building Personal Communication System Design," *IEEE Transactions on Vehicular Technology*, Vol. 43, No. 4, November 1994, pp. 879-891.

[8] Theodore S. Rappaport, Scott Y. Seidel, Koichiro Takamizawa, "Statistical Channel Impulse Response Models for Factory and Open Plan Building Radio Communication System Design," *IEEE Transactions on Communications*, Vol. 39, No. 5, May 1991, pp. 794-806.

[9] Theodore S. Rappaport, "Characterization of UHF Multipath Radio Channels in Factory Buildings," *IEEE Transactions on Antennas and Propagation*, Vol. 37, No. 8, , August 1989 pp. 1058-1069.

[10] Kurt J. Rothenhaus, "Distributed Software Applications in Java for Portable Processors Operating on a Wireless LAN," Master's Thesis, Naval Postgraduate School, Monterey CA, September 1999.

[11] Mark M. Matthews, "Analysis of Radio Frequency Components for Shipboard Wireless Networks," Master's Thesis, Naval Postgraduate School, Monterey CA, December 1999.

[12] Steven M. Debus, "Feasability Analysis for a Submarine Wireless Computer Network Using Commercial off the Shelf Components," Master's Thesis, Naval Postgraduate School, Monterey CA, September 1998.

[13] Eric L. Mokole, et al. "Radio-Frequency Propagation Measurements in Confined Ship Spaces Aboard the *ex-USS Shadwell*," NRL/FR/5340-00-9951, Naval Research Laboratory, 18 August 2000.

[14] *MATLAB: The Language of Technical Computing*, Math Works Inc., Natick MA, 1984.

[15] William C.Y. Lee, "The Proper Statistical Nature of Measuring & Estimating," *IEEE Vehicular Technology Conference 1999*, Houston TX, May 1999.

[16] R. Kattenbach and T. Englert, "Investigation Of Short Term Statistical Distributions For Path Amplitudes And Phases In Indoor Environments," *Proc. VTC'98*, pp. 2114-2118, session 64-4 [CD-ROM], May 1998.

[17] A.J. Poggio and E.K. Miller, "Techniques for Low-Frequency Problems," *Antenna Handbook: Theory, Applications, and Design*, Y.T. Lo and S.W. Lee, eds., New York NY, Van Nostrand Reinhold, 1988, p. 3-28.

[18] *PulsON™ Application Demonstrator Scanning Receiver*, Huntsville AL, Time Domain Corporation, 2000.

[19] Paul Withington, "Impulse Radio Overview," Time Domain Corporation, Huntsville AL.

[20] "Ansoft Corporation – Maxwell3D Main Page," http://www.ansoft.com/products/em/max3d/index.cfm, Ansoft Corporation, Philadelphia PA, 2000.

[21] Steven E. Schwarz, *Electromagnetics for Engineers*, New York, NY: Oxford University Press, Inc., 1990.

[22] H.J. Childs, *Physical Constants: Ninth (SI) Edition*, New York NY: Halsted Press 1972.

[23] www.bluetooth.com, Adcore Pyramid AB, 2001.

[24] James W. Nilsson and Susan A. Riedel, *Electric Circuits*, Reading MA: Addison-Wesley Publishing Co., 1996.

[25] Nadeem Bunni, Ansoft Corporation Technical Support, Email Correspondence, 29 March 2001.

A. Explanation of the Decibel

The decibel is a common unit in the analysis of signal strength. It is a measure of the power, P, of a signal relative to a known quantity, R [24 p. 591]. Mathematically, it is

$$P(\text{in dB}) = 10 \cdot \log_{10}\left(\frac{P(\text{in W})}{R(\text{in W})}\right)$$

That is, the power of a signal (in dB) is ten times the logarithm of that power (in watts) divided by a reference (in watts). This reference value may be a standard unit of power, such as a milliwatt. The decibel's convenience comes from the fact that it transforms proportions into sums. That is, the proportion of one power to another in watts is the (subtraction) difference between them in decibels. Additionally, the decibel allows a large dynamic range to be represented compactly, as shown by the decibel values listed below.

The reference power may be a standard unit of power, such as a milliwatt, the power of another signal, or the power of the same signal at another point. Often, the power of a signal after some event (such as attenuation) is compared to the power before. In such a case, a signal that has lost half of its power is said to have lost 3 dB. If this signal were to lose half its power again, bringing it to 25% of its original strength, it has lost another 3 dB, for a total of 6 dB.

If the decibel is referenced to a standard unit of power, such as a milliwatt, the abbreviation gets a special suffix. That is, a decibel referenced to a watt is a dBW. Likewise, a dBm is a decibel referenced to a milliwatt.

Some common decibel levels include

0 dB	Full power	0 dBm	1 milliwatt
-3 dB	Half power	-3 dBm	500 microwatts
-6 dB	One quarter power	-6 dBm	250 microwatts
-10 dB	One tenth power	-10 dBm	100 microwatts
-20 dB	One hundredth power	-20 dBm	10 microwatts
-30 dB	One thousandth power	-30 dBm	1 microwatt

B. Narrowband Test Analysis Programs

The MATLAB programs included in this appendix were used to analyze the data recorded during the narrowband tests.

ricecalc.m

```
CDF = ricecalc (k_factor,g_sigma,r_values)
Estes, Daniel RJ

This function creates a Ricean CDF with K = k_factor and standard
deviation sigma corresponding to the input vector r_values.  This CDF
output by this function is zero for all input values less than or equal
to zero.

k_factor = Ricean K factor
g_sigma  = standard deviation of component gaussian distributions
r_values = values at which to calculate CDF
```

kfind.m

```
[K,meanerr] = kfind(data,accuracy,PlotFlag)
Estes, Daniel RJ

This program will find the Ricean K factor of a set of data.
It finds the best-fit Ricean distribution for the data by minimizing
the mean square error. The program iteratively refines the k factor and
stops when it is within a given range of the actual k factor, as
defined by input accuracy.

data     - vector of data for which to calculate K (values assumed to
           be in dB)
accuracy - max interval by which calculated K will differ from actual K
PlotFlag - 1 to plot CDFs, 0 to not
K        - Ricean K factor
meanerr  - mean square error between data CDF and ricean curve

K = kfind(data,acc) assumes PlotFlag = 0, will not plot
K = kfind(data) assumes desired accuracy of .1 and PlotFlag = 0
```

shipanalyze.m

```
shipanalyze.m
Estes, Daniel RJ

This program analyzes the data taken aboard a ship for my trident
project.  It requires an information file in text format and data
files, also in text format, saved according to the following
convention: saved in directory d:\tests\xxxx where xxxx = name of the
ship in lower case letters

d_7108_4.txt
d              Type of ship (d = destroyer, c = cruiser, f = frigate,
                            etc)
 _71           Ship number
    08         Test frequency divided by 100 MHz
      _4       Test #

This program requires that at least one measurement has been taken,
labeled as test 1, and stored with the above file name convention.
```

reference.m

```
reference.m
Estes, Daniel RJ

This program will reference the data from one shipboard test to that of
another.  It requires the data to first be analyzed by 'shipanalyze.m'
and that each test contain the same number of data points.
```

```
function CDF = ricecalc (k,sigma,r)
% CDF = ricecalc (k_factor,g_sigma,r_values)
% Estes, Daniel RJ
%
% This function creates a Ricean CDF with K = k_factor and standard deviation sigma
% corresponding to the input vector r_values.  This CDF output by this function is
% zero for all input values less than or equal to zero.
%
% k_factor = Ricean K factor
% g_sigma  = standard deviation of component gaussian distributions
% r_values = values at which to calculate CDF
;
delta=.004;
v=0:delta:50;                                          % initial argument of CDF function
xrice=(v/sigma^2).*exp(-(v.^2+k^2)/(2*sigma^2)).*besseli(0,k*v/sigma^2); % Ricean pdf
ave=delta*sum(v.*xrice);                               % calculate average from pdf
x_vals=v/ave;                                          % x_values corresponding to xrice pdf
rrice=interp1(x_vals,xrice,r);                         % re-map pdf to correspond to input r values
CDF=cumsum(rrice)/sum(rrice);                          % create Ricean CDF by integrating
CDF;
```

```
function [k,meanerr] = kfind (data,acc,pflag)
% [K,meanerr] = kfind(data,accuracy,PlotFlag)
% Estes, Daniel RJ
%
% This program will find the Ricean K factor of a set of data.
% It finds the best-fit Ricean distribution for the data by minimizing the mean square error.
% The program iteratively refines the k factor and stops when it is within a given range of
% the actual k factor, as defined by input accuracy.
%
% data     - vector of data for which to calculate K (values assumed to be in dB)
% accuracy - max interval by which calculated K will differ from actual K
% PlotFlag - 1 to plot CDFs, 0 to not
% K        - Ricean K factor
% meanerr  - mean square error between data CDF and ricean curve
%
% K = kfind(data,acc) assumes PlotFlag = 0, will not plot
% K = kfind(data) assumes desired accuracy of .1 and PlotFlag = 0
;
switch nargin                                       % determine number of input arguments
case 1                                              % if only one argument
   acc=.1;                                          %  assume desired accuracy of .1

   pflag=0;                                         %  assume no plot desired
case 2                                              % if only two arguments
   pflag=0;                                         %  assume no plot desired
case 3                                              % if all arguments defined, do nothing
case 0                                              % if no arguments, declare error
   error('Not enough arguments for function kfind.  Type ''help kfind''.');
otherwise                                           % if too many arguments, declare error
   error('Too many arguments for function kfind.  Type ''help kfind''');
end
%
% First convert data into non-dB values
abs_data=10.^(data/20);                             % convert from dB to absolute values
%
% Normalize data by removing offset and dividing by the mean
%no_off_data=abs_data-min(abs_data);                   % bring lowest value to zero
%norm_data=no_off_data/mean(no_off_data);           % divide by the mean, data is now normalized
```

```
norm_data=abs_data/mean(abs_data);
%
% Create distribution function for data
[hgram,x_vals]=hist(norm_data,200);            % create histogram of normalized data with 200 bins
pdf=hgram/sum(hgram);                          % create pdf from histogram
CDF=cumsum(pdf);                               % integrate pdf to obtain CDF
%
% The K-finding routine will create a ricean CDF for three k-values.  It will then compare the mean
% square error (mse) of each CDF compared to the data CDF.  It then "homes in" on the lowest mse until
% the differences between the possible values of K is less than the user-defined accuracy (acc).
%
% Initialize iteration process
K=[2 3 4];                                     % create initial K vector
errl=ricecalc(K(1),1,x_vals)-CDF;              % find error between lower K and data CDFs
errc=ricecalc(K(2),1,x_vals)-CDF;              % find error between middle K and data CDFs
errh=ricecalc(K(3),1,x_vals)-CDF;              % find error between upper K and data CDFs
mse=[mean(errl.^2) mean(errc.^2) mean(errh.^2)]; % find mean square errors at each K
oot=1;                                         % assume not within desired accuracy (out of
tolerance)
incr=1;                                        % increment k by one when searching for correct value
%
% Iteratively search for k
while(oot)                                          % loop until k is within desired accuracy
   slope(1:2)=(mse(2:3)-mse(1:2))./(K(2:3)-K(1:2));% find differences between successive mse points
                                                    (slopes)
   if ((slope(1)>0)&(slope(2)>0))                 % if both slopes are positive, lower guesses for k
      K=K-incr;                                    %  shift all points down one increment
      errl=ricecalc(K(1),1,x_vals)-CDF;            %  calculate error at new lower bound
      mse=[mean(errl.^2) mse(1:2)];                %  figure new mean square error
   elseif ((slope(1)<0)&(slope(2)<0))             % if both slopes are negative, raise guesses for k
      K=K+incr;                                    %  shift all points up one increment
      errh=ricecalc(K(3),1,x_vals)-CDF;            %  calculate error at new upper bound
      mse=[mse(2:3) mean(errh.^2)];                %  figure new mean square error
   else                        % if one slope is negative and one positive, k is between K(1) and K(3)
      oot=(incr>acc);               %  returns 1 if actual k could differ from real k by more than acc
      incr=incr/2;                                 %  divide increment in half
      K=K(2)+[-incr 0 incr];                       %  create new K vector
      errl=ricecalc(K(1),1,x_vals)-CDF;            %  calculate error at new lower bound
```

```
      errh=ricecalc(K(3),1,x_vals)-CDF;              %  calculate error at new upper bound
      mse=[mean(errl.^2) mse(2) mean(errh.^2)];      %  figure new mean square errors
   end
end
if K(2)>0
   k=K(2);                                           % loop only exited when middle K value within
acc of actual value
else
   k=0;                                              % k will never actually be below zero.
end;
meanerr=mean((ricecalc(k,1,x_vals)-CDF).^2);         % find mean square error associated with K
%
% If desired, show CDF and Ricean CDF
d=0;                                                 % initialize d, the number of decimal places to
show for K
while(floor(acc)~=acc)                               % while acc has at least one decimal place
   d=d+1;                                            % increment d
   acc=acc*10;                                       % move decimal place of acc to the right
end                                                  % d now equals the number of decimal places in
accuracy
kdisp=sprintf(['%0.' int2str(d) 'f'],k);             % write k value into a string with proper number
of decimal places
msedisp=sprintf('%0.6f',meanerr);                    % write mse into a string with six decimal
places
if pflag
   plot(x_vals,CDF,'b');
   axis([0 3 0 1]);
   hold on;
   plot(x_vals,ricecalc(k,1,x_vals),'r:');
   hold off;
   title(['Ricean Distribution with K = ' kdisp ' and mse = ' msedisp]);
   xlabel('Normalized Power');
   ylabel('Cumulative Probability');
   legend('data','Ricean CDF',2);
end
```

```
% shipanalyze.m
% Estes, Daniel RJ
%
% This program analyzes the data taken aboard a ship for my trident project.  It requires
% an information file in text format and data files, also in text format, saved according
% to the following convention:
%
% saved in directory d:\tests\xxxx where xxxx = name of the ship in lower case letters
%
% d_7108_4.txt
% d               Type of ship (d = destroyer, c = cruiser, f = frigate, etc)
%  _71            Ship number
%     08          Test frequency divided by 100 MHz
%       _4        Test #
%
% This program requires that at least one measurement has been taken, labeled as test 1,
% and stored with the above file name convention.
;
% Change to test file directory
sname=input('What is the name of the ship? (Ex: ''Philo'') ');    % Ask for name of ship
cd(['d:\tests\' strtok(lower(sname))]);                           % Open corresponding directory
%
% Find out if the user wants the results plotted and/or printed
plflag=~~input('Do you want the results plotted? (0 = no) ');
if plflag
   prflag=~~input('Do you want the plots printed? (0 = no) ');
end;
%
% Find the type and number of ship
test=dir('*_1.txt');                                              % find the first test's files
type=test(1).name(1);                                             % read first letter
cnumber=test(1).name(2:4);                                        % read hull number as characters
if cnumber(2)=='_'                                                % if the number is 1 digit
   h_number=str2num(cnumber(3));                                  % read in 1 digit
elseif cnumber(1)=='_'                                            % if the number is 2 digits
   h_number=str2num(cnumber(2:3));                                % read in 2 digits
else                                                              % otherwise number is 3 digits, so
   h_number=str2num(number);                                      % read in 3 digits
```

```
end
%
% determine number of measurements in first test
n=1;                                                    % n = test to find measurements for
n_test='_1';                                            % also create ascii label for the
test number
[i k] = size(test);                                     % i = number of measurements
%
% loop through all tests
while i                                                 % quit if there were 0 measurements
in test
   for j=1:i
      file(j,:)=test(j).name;                           % read list of files into array
   end
   file=sortrows(file);                         % put files in numerical (therefore frequency) order
   freq=[];                                             % reinitialize variables
   pave=[];
   pvar=[];
   pmax=[];
   pmin=[];
   weight=[];
   abspave=[];
   err=[];
   kfact=[];
   mse=[];
   for j=1:i                                            % loop through all measurements
      freq(j)=str2num(file(j,5:6))/10;                  % find frequency in GHz
      data=load(file(j,:));                             % read in data
      absdata=10.^(data/10);                            % convert data from dB to W
      [kfact(j),mse(j)]=kfind(data,.1,plflag);  % calculate K factor within .1 of actual K (convert
                                                  power dB to voltage dB)
      abspave(j)=mean(absdata);                         % find mean power in W
      pave=10*log10(abspave);                           % convert mean power into dB
      pvar(j)=var(data);                                % find variance
      pmax(j)=max(data);                                % find maximum power received
      pmin(j)=min(data);                                % find minimum power received
      weight(j)=length(data);                           % find number of points
      err(j)=sqrt(pvar(j)/weight(j));                   % find the error value
```

```
   if plflag
      title(['K factor from test ' int2str(n) ' aboard ' sname ' at ' num2str(freq(j)) ...
               ' GHz; K = ' num2str(kfact(j))]);
      text(2,.4,['K   =  ' num2str(kfact(j),'%4.1f') ],'FontName','Courier New','Fontsize',10);
      text(2,.365,['mse =  ' num2str(mse(j),'%10.7f')],'FontName','Courier New','Fontsize',10);
      text(2,.330,['ave = ' num2str(pave(j),'%6.2f') ' dBm'],'FontName','Courier New',...
               'Fontsize',10);
            text(2,.295,['std =  ' num2str(sqrt(pvar(j)),'%6.2f') ' dBm'],'FontName',...
               'Courier New','Fontsize',10);
            text(2,.260,['max = ' num2str(pmax(j),'%6.2f') ' dBm'],'FontName','Courier New',...
               'Fontsize',10);
            text(2,.225,['min = ' num2str(pmin(j),'%6.2f') ' dBm'],'FontName','Courier New',...
               'Fontsize',10);
      text(2,.190,[int2str(weight(j)) ' Data Points'],'FontName','Courier New','Fontsize',10);
      if prflag
         print;
      else
         pause;
      end;
   end;
end
save([type cnumber n_test],'freq','pave','pvar','pmax','pmin','weight','kfact','mse','err');
                                                                  % save analysis for this test
%
% Display results in table format
disp(' ');
disp(['Test aboard USS ' sname]);
disp(' ');
disp(['Test number: ' int2str(n)]);
disp(['Frequency (GHz)  Ricean K           K MSE        Max Power (dBm)  Ave Power (dBm)  '...
            'Min Power (dBm)  Power STD (dBm)  Error Value  Number of Points']);
for j=1:i
   fprintf(1,'   %6.3f           %2.1f        %12.6f            %5.1f           %5.1f         '...
      '%5.1f         %5.1f         %10.2f      %10.0f\n',freq(j),kfact(j),mse(j),...
      pmax(j),pave(j),pmin(j),sqrt(pvar(j)),err(j),weight(j));
end
%figure(n+1);                                              % plot results on figure n
%errorbar(freq,pave,err,'*');                              % plot average power response as a
```

```
   %plotid=['Test aboard USS ' sname];
   %testid=sprintf('; test number %d', n);
   %title([plotid testid]);
   %xlabel('Frequency (GHz)');
   %ylabel('Received Power (dBm)');

   %print -dmeta                                          % copy plot to the clipboard as a meta file

   disp('Press any key to continue');
   pause;

   n=n+1;                                                 % increment test to find measurements for
   switch n>9
   case 0,                                                      % if this is the 9th test or less
      n_test=['_' int2str(n)];                                  % add a '_' to the number (_2 to _9)
   otherwise,                                                   % if not
      n_test=int2str(n);                                        % just turn number into ascii
   end
   test=dir(['*' n_test '.txt']);                         % find files corresponding to this test
   [i k] = size(test);                                    % i = number of measurements in test n
end
%
% Save file with ship information in directory
num_tests=n-1;
save('shipinfo','sname','type','cnumber','num_tests');
```

```
% reference.m
% Estes, Daniel RJ
%
% This program will reference the data from one shipboard test to that of another.
% It requires the data to first be analyzed by 'shipanalyze.m' and that each test contain
% the same number of data points.
;
% Change to test file directory
sname=input('What is the name of the ship? (Ex: ''Philo'') ');    % Ask for name of ship
cd(['d:\tests\' strtok(lower(sname))]);                           % Open corresponding directory
%
% Read in ship data
load shipinfo;                      % This automatically loads sname, h_number, num_tests_, and type
%
% Find out which test to reference to which
i=1;
while(i)
   base=input(sprintf('Which of these %d tests would you like to be the baseline? ',num_tests));
   i=((base<1)|(base>num_tests));
end
i=1;
while(i)
   refd=input(sprintf('Which of these %d tests would you like to be referenced? ',num_tests));
   i=((refd<1)|(refd>num_tests));
end
%
% Load baseline file
switch (base>9)
case 0,                                                  % If the base test has a single digit
   b_test=['_' int2str(base)];                              % add a '_' to the front (_1 to _9)
otherwise,                                                  % if it has two
   b_test=int2str(base);                                 % just convert the number into a string
end
b=load([type cnumber b_test]);
%
% Load referenced file
switch (refd>9)                                       % perform same number to string conversion
case 0,
   r_test=['_' int2str(refd)];
```

```
otherwise,
   r_test=int2str(refd);
end
r=load([type cnumber r_test]);
%
% Reference power levels, variance, error vaule, and K factor.
ploss=b.pave-r.pave;                                                    % Power loss is simply subtraction
tot_var=(b.pvar.*b.weight+r.pvar.*r.weight)./(b.weight+r.weight); % Variance is scaled by weight,
                                                                         added, then divided by total weight
tot_err=b.err+r.err;
kdiff=b.kfact-r.kfact;                                                  % find difference between K factors
aveloss=mean(ploss);                                                    % The average loss is the mean of
the losses
%
% Transfer frequency information to saveable information
freq=b.freq;
%
% Save referenced information
desc=input('Please enter a brief description of this data. (Ex: ''Power Loss across 1-100-2'') ');
save([type cnumber r_test b_test],'freq','ploss','tot_var','tot_err','desc','kdiff');
%
% Display results in table format
disp(' ');
disp(['Test aboard USS ' sname]);
disp(' ');
disp(desc);
disp(['Frequency (GHz)     ' num2str(freq,'%7.3f')]);
disp(['Power Loss (dBm) ' num2str(ploss,'%7.1f')]);
disp(['Power St. Dev. (dBm)   ' num2str(sqrt(tot_var),'%7.1f')]);
disp(['Error Val (dBm)     ' num2str(tot_err,'%7.2f')]);
disp(['K Difference     ' num2str(kdiff,'%7.2f')]);
disp(' ');
disp(['Average Loss (dBm)  ' num2str(aveloss,'%7.2f')]);
disp(['Average K Difference   ' num2str(mean(kdiff))]);
disp(' ');
%
% Plot referenced information
errorbar(freq,ploss,sqrt(tot_err),'*');                                 % plot power difference
hold on
```

```
plot(freq,aveloss*ones(1,length(freq)),':');                    % plot dotted line at mean
hold off
plotid=['Test aboard ' sname];
refid=sprintf('; Test %d referenced to test %d',refd,base);
title([plotid refid ' ; ' desc]);
if aveloss>10
   lossdisp=sprintf('%4.1f',aveloss);
else
   lossdisp=sprintf('%4.2f',aveloss);
end
xlabel(['Frequency (GHz); Average Loss ' lossdisp ' dB']);
ylabel('Power Loss (dB)');
%
% Save a copy of the graph on the clipboard as a meta file
print -dmeta;
```

C. Maxwell3D

Ansoft Corporation's electromagnetic field solver, Maxwell3D, was used for computer simulations during this project. This program is a finite-element modeling program, which iteratively solves Maxwell's Equations, the characteristic differential equations for electromagnetic systems, at points located throughout the geometry of the simulation. This set of points is referred to as the "mesh", and is refined between iterations—in areas of high field gradient, for example—to make the solution more accurate.

Before Maxwell3D was started, an environmental variable was created in the operating system. The variable use_abc_boundary was set to 1. This instructed the program to not simulate reflections from the boundaries of the solution region. The program was then started and operated in steps, including *Create*, *Draw*, *Setup Materials*, *Setup Boundaries/Sources*, *Setup Solution*, *Solve*, and *Post Process* (Fig. 52).

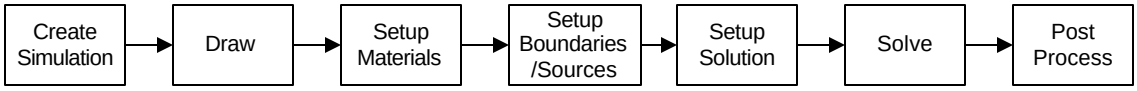

Figure 52 Simulation Process.

Create

First the simulation had to be created. This was done from the Maxwell3D project manager by clicking the "New" button (Fig. 53). This prompted the user to enter a name for the simulation. Once it was named and created, it was defined as an eddy current simulation from the field simulator interface (Fig. 54).

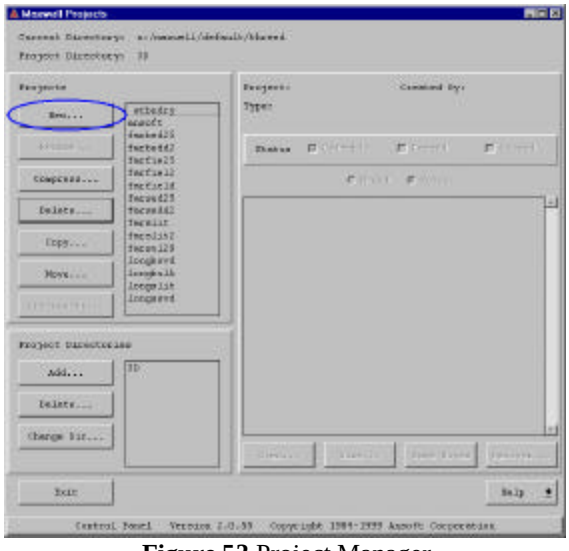

Figure 53 Project Manager.

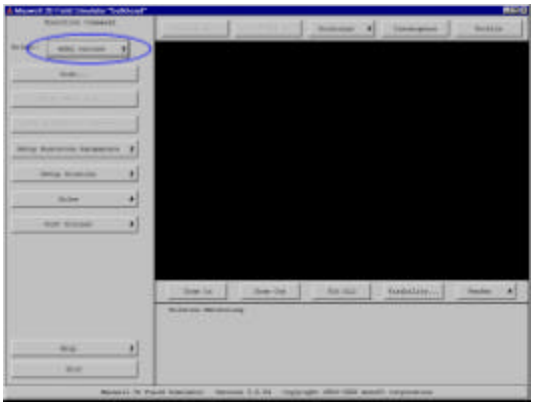

Figure 54 Field Simulator Interface.

Draw

Before drawing the scenario, it was decided that the simulation would be run for radio waves at 800 MHz. This is due to the fact that, according to the relation

$$c = f \cdot l$$

this frequency has the longest wavelength, ë, of all frequencies studied in this project—14.9 inches. This allows mesh points to be spaced farther apart, thereby requiring fewer points and making the simulation smaller.

The *Draw* module allowed the user to create the objects to be included in the simulation. These objects were drawn in a three-dimensional coordinate system (x, y, z). The unit of distance had to be chosen so that all dimensions in the simulation were between 1e-5 and 10000. For best results, the dimensions should be between 0.1 and 100. Based on these requirements, the best unit for this simulation was determined to be the inch. Therefore, all coordinates are expressed in terms of inches.

Simulation Region

Maxwell3D solves for fields within a region in space. All objects must be located inside this region. To define this region, the menu option **Options→Region→Define** was selected. This prompted the user to enter two points. The region created was a rectangular prism (box) with opposite vertices on these two points. The points chosen for the simulations done in this project were at (0, 15, 15) and (195, -15, -15), meaning that the region stretched from 0 to 195 in the x direction, -15 to 15 in the y direction, and -15 to 15 in the z direction (Fig. 55).

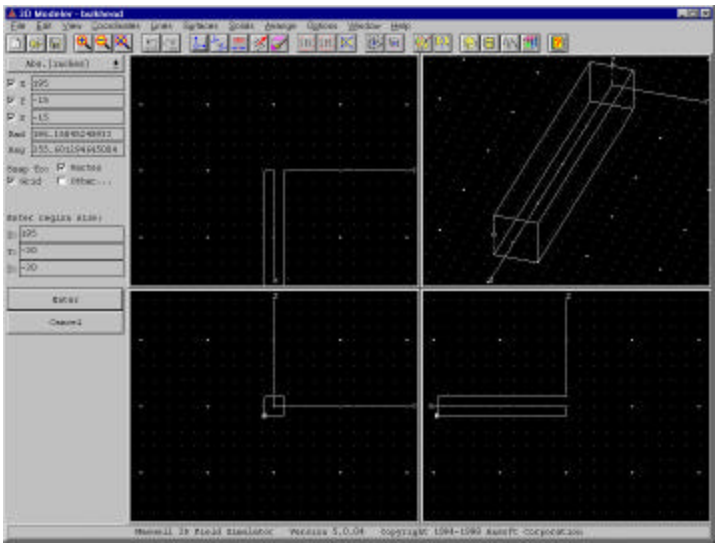

Figure 55 Defining The Simulation Region.

Antenna

The antenna was a section of a rectangular coil. It was created by the following steps:

The outer wall of the coil was defined as a rectangle. Menu option **Lines→ Rectangle** was selected. The user was prompted for two points. The first point was selected as (3.8, 0.1, 7.5). The second point was chosen as (-3.8, 0.1, -7.5), and was defined as being parallel to the XZ plane. The rectangle was defined as "not covered", meaning it created a loop rather than a plate, and was named coil_out. The color bright green was selected for this rectangle (Fig. 56).

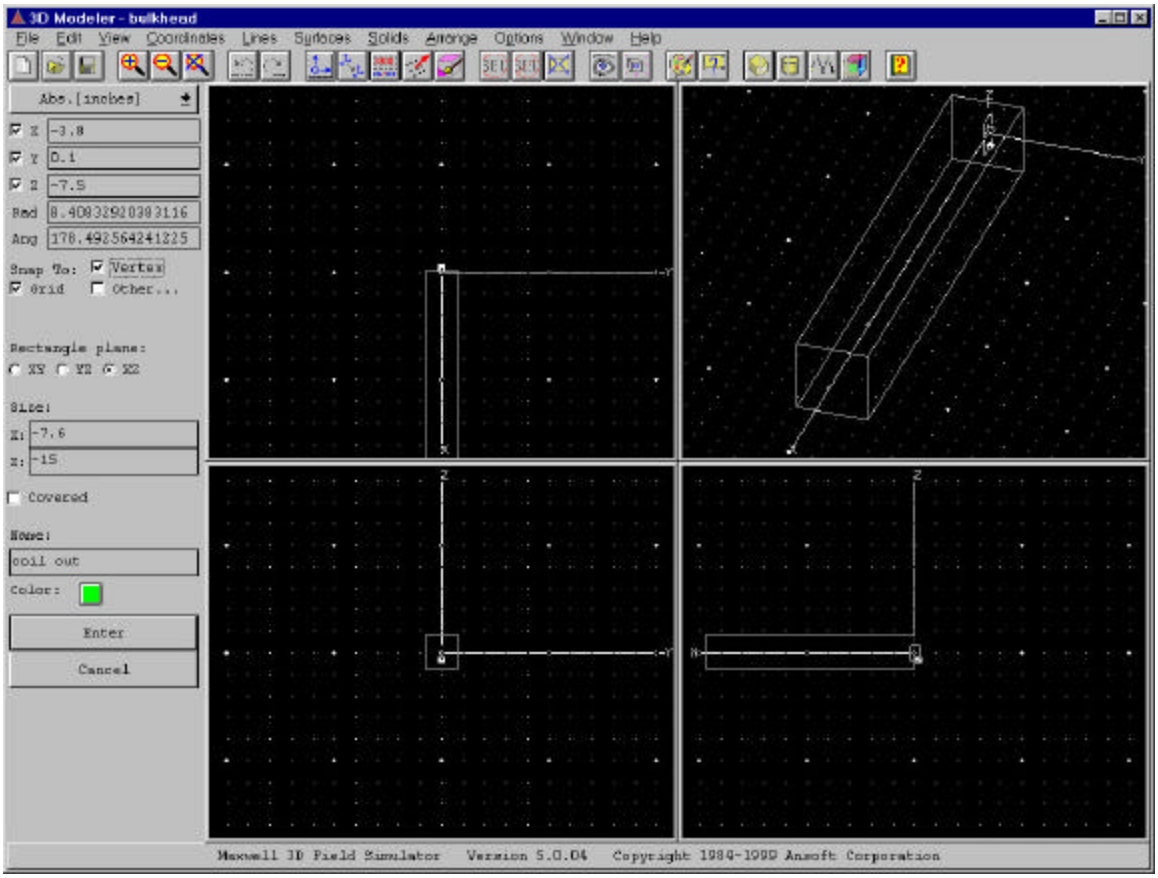

Figure 56 Defining coil_out.

The coil inner wall was also defined as a rectangle loop in the same fashion. The two points chosen for this coil were (3.6, 0.1, 7.3) and (-3.6, 0.1, -7.3), and it was named coil_in.

These two rectangles were then "connected", to create a new object, which had the shape of a picture frame. This was done by selecting **Surfaces→Connect**, which prompted the user to choose the objects to be connected; coil_out and coil_in were chosen. This created a light gray picture frame-shaped object named Connect. The option **Edit→Attributes→By Clicking** was then selected, and the object was renamed coil. The color changed to bright green (Fig. 57).

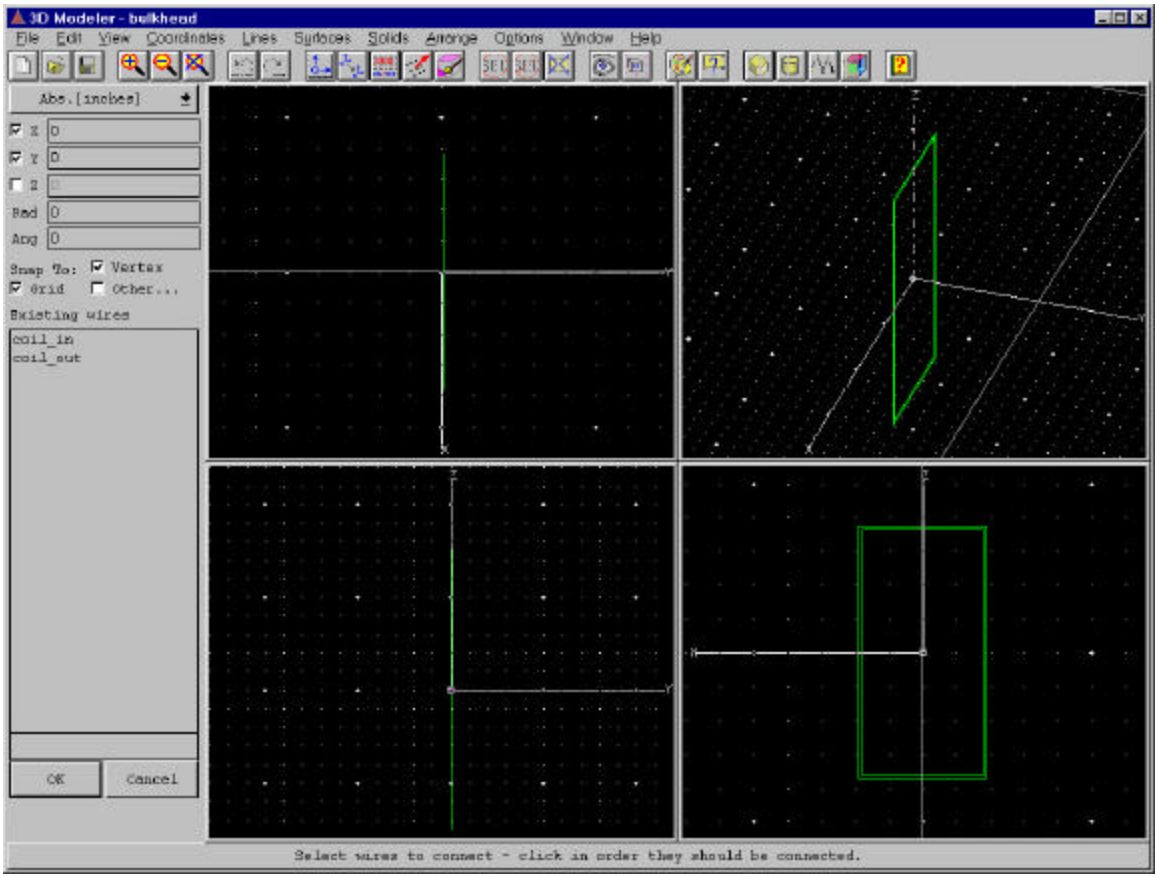

Figure 57 Connecting coil_out and coil_in.

In order to run the simulation, no objects could extend outside of the simulation space. Since this space had been defined to not extend into the negative-x region, any object which did had to either be deleted or modified. Since coil_out and coil_in had been used to create the coil, and were no longer needed, they were deleted. This was done by pressing the "Sel" (select) button on the tool bar, choosing the names coil_out and coil_in from the list of objects that appeared, and pressing the delete button.

However, the coil was modified. This was done by deleting only the part which extended outside the simulation space. The menu option **Solids → Split** was selected, which prompted the user to select the plane to cut across, the region to retain, and the object to split. The YZ plane was chosen, and the option "Above Plane" was selected. Then the coil was selected. This cut the coil at the x=0 plane and deleted everything in the negative-x region (Fig. 58).

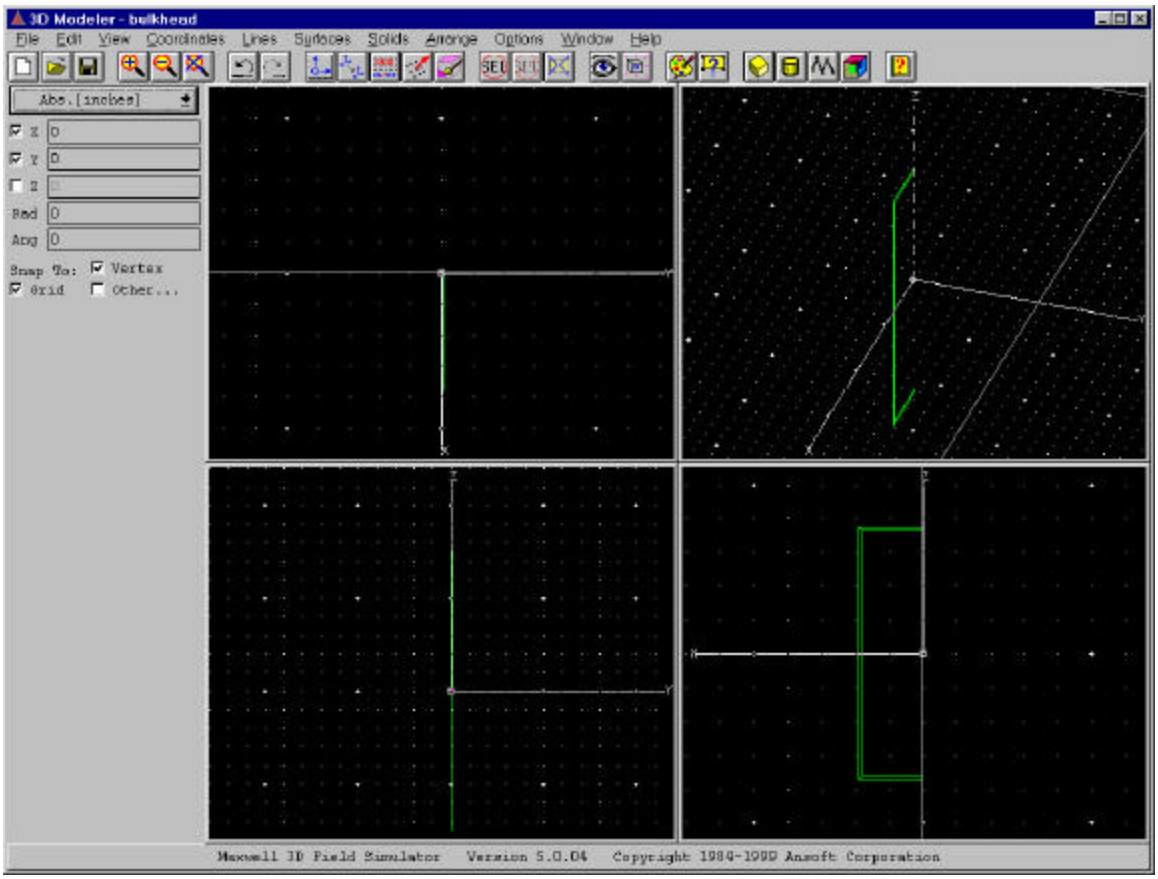

Figure 58 Result of Split Command.

The antenna was then finished by creating a solid from the two-dimensional coil. The menu option **Solids → Sweep → Along Vector** was chosen, which prompted the user to select an object. The coil was selected, at which point the user was prompted for the vector to sweep the object along, which was defined as (0, -.2, 0). This expanded the coil from a two-dimensional object to a three-dimensional solid extending it in the y direction from -0.1 to 0.1 (Fig. 59).

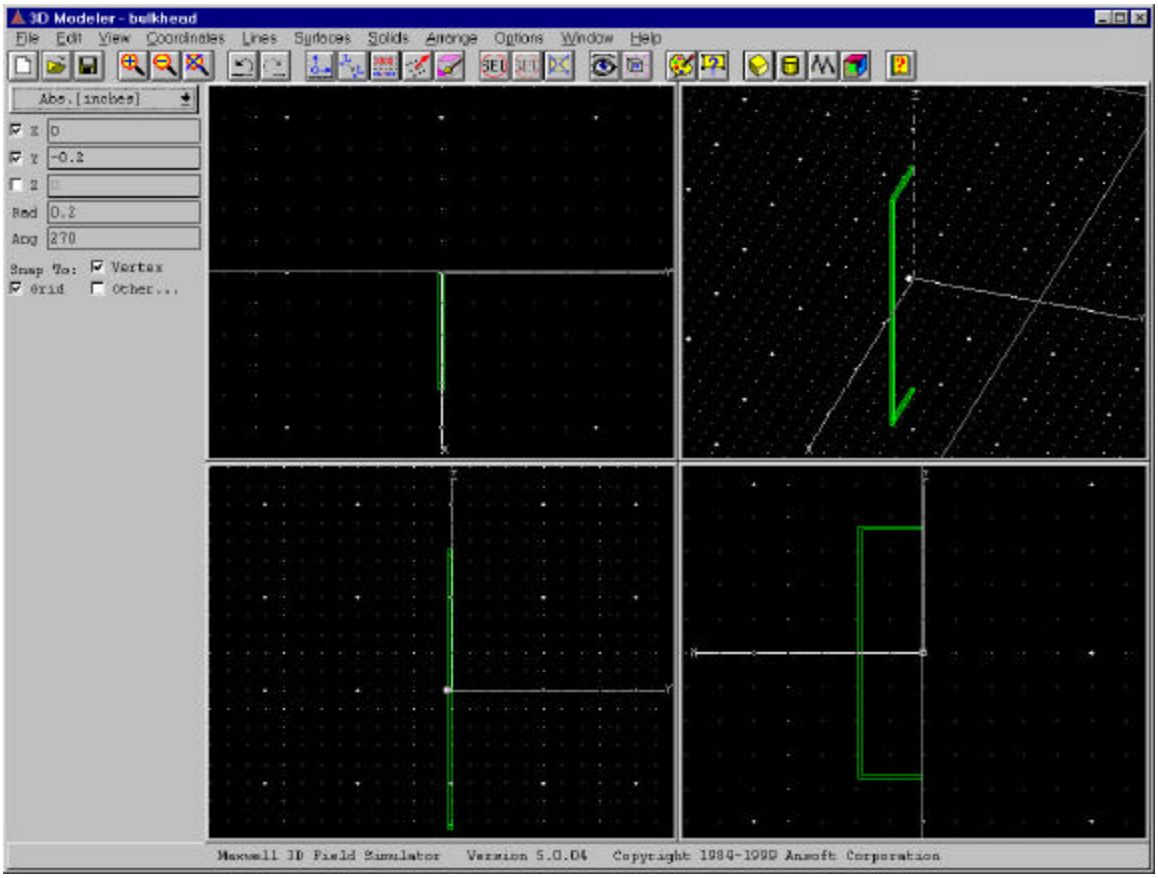

Figure 59 Result of Sweep—Create coil.

In order to provide current to the coil later—during the *Setup Boundaries/Sources* step—two terminals were created on the ends of the coil at the intersection with the simulation boundary. The top terminal, named "top", was created by selecting **Lines→ Rectangle** and choosing points (0, 0.1, 7.5) and (0, -0.1, 7.3). The bottom terminal, "bottom" was similarly created with points (0, 0.1, -7.5) and (0, -0.1, -7.3). The option "covered" was selected when these objects were created, and the color selected for these terminals was yellow (Fig. 60).

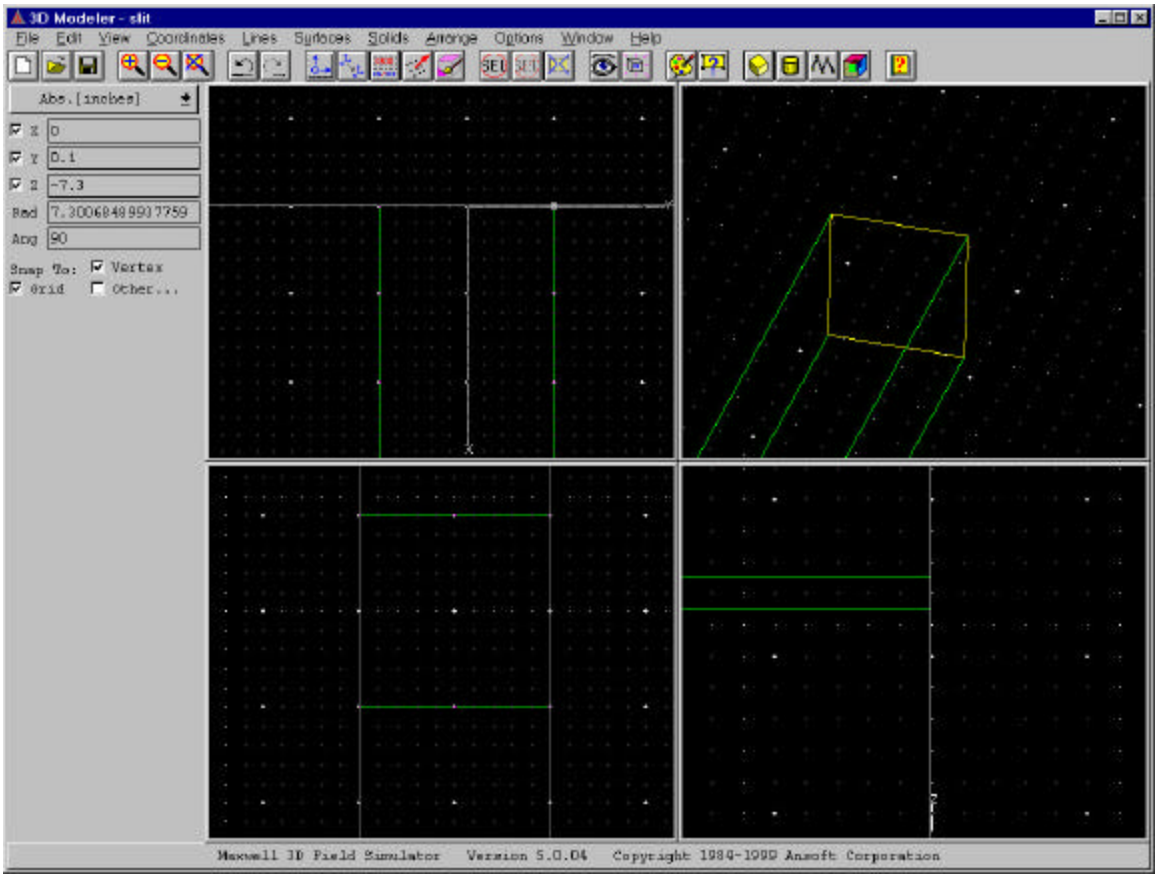

Figure 60 Creation of Terminal Object.

Bulkhead

A bulkhead was simulated by a .5-inch-thick box parallel to the YZ plane and extended across the entire cross-section of the simulation space. This box was defined by selecting menu option **Solids → Box**. The user was prompted for two points, the first point was selected as (165, 15, 15). This placed the bulkhead 165 inches from the antenna—over ten wavelengths away. This was done so the effect of the bulkhead on the antenna would be negligible. The second point was chosen as (165.5, -15, -15). Therefore, the box was .5 inches thick and extended across the entire simulation space in the Y and Z directions. The box was named "bulkhead", and the color was selected as light blue (Fig. 61).

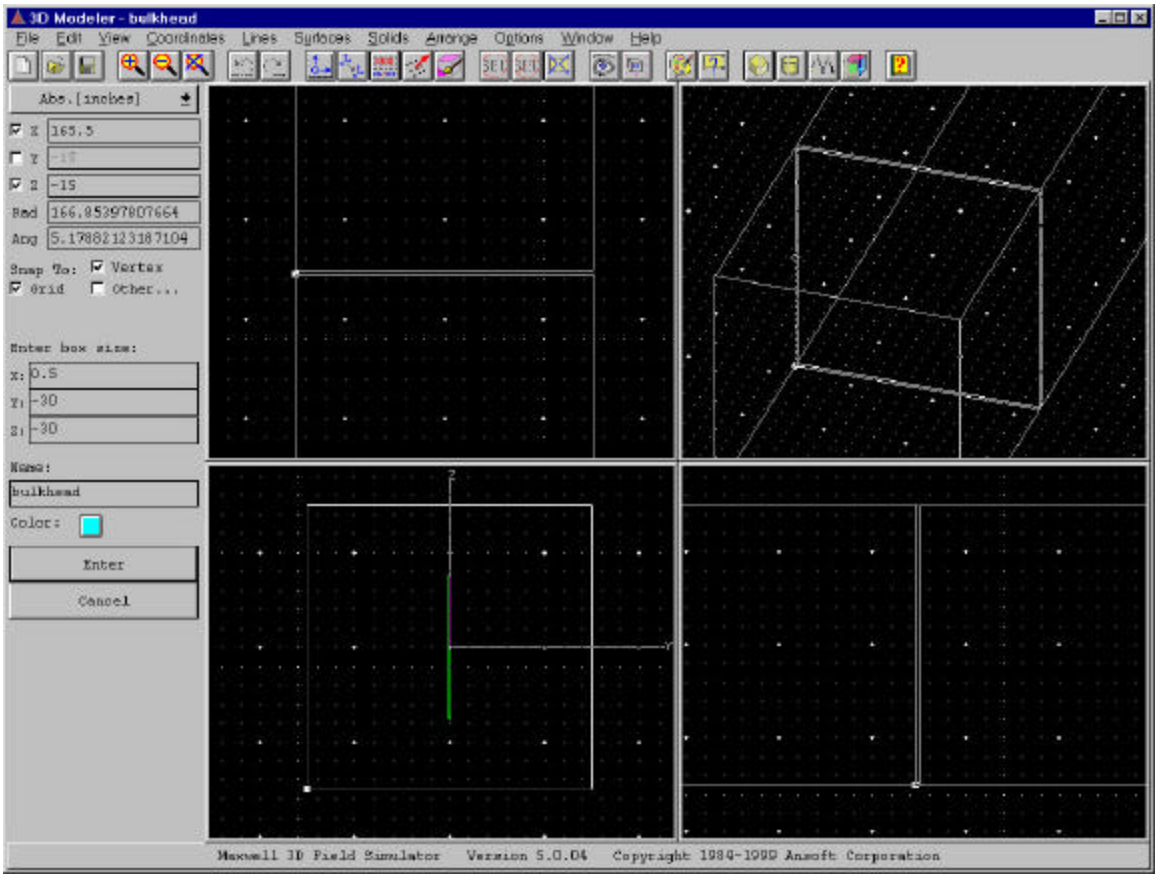

Figure 61 Defining bulkhead**.**

Other Objects

Several other objects were created to help analyze the results. Rather than representing physical objects in the scenario, these were surfaces to be used for calculations. Two rectangles were defined along the x axis to allow a representation of the electromagnetic wave to be displayed during the *Post Process* step. The first

rectangle, x_axis, extended from (5, 0, 0.1) to (150, 0, -0.1), and the second, far_x, from (150, 0, 0.1) to (195, 0, 0.1).

The two most important surfaces, however, were those used to calculate the power in the electromagnetic wave. They were placed 15 inches on either side of the bulkhead and extended from (150, -10, -10) to (150, 10, 10) and from (180., -10, -10) to (180, 10, 10). They were named near_int and int_surf, respectively. After the electromagnetic fields were solved, the power flowing through these two surfaces would be compared to determine the effect of the bulkhead on the transmitted wave (Fig. 62).

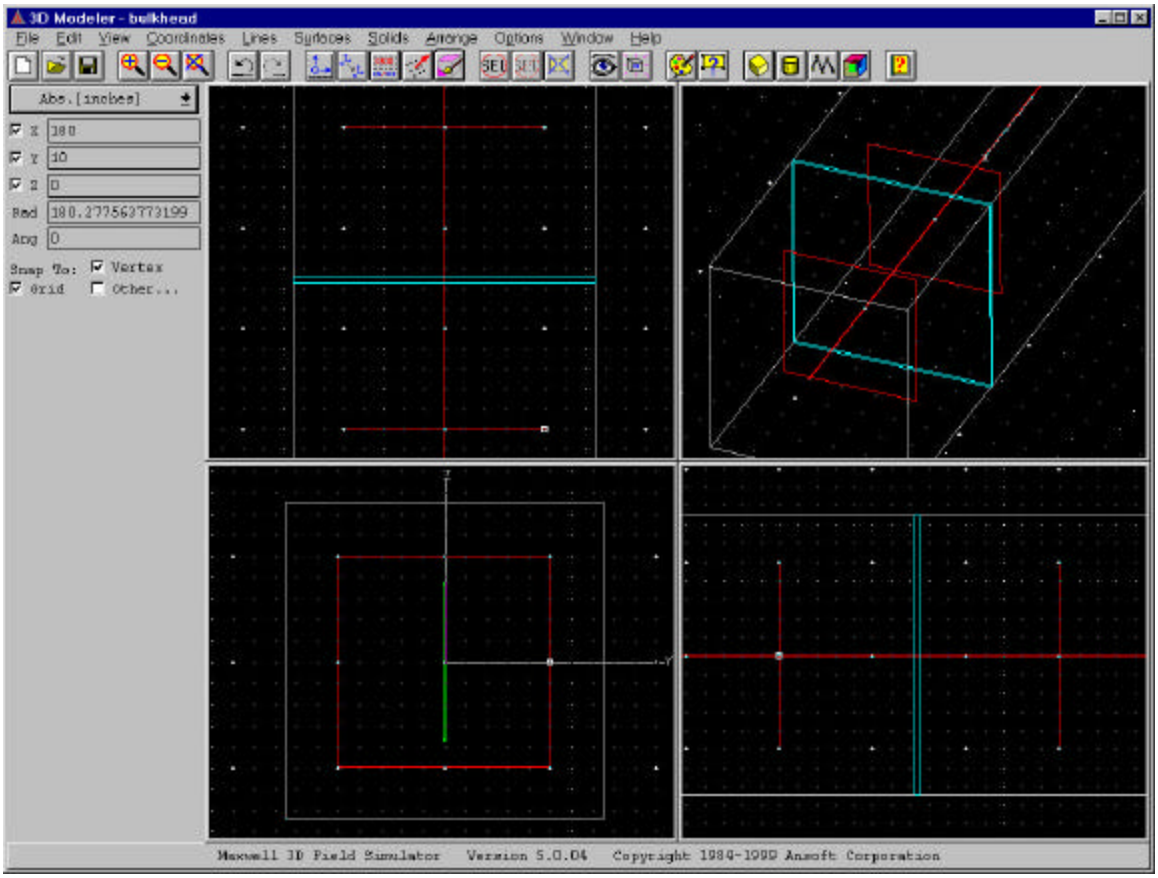

Figure 62 Surfaces Included in Model.

Two scenarios

At this point, the simulation was copied to another file in order to have two scenarios: one with a solid bulkhead, and one with a slit through the middle of the bulkhead. The slit was added to the second scenario by defining a new box, named slit, from (165, 0.1 , 15) to (165.5, -0.1, -15). This slit was then incorporated into the bulkhead in the following manner:

The area where the slit was to go was subtracted from the bulkhead. Doing this would split the bulkhead into two objects and would delete the slit object entirely. Therefore, the slit was copied to the clipboard before the operation was performed. The menu option **Solids → Subtract** was selected. The user was prompted to select the object *to be subtracted from*—in this case, the bulkhead. The user was then prompted for the object *to subtract*. For this, the slit was selected. This removed the intersection of the bulkhead and slit, effectively splitting the bulkhead into two parts and creating a .2-inch gap between them (Fig. 63). These two parts were renamed bulkheadr (for bulkhead right) and bulkheadl. The slit was then pasted back into the model to simulate a rubber seal between the two sections of the bulkhead (Fig. 64).

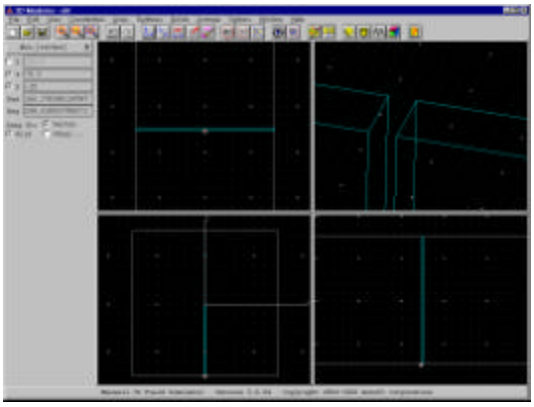

Figure 63 Slit Region Removed From bulkhead.

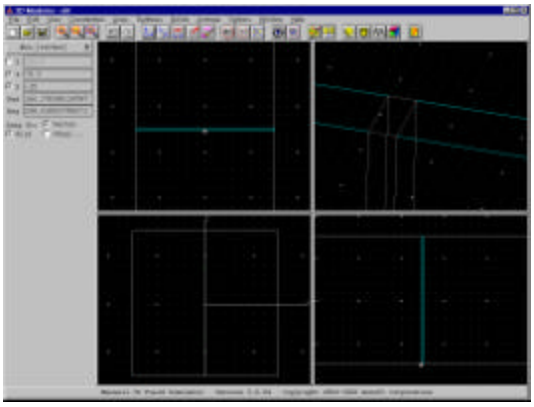

Figure 64 Slit Embedded in bulkhead.

Setup Materials

Once the scenario was drawn, the material properties of the objects needed to be assigned. This was accomplished in the *Setup Materials* module. In this module, the user was able to select three-dimensional objects and assign a material to that object.

Copper was selected as the material for the coil, and hard rubber for the slit. These two materials were already defined within the program. The steel for the bulkhead, however, had to be defined by the user because Maxwell3D's Eddy Current Solver could not operate with non-linear materials, as the two types of steel already included in Maxwell3D were. That is, the Eddy Current solver could not simulate materials whose response to an applied magnetic field changes with the magnitude of that field. This does not affect the accuracy of the simulation, because these non-linearities occur at much higher field intensities than those in electromagnetic waves.

This material was defined by selecting steel_1010, one of the non-linear steels already included in the software, and selecting **Material→Derive** to create a new material with the same characteristics. Because the effect of the bulkhead is so great that it can be modeled as a perfect conductor, this option was selected. The material was renamed "steel" (Fig. 65).

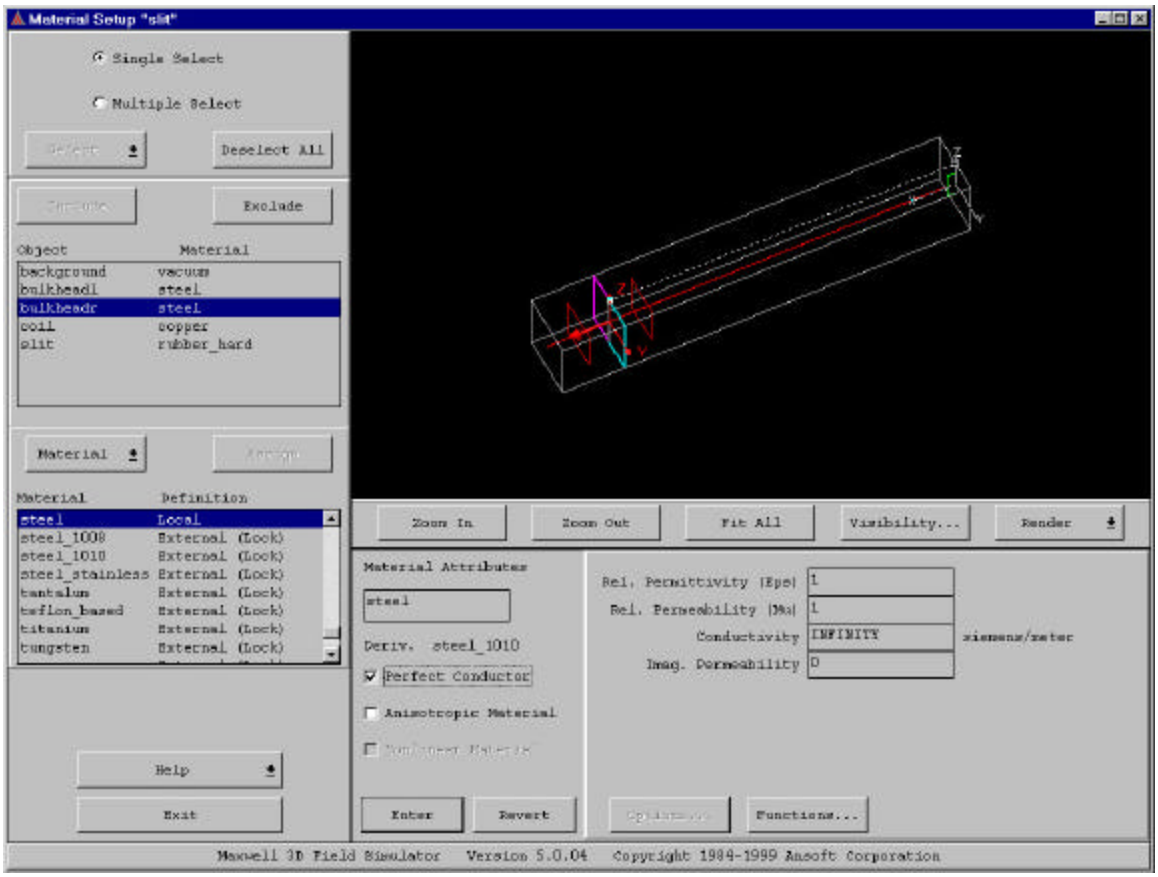

Figure 65 Material Assignment—Derivation of Steel.

Setup Boundaries/Sources

After the geometry was created and the materials assigned, the boundary conditions and current source had to be defined. This was done in the *Setup Boundaries/Sources* module of Maxwell3D. Additionally, this module prompted the user to identify whether or not to solve for eddy current and displacement current in each object. Since none of the objects in the simulation are perfect conductors, there is displacement current—time-varying electric fields induced by time-varying magnetic fields—in all objects. Therefore, the program was instructed to solve for this effect in all objects. Eddy current—movement of charge induced by time-varying magnetic fields—only occurs in conductive objects. Therefore, the program was only instructed to solve for eddy current in the bulkhead and in the rubber slit, which had a conductivity of 1e-15 Siemens per meter (Fig. 66).

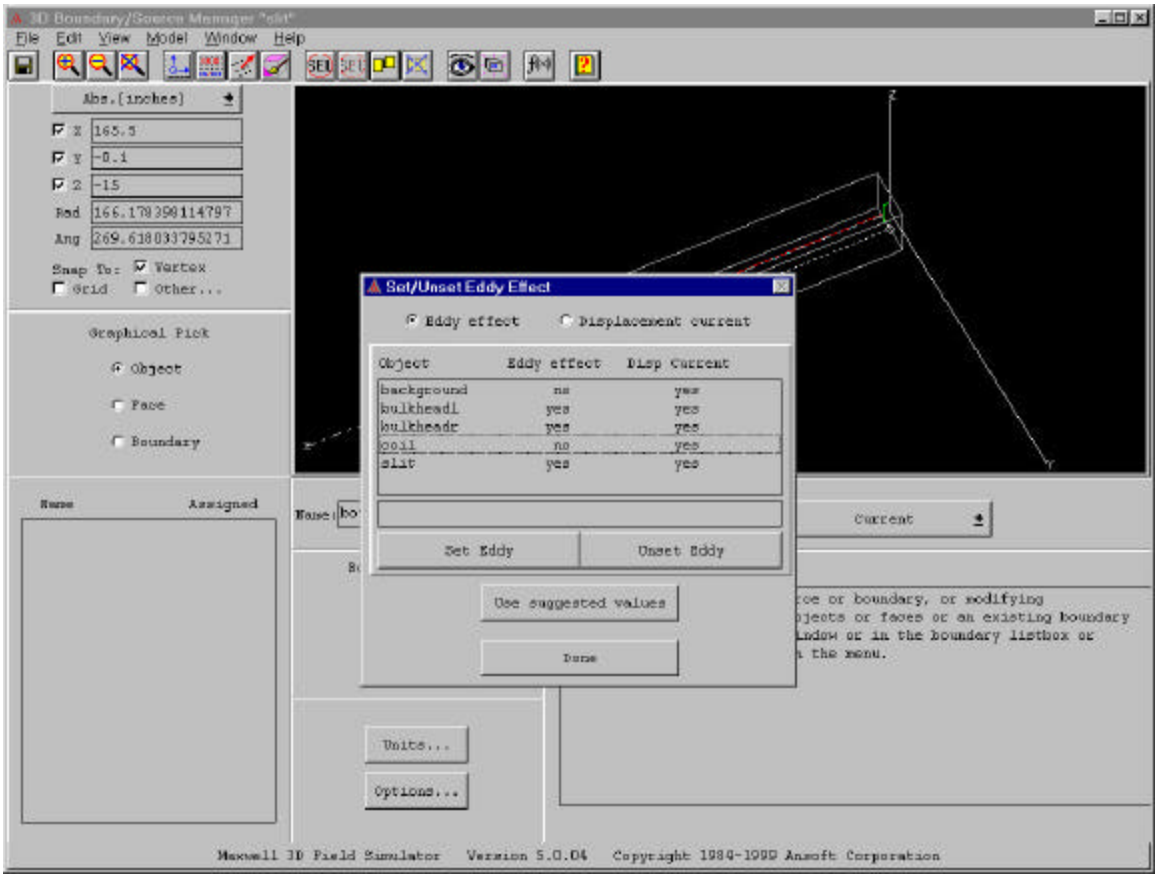

Figure 66 Solve for Eddy and Displacement Currents.

To drive the current in the antenna, the two terminals defined in the *Draw* section were chosen as current sources. First, the top terminal was selected, and was assigned a current source of 1 amp, named “upper”. The direction of the current was chosen as into the coil. Then the bottom terminal was assigned 1 amp source, named “lower”, directed out of the coil (Fig. 67).

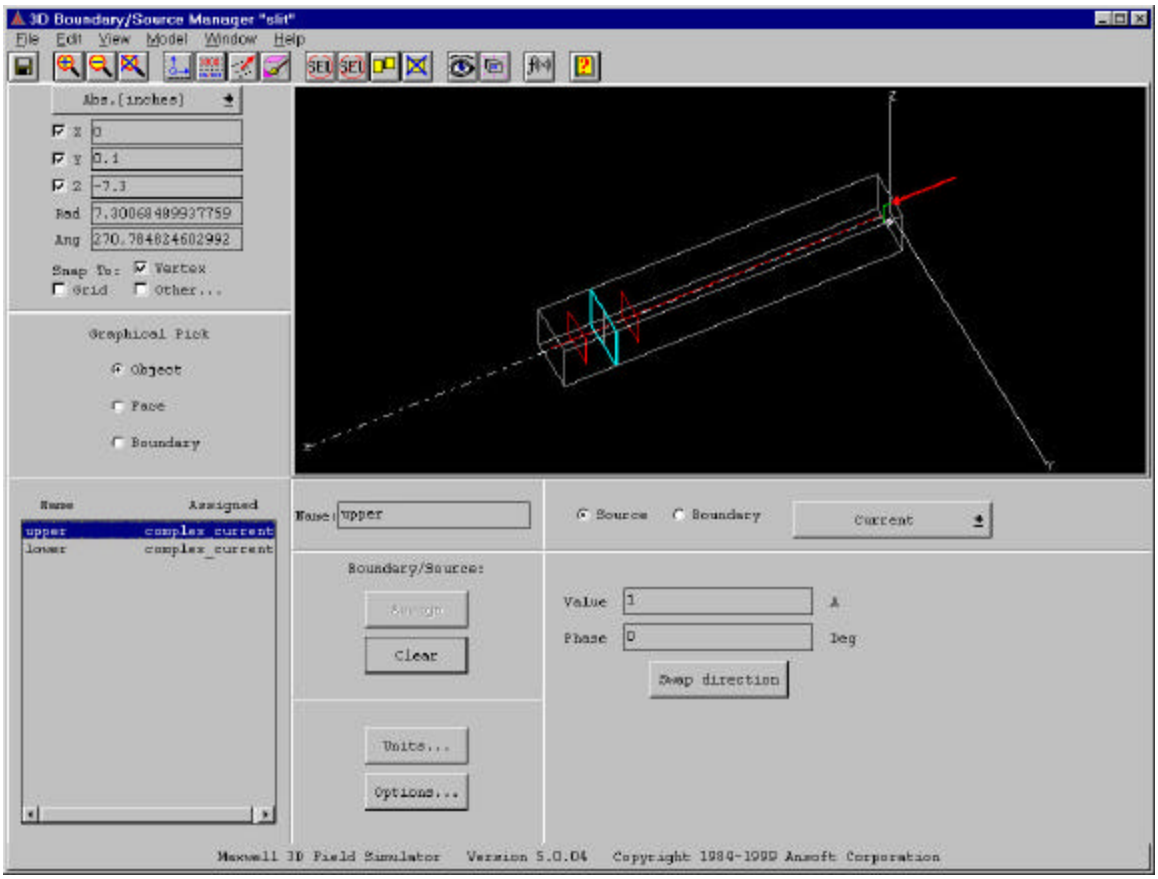

Figure 67 Assignment of Current Source.

The other five faces of the simulation region were selected to be an impedance boundary, meaning the electromagnetic fields were not forced to any particular value at the boundary. This, coupled with the previously defined environmental variable use_abc_boundary, caused the edges of the simulation region to have no effect on the electromagnetic wave (Fig. 68).

The program failed each time it a simulation was attempted with the perfectly conductive bulkhead in contact with the impedance boundary. Therefore, the bulkhead was isolated by creating an insulating boundary around the edges of the plate, wherever it came into contact with the impedance boundary. The program warned the user that these two boundaries were in contact, and that in the region of overlap the insulating boundary would supersede the impedance boundary. As this was the desired effect—isolating the perfect conductor from the impedance boundary—this setup was not changed.

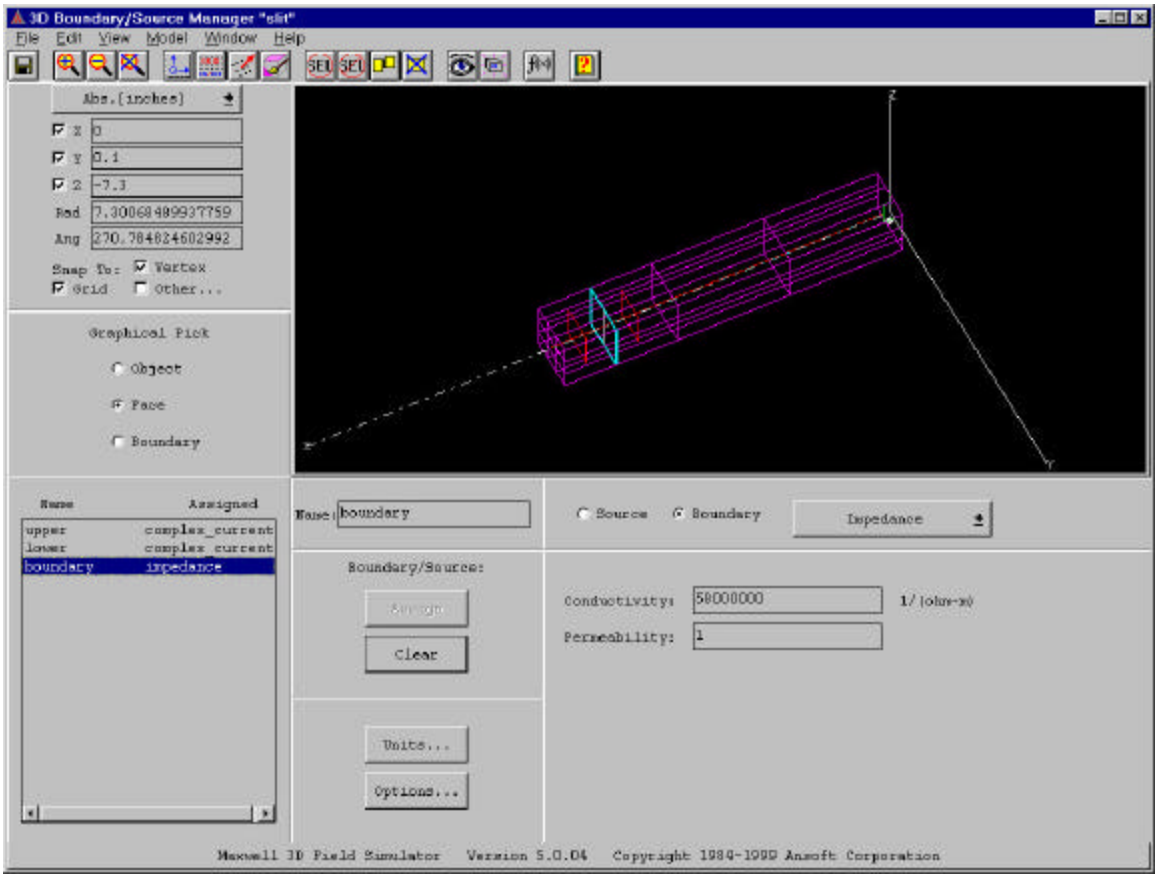

Figure 68 Assignment of Impedance Boundary.

Setup Solution

After the boundaries and sources were defined, several final parameters were entered. Most importantly, the frequency at which to solve the problem was defined as 800 MHz. Additionally, the solver was instructed to iterate until the energy error (as calculated by the simulator) was less than 0.1% or two passes had been completed, whichever came first, and to refine the mesh 30% (by number of mesh points) each pass (Fig. 69).

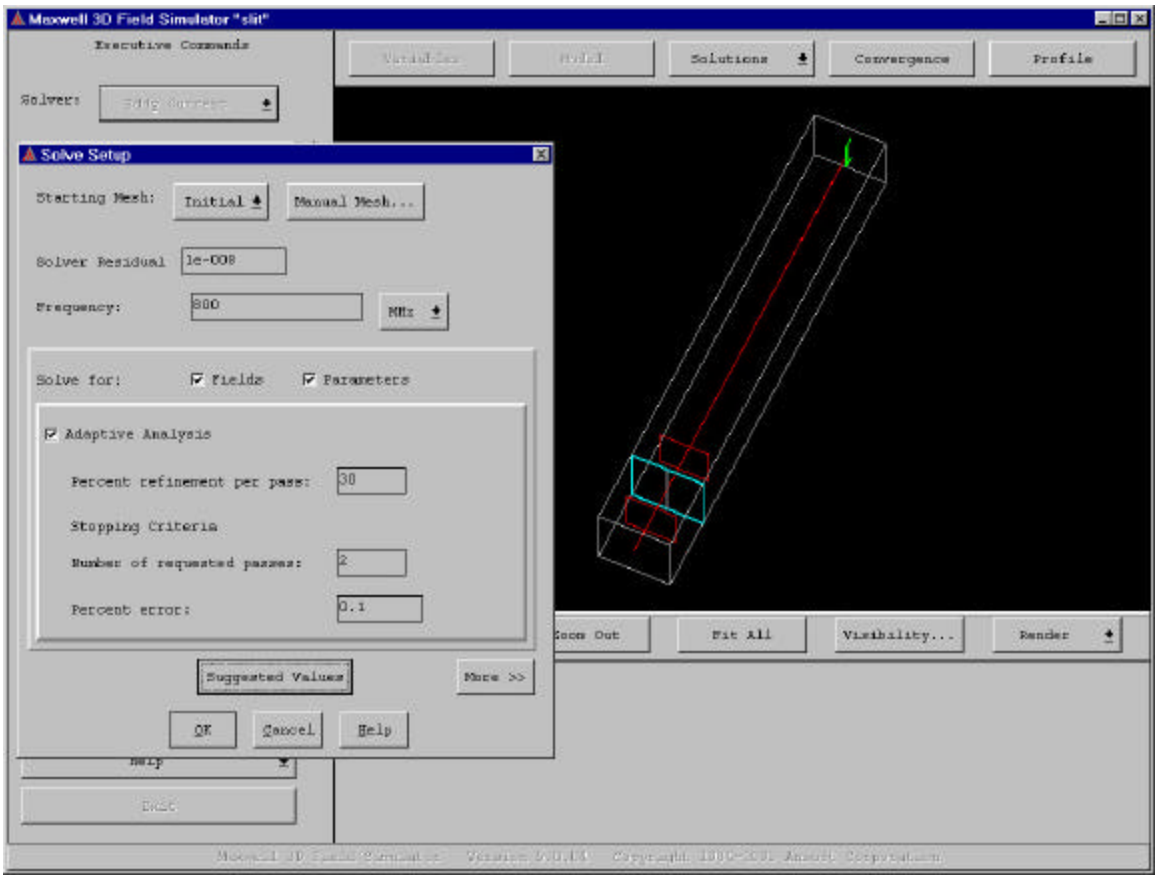

Figure 69 Solution Parameters.

Finally, the initial mesh was created. The "Manual Mesh" button was pressed to access the mesh module. From this module, the simulation space could be seeded with mesh points and the mesh created and modified. In order to accurately model the electromagnetic wave, the mesh needed to contain several points per wavelength. Therefore, the objects background, bulkheadr, bulkheadl, and slit were seeded with points approximately 5 inches apart. This was done by selecting these objects, then choosing menu option **Seed→Object→By Length**, deselecting the option to limit the number of points added, and entering 5 for the maximum element length. Once this seeding information was entered, the module was instructed to calculate the mesh by selecting **Mesh→Make** (Fig. 70).

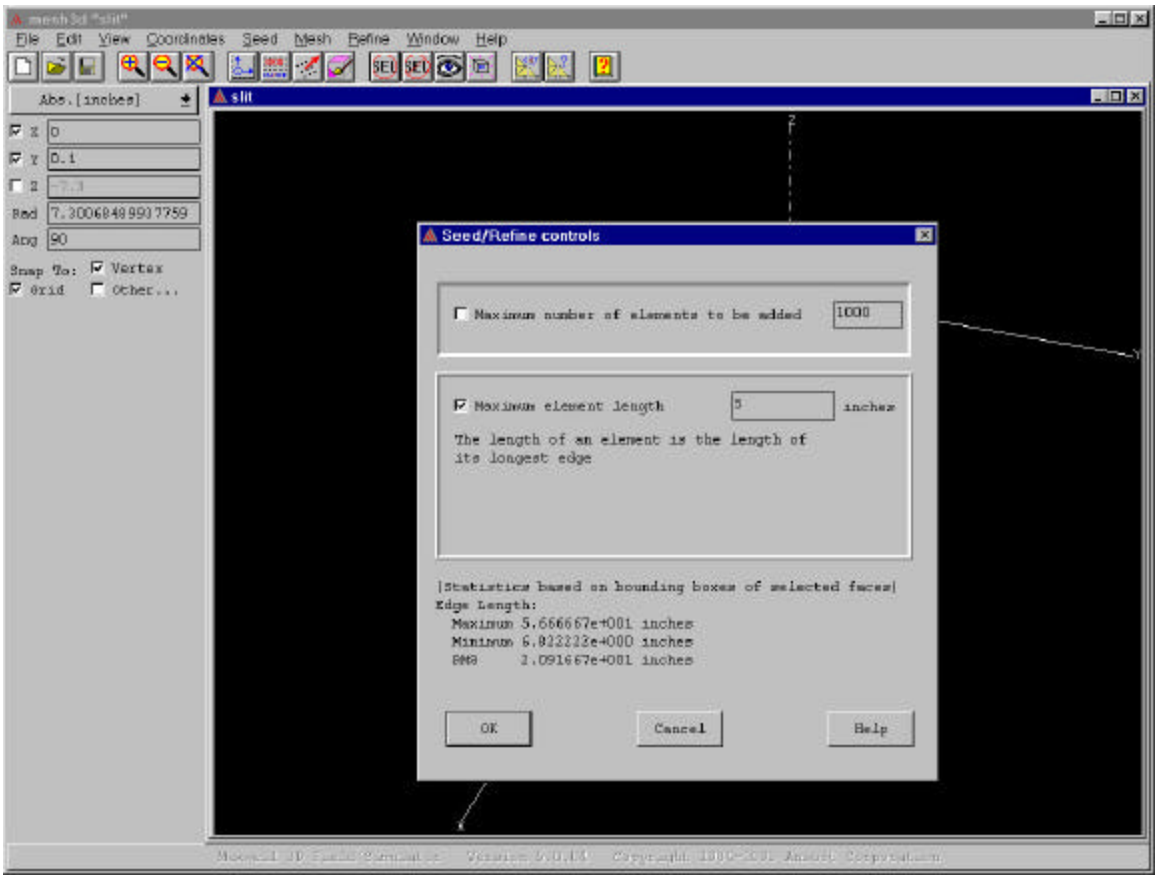

Figure 70 Seeding Control.

Once the solve parameters were defined and the mesh created, Maxwell3D was instructed to run the simulation by selecting **Solve→Nominal Problem** on the field simulator interface. On a 700 MHz Pentium III desktop computer, the program took approximately 3.5 hours to perform two iterations. During the solving process the hard drive space occupied by this simulation expanded to over 500MB. Once a simulation had been completed, it occupied approximately 100 MB of disk space.

Post Process

After the simulation had been completed, the results were analyzed in the *Post Process* module. This module allowed the electromagnetic fields and the Poynting vector to be calculated and plotted.

To investigate the electromagnetic fields the data calculator was used. This feature of the *Post Process* module allowed the results of the simulation to be entered into calculations and displayed (Fig. 71).

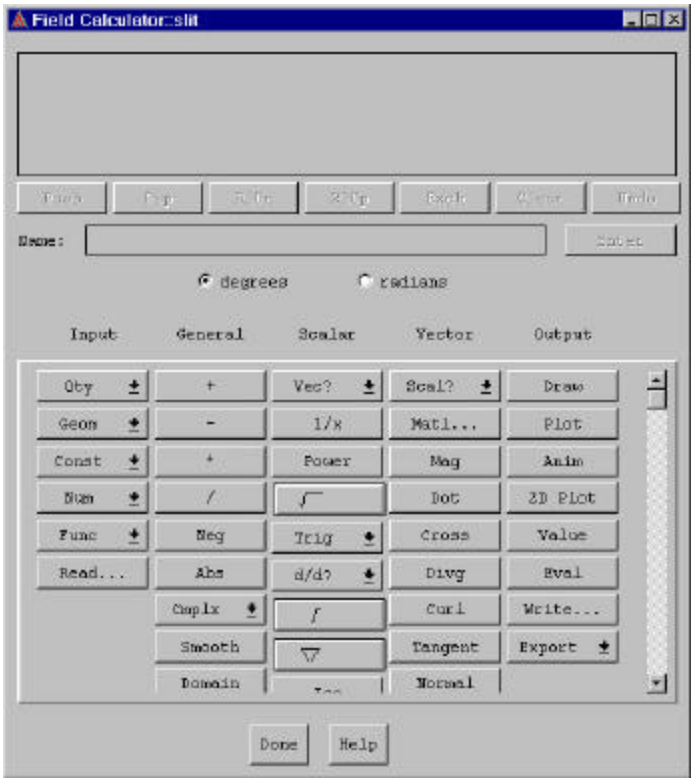

Figure 71 Data Calculator.

The quantity solved for by the program that was of interest was the magnetic intensity field, the H field. From this field, the electric field, the E field, was calculated. Using the H and the E fields, the Poynting vector, which described the magnitude and direction of the power in the wave, was calculated.

First, the equations to use to calculate these values were derived.

Derivation of Power Calculation Equation

An electromagnetic wave can be considered as having two components—a time varying electric field and a time varying magnetic field. These vectors are represented by

the symbols $\vec{\mathbf{E}}$ and $\vec{\mathbf{H}}$, respectively, where the arrow indicates a space vector and the boldface indicates a phasor—a representation of time dependence.

A phasor indicates a sinusoidal time dependence [21 p. 8]. Mathematically, a phasor is defined in the following manner:

$$\vec{\mathbf{E}} = \mathrm{Re}\left\{\vec{E}\cdot e^{j\cdot 2p\, f\cdot t}\right\}$$

where Re{*}extracts only the real component, j is the imaginary constant, f is the frequency of oscillation, t is time, and $e^{j\theta}$, according to Euler's identity, is:

$$e^{jq} = \cos(q) + j\cdot\sin(q)$$

Ampere's law, one of Maxwell's Equations, the characteristic equations of electromagnetic systems, states that

$$\vec{\nabla}\times\vec{\mathbf{H}} = \vec{\mathbf{J}} + \frac{\partial\vec{\mathbf{D}}}{\partial t}$$

where $\vec{\nabla}\times$ is the curl operator, $\vec{\mathbf{J}}$ is current density and $\vec{\mathbf{D}} = e\vec{\mathbf{E}}$ is the electrical field density [21 p. 202].

In free space—where the simulated fields were to be analyzed—$\vec{\mathbf{J}} = 0$ and the permittivity, ε, is that of free space, ε_0=8.85e-12. Therefore, this equality can be written as

$$\begin{aligned}\vec{\nabla}\times\vec{\mathbf{H}} &= \frac{\partial\vec{\mathbf{D}}}{\partial t}\\ &= \frac{\partial}{\partial t}\left(e_0\vec{E}\cdot e^{j\cdot 2p\, f\cdot t}\right)\\ &= j\cdot 2pf\cdot e_0\vec{E}\cdot e^{j\cdot 2p\, f\cdot t}\\ &= j\cdot 2p\, f\cdot e_0\cdot\vec{\mathbf{E}}\end{aligned}$$

which can be rearranged to yield

$$\vec{\mathbf{E}} = \frac{\vec{\nabla}\times\vec{\mathbf{H}}}{j\cdot 2pf\cdot e_o}$$

Once the electric field is found, the Poynting vector, $\vec{\mathbf{S}}$, can be calculated as the cross product of the electric and magnetic fields. The average amount of power, P_{av}, flowing through a region, A, can be found by integrating the real component of the Poynting vector [25].

$$P_{av} = \int_A \frac{1}{2} \mathrm{Re}\left(\vec{\mathbf{E}} \times \vec{\mathbf{H}}^*\right) \cdot d\vec{A}$$

The data calculator was used to find the power flowing through the surfaces int_surf and near_int.

Using the Data Calculator

The H field was entered into the calculator by selecting **Qty→H** (Fig. 72).

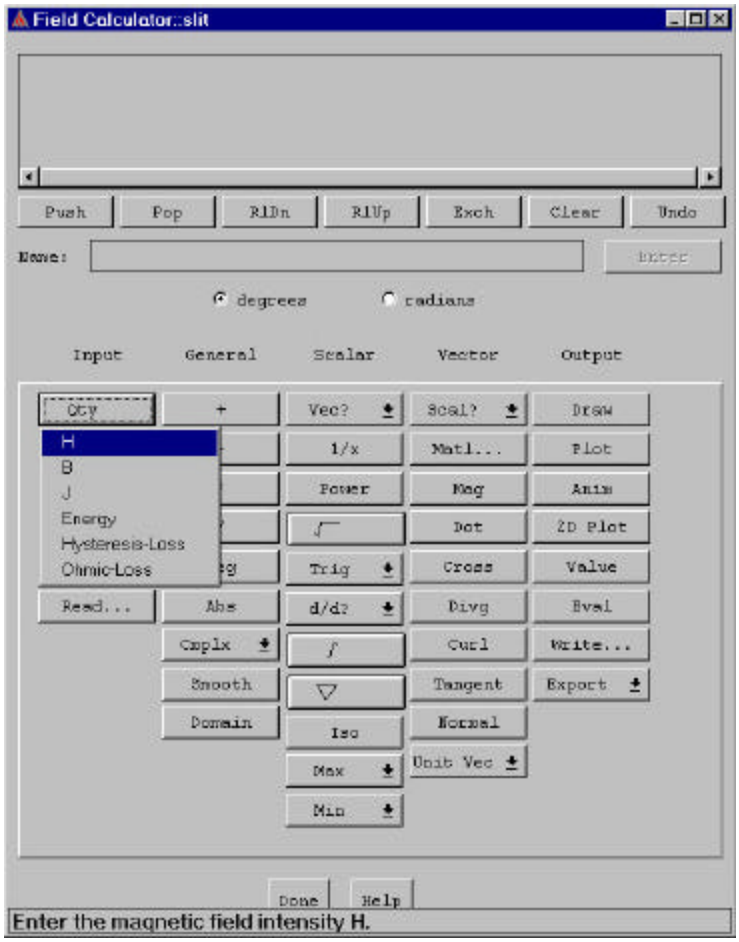

Figure 72 Entering H to the Data Calculator.

Calculating the E field

The H field was used to calculate the E field by entering this equation:

$$\vec{\mathbf{E}} = \frac{\vec{\nabla} \times \vec{\mathbf{H}}}{j \cdot 2\pi f \cdot \varepsilon} = \frac{curl\left(\vec{\mathbf{H}}\right)}{j \cdot 0.044506}$$

Enter the H field by selecting **Qty→H**.
Calculate the curl of the H field by selecting **Curl**.
Enter jωε by selecting **Num→Complex** and entering 0 for real value and .044506 for imag value.
Perform the division by clicking / (Fig. 73).

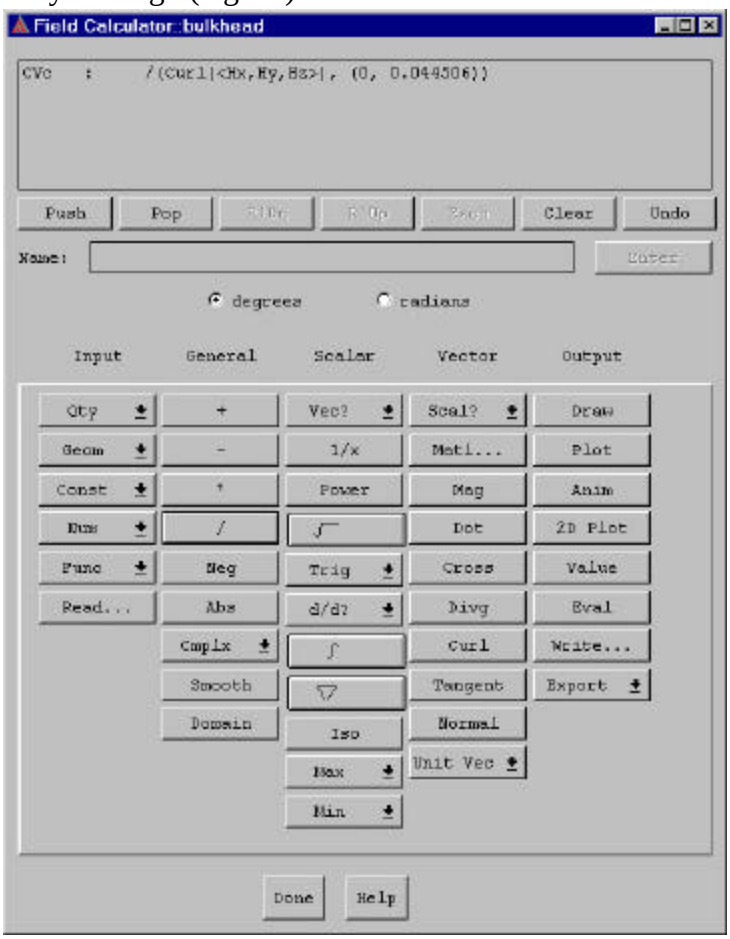

Figure 73 Calculation of E Field.

Calculating Power

The power in the wave flowing through a surface, *A*, was then calculated by entering the equation:

$$P_{av} = \int_A \frac{1}{2} \mathrm{Re}\left(\vec{\mathbf{E}} \times \vec{\mathbf{H}}^*\right) \cdot d\vec{A}$$

Calculate the E field by performing the steps listed above.
Enter the H field by selecting **Qty→H**.
Find the complex conjugate by selecting **Cmplx→Conj**.
Take the cross product of these fields by clicking **Cross**.
Find the real component of these by selecting **Cmplx→Real**.

Enter .5 by selecting **Num→ Scalar** and entering .5.
Multiply by selecting ***.**
Select the surface to integrate over by selecting **Geom→ Surface** and choosing the desired surface (int_surf or near_int).
Calculate the power flowing through the surface by clicking **Normal**.
Integrate over the surface by clicking $\int$.
Display the result numerically by clicking **Eval** (Fig. 74).

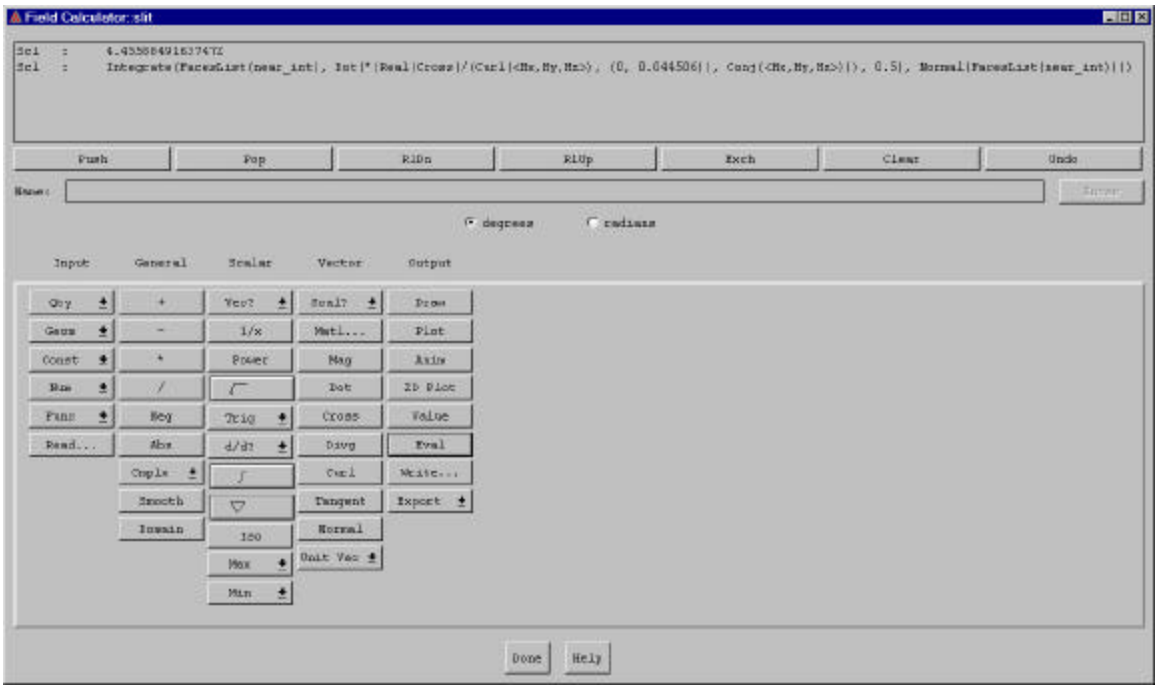

Figure 74 Power Calculation.

Wave Display

In addition to these calculations, plots were made representing the wave propagation through the space. No analysis was performed with these plots, save to verify that the simulation (correctly) showed a wavelength of approximately 15 inches. These plots also appear in this report to illustrate the wave propagation. To make these plots, the electromagnetic fields were plotted along the surfaces x_axis and far_x after being manipulated to show constant signal power along the length of the plot. This was done by dividing the field by its maximum value in the following manner.

Enter or calculate the desired field.
Enter the field again or click the **Push** button to create another copy of the field in the calculator.
Enter the variable PHASE to the calculator by selecting **Func→ Scalar** and choosing PHASE.
Have the calculator treat the field as a function of phase by selecting **Cmplx→ AtPhase**.

Move the AtPhase function down in the list and the other field entry up by clicking **Exch**.

Find the vector corresponding to the largest signal in the field by selecting **Cmplx→ CmplxMag**.

Find the magnitude of this vector by clicking **Mag**.

Divide the field (as a function of PHASE) by its magnitude by clicking /.

Select the surface on which to plot the wave shape by selecting **Geom→ Surface** and choosing the desired surface (Fig. 75).

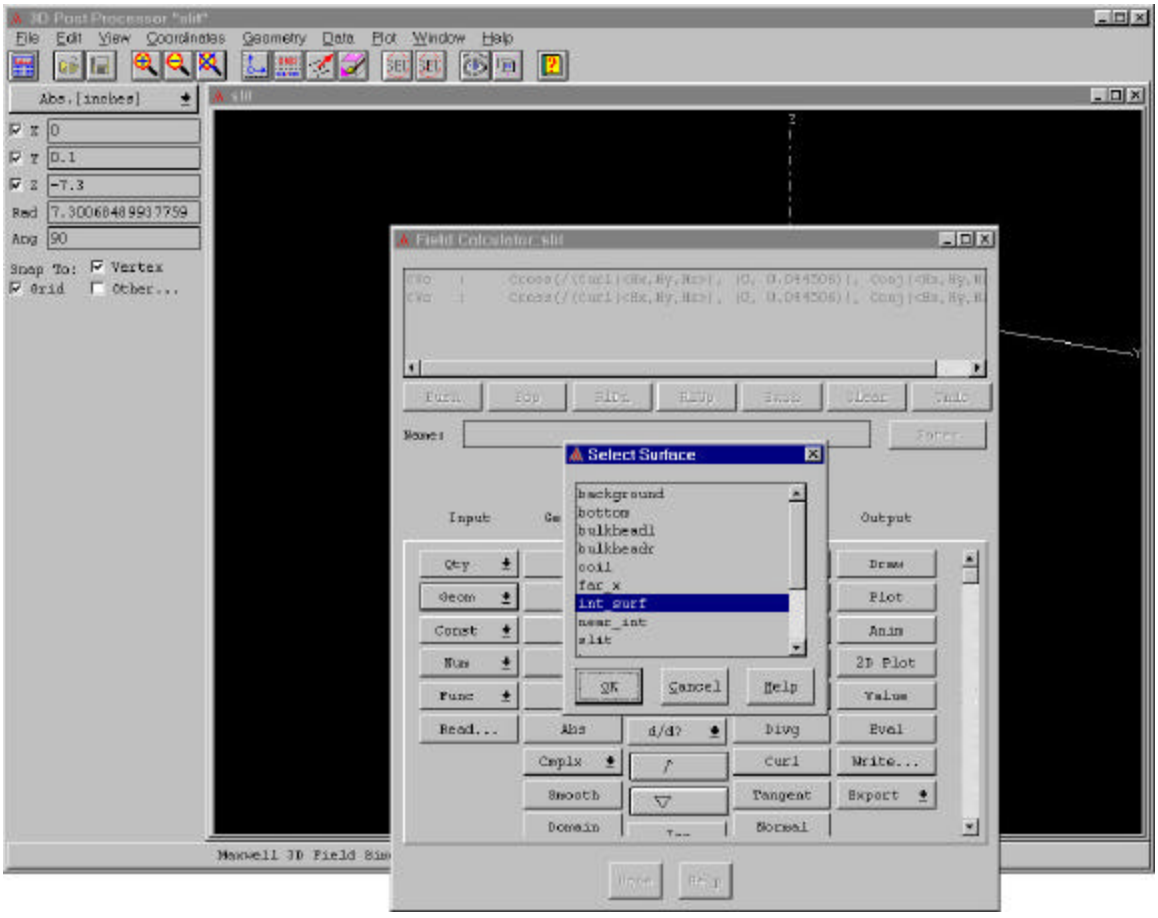

Figure 75 Selecting Surface For Power Calculation.

Create an animation plot by clicking on **Anim**, selecting PHASE as the variable, and enter 0 for start, 351 for stop, and 9 for delta. Select "Store Frames" to allow the animation to be viewed from different angles without having to manually redo the plot at each point of view (Fig. 76).

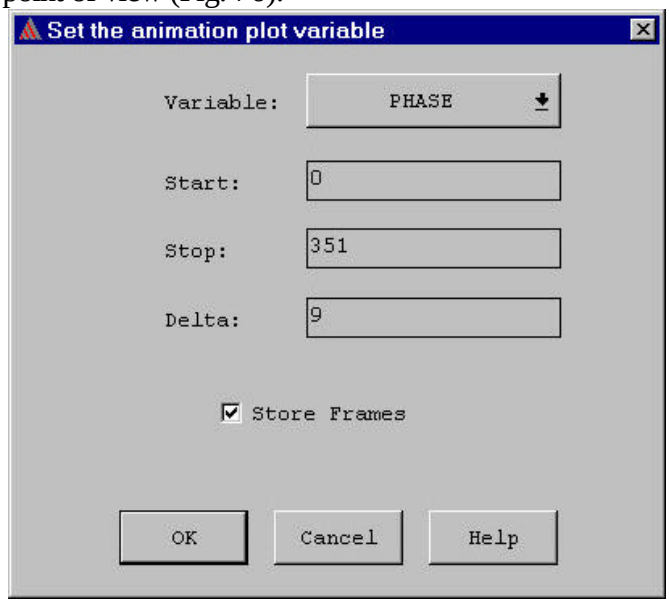

Figure 76 Animation Setup.

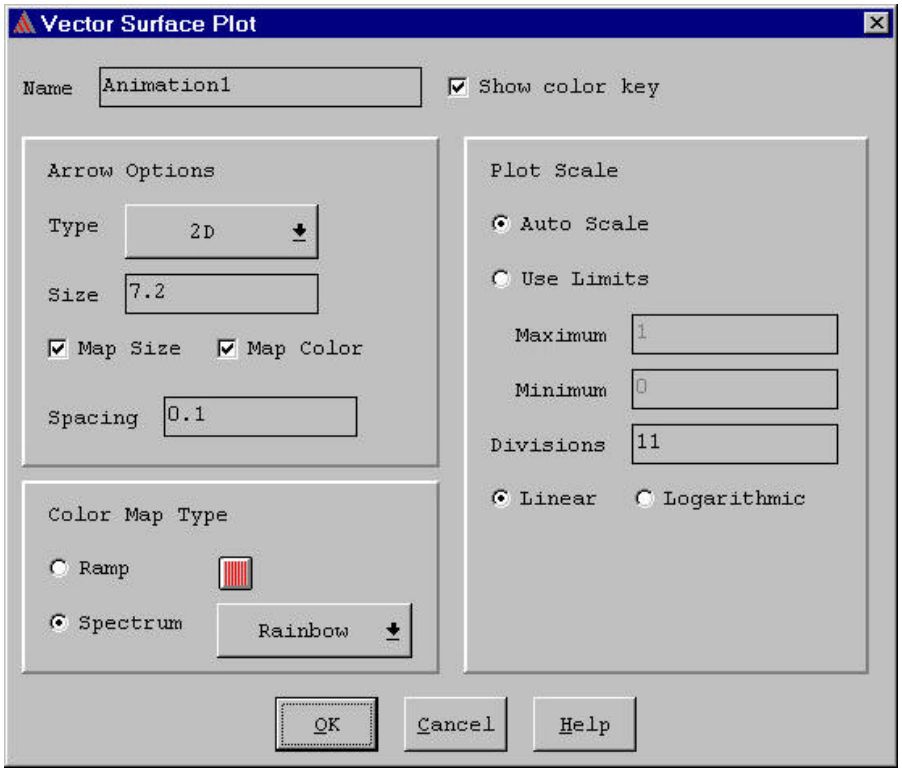

Figure 77 Plot Options.

Select 2D as the plot type and enter 0.1 as the spacing (Fig. 77).

Use the buttons on the animation control to investigate the wave propagation. Select a particular frame for display by double clicking that frame with the animation stopped (Fig. 78).

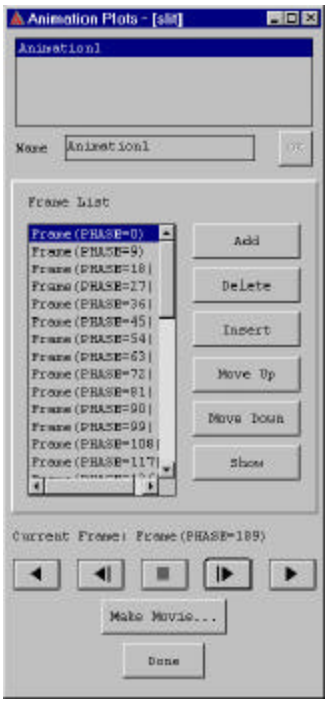

Figure 78 Animation Control.

Repeat these steps for all desired waves and surfaces. The plots included in this report (Figures 79 and 80) were made by plotting both electromagnetic waves on both x_axis and far_x.

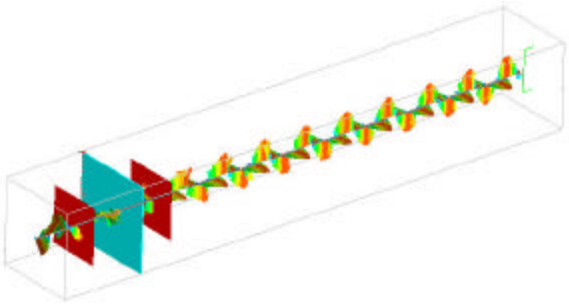

Figure 79 Solid Bulkhead Simulation.

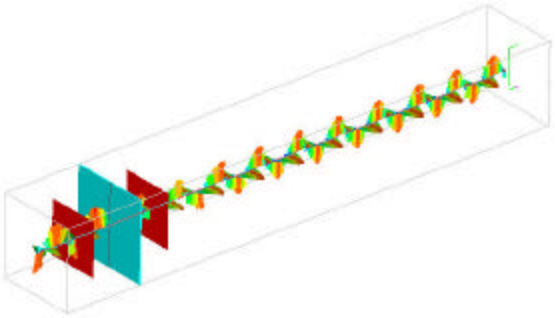

Figure 80 Slit Bulkhead Simulation.